SUPERCONDUCTING TECHNOLOGY FOR ELECTRIC PROPULSION

by

Eric F. Keamy

B.S.E.E., The Citadel, 1981

Submitted to the Department of Ocean Engineering
in Partial Fulfillment of the Requirement for the Degree of

MASTER OF SCIENCE IN NAVAL ARCHITECTURE
AND MARINE ENGINEERING

at the

MASSACHUSETTS INSTITUTE OF TECHNOLOGY

June 1988

Signature of Author: Eric F. Keamy
Department of Ocean Engineering, 10 May 1988

Certified by: Koichi Masubuchi
Koichi Masubuchi, Thesis Supervisor

Accepted by: A. Douglas Carmichael
A. Douglas Carmichael, Chairman
Departmental Graduate Committee
Department of Ocean Engineering

SUPERCONDUCTING TECHNOLOGY

FOR ELECTRIC PROPULSION

by

Eric F. Keamy

ABSTRACT

Submitted to the Department of Naval Architecture and Marine Engineering on May 1, 1988 in partial fulfillment of the requirements for the Degree of Master of Science in Naval Architecture and Marine Engineering

The thesis analyzes the superconducting technology for a shipboard electric propulsion system. Superconductor operational limits, and magnet design requirements were established. The magnetic field reqirements for a large scale superconducting propulsion plant were analyzed from.experimental information on copper and aluminum-stabilizied NbTi superconductors. Experimental results were followed with a feasibility study in the convertion of a DD963 Spruance Class Destroyer from mechanical to superconducting electric drive. The results of the conversion are an increase in survivability, speed, usable deck area (4,954 ft^2), maintainability, propeller efficiency and endurance range (+71%) along with a decrease in displacement (-2.83%) and self radiated noise without compromising existing mission capabilities. The estimated cost of the conversion is $118.8 million dollars.

SUPERCONDUCTING TECHNOLOGY

FOR ELECTRIC PROPULSION

by

Eric F. Keamy

ABSTRACT

Submitted to the Department of Naval Architecture and Marine Engineering on May 1, 1988 in partial fulfillment of the requirements for the Degree of Master of Science in Naval Architecture and Marine Engineering

The thesis analyzes the superconducting technology for a shipboard electric propulsion system. Superconductor operational limits, and magnet design requirements were established. The magnetic field reqirements for a large scale superconducting propulsion plant were analyzed from.experimental information on copper and aluminum-stabilizied NbTi superconductors. Experimental results were followed with a feasibility study in the convertion of a DD963 Spruance Class Destroyer from mechanical to superconducting electric drive. The results of the conversion are an increase in survivability, speed, usable deck area (4,954 ft^2), maintainability, propeller efficiency and endurance range (+71%) along with a decrease in displacement (-2.83%) and self radiated noise without compromising existing mission capabilities. The estimated cost of the conversion is $118.8 million dollars.

ACKNOWLEDGEMENT

The author is deeply indebted to his advisor, Professor Koichi Masubuchi for his guidance during the difficult period of authorship. A deep debt of gratitude is also owed to the following individuals:

Don Waltman, David Taylor Naval Research Laboratory
Neal Sonderguard,.David Taylor Naval Research Laboratory
Jeff Green, David Taylor Naval Research Laboratory
Mike Cannell, David Taylor Naval Research Laboratory
Phil Clark, David Taylor Naval Research Laboratory
Mike Supercynski, David Taylor Naval Research Laboratory
LT Greg Kolodziejczak, David Taylor Naval Research Laboratory
Don Schmucker, NAVSEA Code 56Z31
Don Gubsner, United States Naval Research Laboratory
Stewart Wolf, United States Naval Research Laboratory
Wendy Fuller, United States Naval Research Laboratory
John Clausser,.United States Naval Research Laboratory
Mike Ossokey, United States Naval Research Laboratory
Jack Ekin, National Bureau of Standards
1ST LT Steve Devers, Wright Peterson Air Force Superconductivity Laboratory
Charles Oberly, Wright Peterson Air Force Superconductivity Laboratory
Sebash Karmarkar,.Naval Surface Weapons Center
John Barclay, Astronautics Corporation
Eric Gregory, Supercon Corporation
Bob Schwell, International Business Corporation
Terry Orlando, M.I.T.
Si Foner, M.I.T.
LT Joeseph Stiglich, M.I.T.
LT Erik Christiensen, M.I.T.
LT Randy Grigg, M.I.T.

Finally, the author wishes to thank Maria for her patience during my 2 years at M.I.T.

TABLE OF CONTENTS

LIST OF FIGURES

LIST OF TABLES

INTRODUCTION

A "superconductor" is a material which loses all electrical resistance when subjected to reduced temperatures. This allows current to flow freely through the material with no associated energy loss. Superconductivity was first discovered in 1911 by G. Kammerlingh Onnes who found that mercury at temperatures near absolute zero (4.12 K) had almost zero electrical resistance. Shortly thereafter, similar phenomena was discovered in a variety of other pure metals. Today, over 1,000 different materials have been identified as having superconductive properties, including such common metals as pure tin and lead. Superconducting properties have only been found at very low temperatures and the phenomena drops off rapidly as temperature increases above absolute zero. Superconductivity has also been found to diminish in the presence of a magnetic field. The critical field intensity (Hcr), defined as the strength of magnetic field at which superconductive properties are no longer present, varies greatly with temperature; the lower the temperature of the superconductor, the higher the critical field intensity. As early as 1933, researchers discovered that the magnetic field did not penetrate the superconductor as with conventional materials but is excluded from the inside of the material. This phenomena, known as the Meissner effect, has become one of the fundamental properties of superconductivity. Because the critical fields of pure superconductors were of such a small magnitude and therefore not practical for any large scale applications, research into superconductivity remained stagnant until the early 1960's when it was discovered that critical fields of alloys and impure materials exhibited much higher intensities. With the discovery that the superconducting properties of both niobium strannide (Nb3Sn) and niobium titanium (NbTi) did not diminish in large magnetic fields, worldwide interest focused on further development of alloy superconductors.

Within the last decade, the availability of superconductors of a large enough size for practical applications has provided the impetus for the development of electric machinery using superconducting windings. Because superconductors support very high currents with negligible resistance loss, superconducting machines can produce large magnetic fields which are needed for high power output. Since there is minimal energy loss associated with these machines, their efficiency is significantly higher than that of conventional machines. One promising application is a superconducting marine electric drive propulsion system; an idea which has previously been impractical due to size and weight considerations. This technology may now be applied to large scale superconducting machines aboard ships.

The role of superconductors in both AC and DC machines is the same; to produce a magnetic field without the use of bulky and heavy ferrous materials. Since a powerful magnetic field is a major driving force in successful implementation of this technology, materials for a high field superconducting magnet were examined. High temperature superconductors were analyzed first since successful implementation would have lead to replacement of expensive liquid helium coolant with cheaper liquid nitrogen coolant. The upper critical field of these materials is sufficient for a large scale superconducting propulsion application. However, technical barriers still exist such as low critical current densities and manufacturing difficulties. The most current density that high temperature wires have been made to carry is1000 amperes per square centimeter at 1 Tesla. Superconductors used in motors must be able to carry up to 100 times this amount. The ceramic's low current density problem appears to be attributed to their anisotropic character. The ceramic samples consist of individual superconducting crystals with nonsuperconducting areas in between. This results in noncontinuos current. Also, the superconducting ceramics like other ceramics are brittle, break easily, and are difficult to manufacture into coil shapes. In addition, the ceramics are highly susceptible to environmental degradation because of their extreme sensitivity to oxygen, water, and carbon dioxide.

Because of the reasons mentioned above, high temperature superconducting ceramics will not be considered technically feasible for a superconducting propulsion system.

Next, the type 2 superconducting materials. were examined. These materials operate in the liquid helium cooling range. The most promising type 2 materials were Nb3Sn, V3Ga, Nb3(AlGe), Nb3Ge, and NbTi. Nb3Sn can generate a magnetic field of over 15 tesla. A process has been developed for manufacturing this brittle material into a coil shape. However, the material is very likely to fracture under the strains and forces of the strong magnetic field. V3Ga, Nb3(AlGe), and Nb3Ge have high critical field intensities but lack a practicle fabrication technique. NbTi can generate a magnetic field of up to 9 tesla (nearly five times that of an iron magnet). NbTi is ductile and can be easily be wound into the spiral shape necessary for a magnet. Therefore, NbTi was selected as the material for a high field superconducting magnet.

Chapter 1 will begin with an overview of superconducting properties and operational limits for NbTi.

The objective of Chapter 2 is to determine the performance and quench behavior of a copper-stabilized NbTi superconducting coil and access the feasibility of application in a superconducting shipboard propulsion system. Copper was selected as the stabilizing element to provide protection to the superconductors in the event of a quench. Stability measurements were conducted with a copper-stabilized NbTi magnet. For a shipboard superconducting propulsion system operating in an adverse environment, stability appears to be the major issue. Aluminum stabilized NbTi superconductors are expected to have an improvement in stability over copperstabilized NbTi superconductors. The disadvantage is that compared to copper, aluminum matrix material is much more difficult to combine with NbTi. The aluminum stabilizer has improved thermal conductivity, heat capacity, and electrical conductivity at 4.2 degrees Kelvin compared with the copper stabilizer. Therefore, in Chapter 3, the stability of NbTi/Al will be compared with the stability of NbTi/Cu.

In Chapter 4 the NbTi superconducting technology is applied to a shipboard propulsion system. The propulsion system that will be considered will be a U.S. Navy Spruance Class Destroyer (DD963). A feasibility study will be conducted in converting the DD963 Class destroyer from mechanical to superconducting electric drive. The anticipated benefits from this conversion are an anticipated increase in survivability, available deck area, maintainability, propeller efficiency, speed, and endurance range along with a decrease in displacement and selfradiated noise without compromising existing mission capabilities.This paper will only investigate the impact on the ship caused byconverting from mechanical to electrical drive; specific use of anyweight, space, or power "savings" will not be addressed. After successful installation and evaluation of this conversion, a follow-on study could be made to determine how to most effectively use the"gains" realized by this modification.

The existing DD963 Spruance Class of U.S. Navy destroyers was designed with the primary mission of submarine tracking and antisubmarinewarfare. The first vessel of the class, the USS Spruance (DD963),was introduced into the fleet in the mid 1970's. Follow-on production continued until a total of 31 vessels entered the U.S. Navy inventory. These ships are very versatile and can operate with equal success either alone or as part of a multiship carrier task force.The addition of the DD963 class into the inventory of the U.S. Navyrepresented many "firsts" (Ware, 1975):

first U.S. warship to use gas turbines for main propulsion

first warship to use gas turbines for electrical generation

first destroyertype ship with an automated engineering plant

first warship with all digital fire control

first vessel designed by a contractor and subject to performance proof tests

first vessel with a warranty/guarantee clause covering proof of design performance

first modern warship with contractor developed computer software

A significant part of the design philosophy of the Spruance class ships was to ensure that sufficient margin would be available for upgrades to the combat systems and supporting electronic equipment at regular intervals during the ships' expected 30 year life as new technology emerged. Therefore, the DD963 was selected as the ideal platform to analyze the effects of applying superconductivity technology to a marine propulsion system and to provide a basis for designing future shipboard systems. Table I.1 provides a list comparing the principal characteristics of the existing configuration to the proposed electrical drive variant.

	BASELINE	ELECTRIC DRIVE VARIANT
Displacement	8014.7 LT	7785.9 LT
LOA	563.3 FT	563.3 FT
LBP	529.0 FT	529.0 FT
B	55.0 FT	55.0 FT
T	19.9 FT	19.5 FT
KM	26.2 FT	26.3 FT

GM	3.9 FT	4.2 FT
GM/B	0.071	0.077
VCG	22.30 FT	22.04 FT
LCG	272.4 FT	276.5 FT
TCG	0.01 FT (stbd)	0.01 FT (port)
HEEL	0.02 deg (stbd)	0.24 deg (port)
TRIM	0.72 FT by bow	0.12 FT by bow
FULL POWER	80,000 SHP	78,834 SHP
CRUISING	10,548 SHP	10,232 SHP
AVE SS ELECT LOAD	1,600 KW	2,839 KW
MAX SS ELECT LOAD	2,408 KW	4,273 KW
MAIN ENGINES	4 LM2500 gas turb.	3 LM2500 gas turb.
S.S. ENGINES	3 2000 KW gas turb.	2 2000 KW gas turb.
PROPELLER	CRP	FIXED PITCH
COMPLEMENT	296	296
ENDURANCE	6,000 NM	10,251 NM

TABLE 1.1 SHIP CHARACTERISTICS SUMMARY (MIT 13A VAULT)

ELECTRICAL DRIVE VARIANT

Electric propulsion systems can be either direct current (DC) or alternating current (AC). Power can be supplied by any of a number different types of prime movers; gas turbines, diesel generators, or steam plants. DC electric drive systems are considered more desirable for naval combatants since they allow a more rapid and continuous control of the propeller shaft which is essential in maneuvering situations. Each shaft would be directly coupled to a largepropulsion motor with a widely variable reduction ratio. The propulsion motors are connected to the propulsion generators through parallel cabling via a main switchboard. The propulsion generators are directly coupled to the prime movers. Historically, there has been a continual interest in using electric propulsion systems aboard naval ships because of their ability to provide a direct speed reduction between a high speed lightweight prime mover (i.e. gas turbine) and a much slower propeller. The advantages of electric drive propulsion include:

greater operational flexibility in the selection of on line equipment at lower speeds since all generators tie into a common bus. Prime movers can be run at most economical loading configurations and hence reduce fuel consumption and propulsion plant installed horsepower.

engine location can be varied to improve survivability and compartment arrangement since prime movers are no longer constrained to be directly attached to the shaft.

the elimination of heavy reduction gears and shortened shaft lengths both help to improve survivability and lower overall ship weight.

the replacement of the heavy and less efficient CRP propellers with a conventional fixed pitch propellers. Reversing direction of electric motors is easily accomplished with minimum of controls.

Although electrical drive systems have many advantages over the more conventional mechanical drive systems, they have not been used extensively in naval applications, primarily for the following reasons:

higher acquisition costs

increased weight and volume requirements

lower efficiency due to higher transmission losses

higher fuel consumption

However, with the recent developments in superconductivity, superconducting electric drive propulsion may now be a very attractive alternative to the conventional mechanical drive system and deserves a renewed interest for the following reasons:

the use of superconducting machinery incorporates all the advantages of an electrical propulsion system combined with an expected actual weight and volume savings over conventional mechanical drive systems.

an expected reduction in the engineering plant would allow for a greater area and weight to be available for other ship's functions.

CHAPTER 1
OVERVIEW OF SUPERCONDUCTOR PROPERTIES AND OPERATIONAL LIMITS FOR A SHIPBOARD ELECTRIC PROPULSION SYSTEM

1.1 INTRODUCTION

The objective of this chapter is to provide an overview of superconductor properties and operational limits for a shipboard electric propulsion system.

1.2 CRITICAL PARAMETERS

The three critical parameters that are used to describe superconductors are critical temperature, critical field, and critical current.

a. CRITICAL TEMPERATURE

The critical temperature is the temperature at which superconductivity begins to occur. (Ekin, J.W., 1988) During this condition the resistivity of the material suddenly drops to approximately zero. Figure 1.1 shows a graph of this characteristic of superconductivity. The critical temperature of pure superconductors is well defined as shown by the sharp transition temperature in Figure 1.1. However, superconducting materials suitable for an electric propulsion system (type2) superconductors are inhomogeneous.in nature and have a poorly defined transition temperature. The transition temperature of these materials is normally defined as the point where the resistivity decreases to half its normal value. The inhomogeneous material (Nb-Ti) was selected as the superconducting material to be examined in this paper. The critical temperature was determined to be 10.2 degrees Kelvin. (Ekin, J.W., 1988) The method used to determine this temperature was the inductive technique. A schematic of the

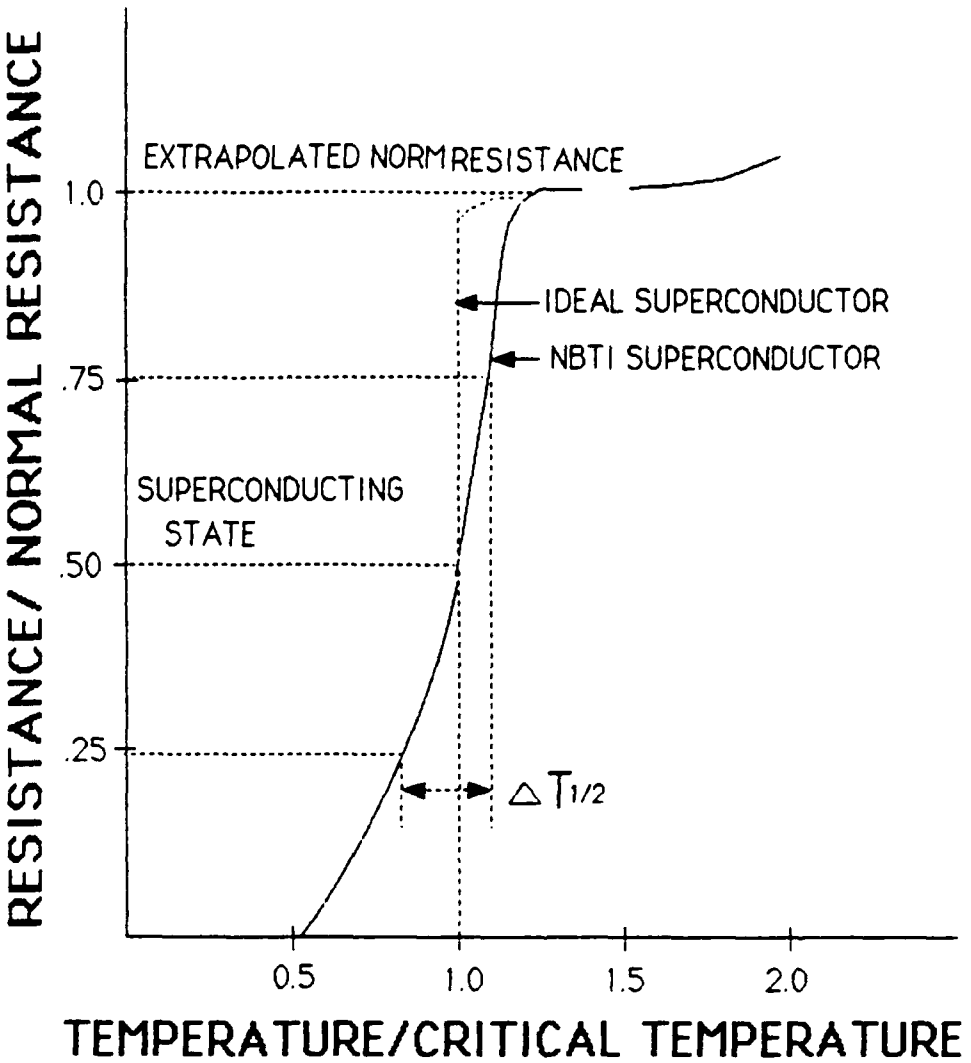

FIGURE 1.1 SCHEMATIC SHOWING RESISTANCE VERSES TEMPERATURE FOR NBTI SUPERCONDUCTOR

inductive technique is shown in Figure 1.2. As can be seen from this figure, fig 1.1penetration of the material is not required. This technique relies on a drastic decrease in magnetic permeability of the Nb-Ti material as it passes into the superconducting state.

b. CRITICAL MAGNETIC FIELD

The critical magnetic field is defined as the value of the applied magnetic field that fully penetrates the material such that the superconductor converts to a normal conductor. When in the superconducting state currents are created to produce an internal opposing magnetic field that cancels the applied magnetic field. Figure 1.3 is a schematic showing the expulsion of flux from an ideal superconductor. NbTi superconductors behave differently than ideal superconductors. Ideal superconductors completely exclude the field from the internal of the superconductors at all fields less than the critical field. However, complete flux penetration occurs once the critical field is exceeded. Contrary to ideal superconductors, magnetic field penetrates NbTi superconductors at a value considerably below the ideal critical field value. However, NbTi remains superconducting up to a much higher critical field.

The high upper critical field value of NbTi make it a prime material for a superconducting shipboard propulsion system. The upper critical field value for NbTi at 4.2 degrees Kelvin is 12 Tesla while the critical field of all ideal superconductors is below 1 Tesla. Figure 1.4 shows a schematic of the magnetization of NbTi compared to an ideal superconductor. Between the lower critical field and upper critical field the flux penetrates the material in the form of flux tubes. Figure 1.5 is a schematic of flux tubes penetrating NbTi material. As can be seen from Figure 1.5, the material surrounding each tube remains supperconducting while the core material becomes superconducting. When the magnetic field is increased in value the number of flux tubes penetrating the material is increased accordingly. The number of vortex flux tubes will eventually

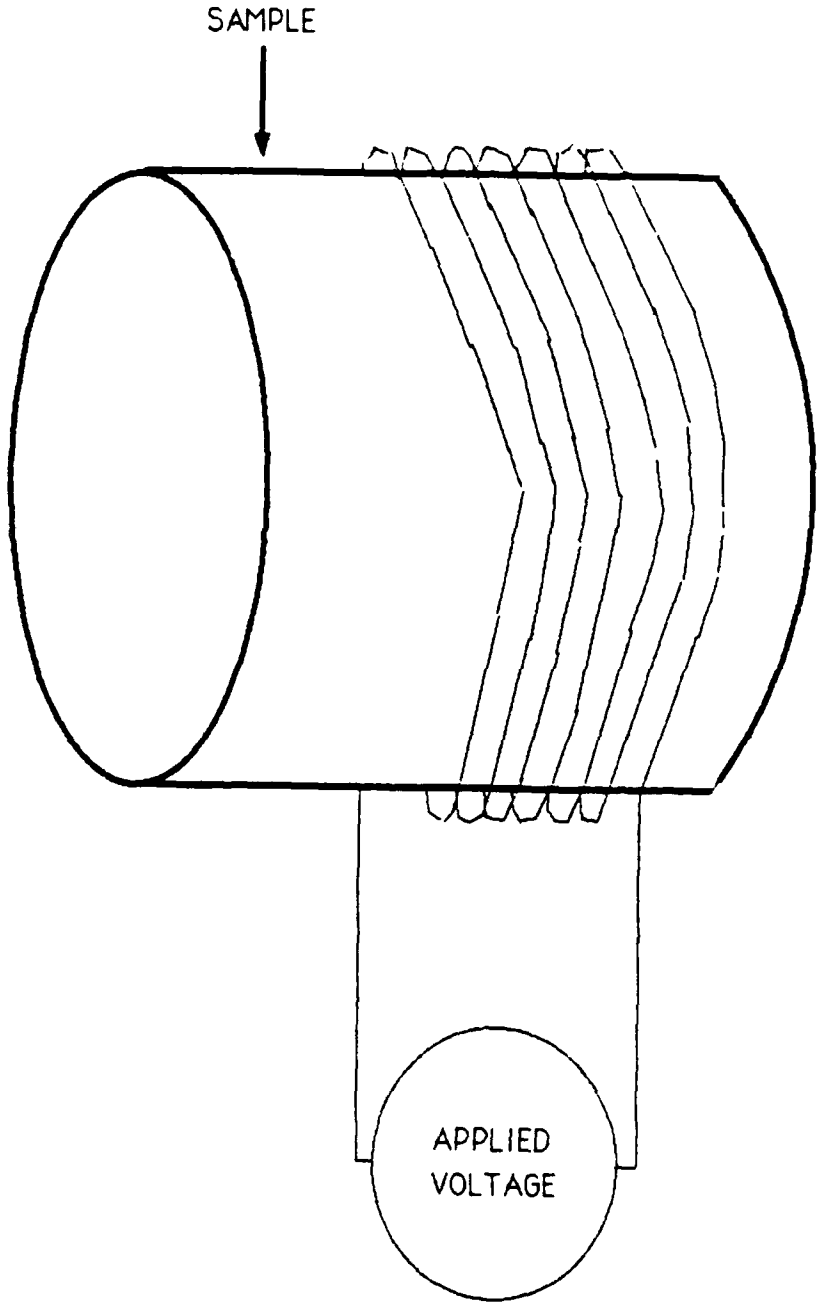

FIGURE 1.2 INDUCTIVE TECHNIQUE FOR DETERMINING CRITICAL TEMPERATURE

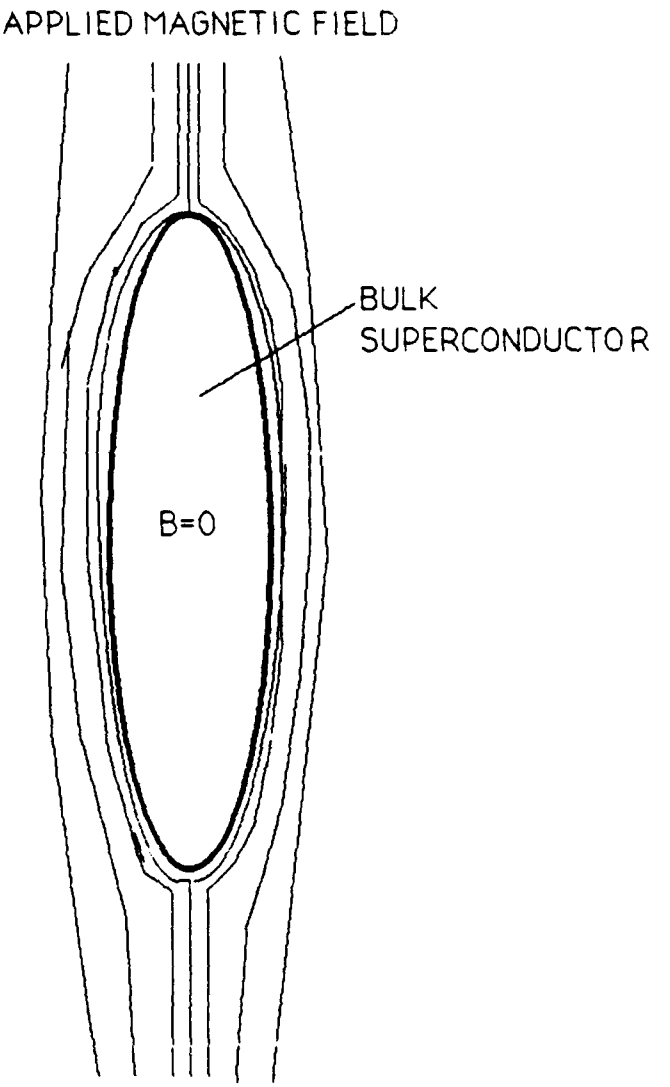

FIGURE 1.3 SCHEMATIC SHOWING EXPULSION OF FLUX FROM INTERIOR OFIDEALSUPERCONDUCTOR

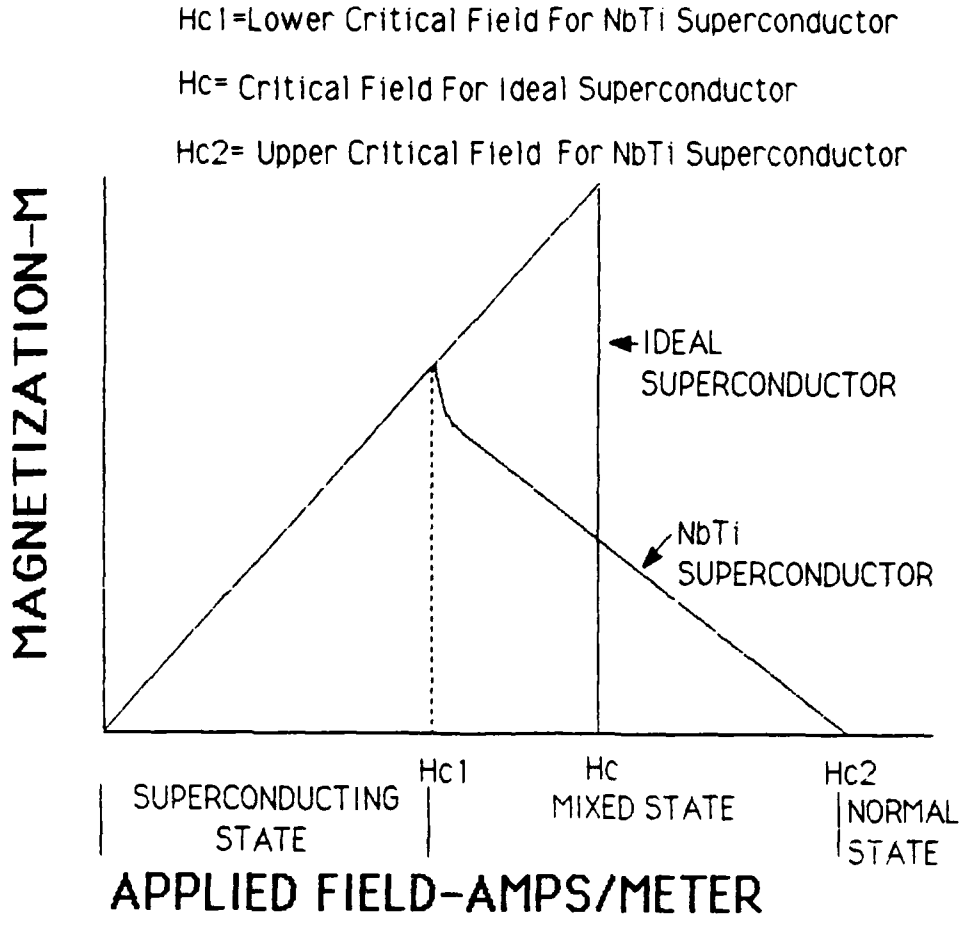

FIGURE 1.4 MAGNETIZATION CURVES FOR NbTi SUPERCONDUCTOR AND IDEAL SUPERCONDUCTOR

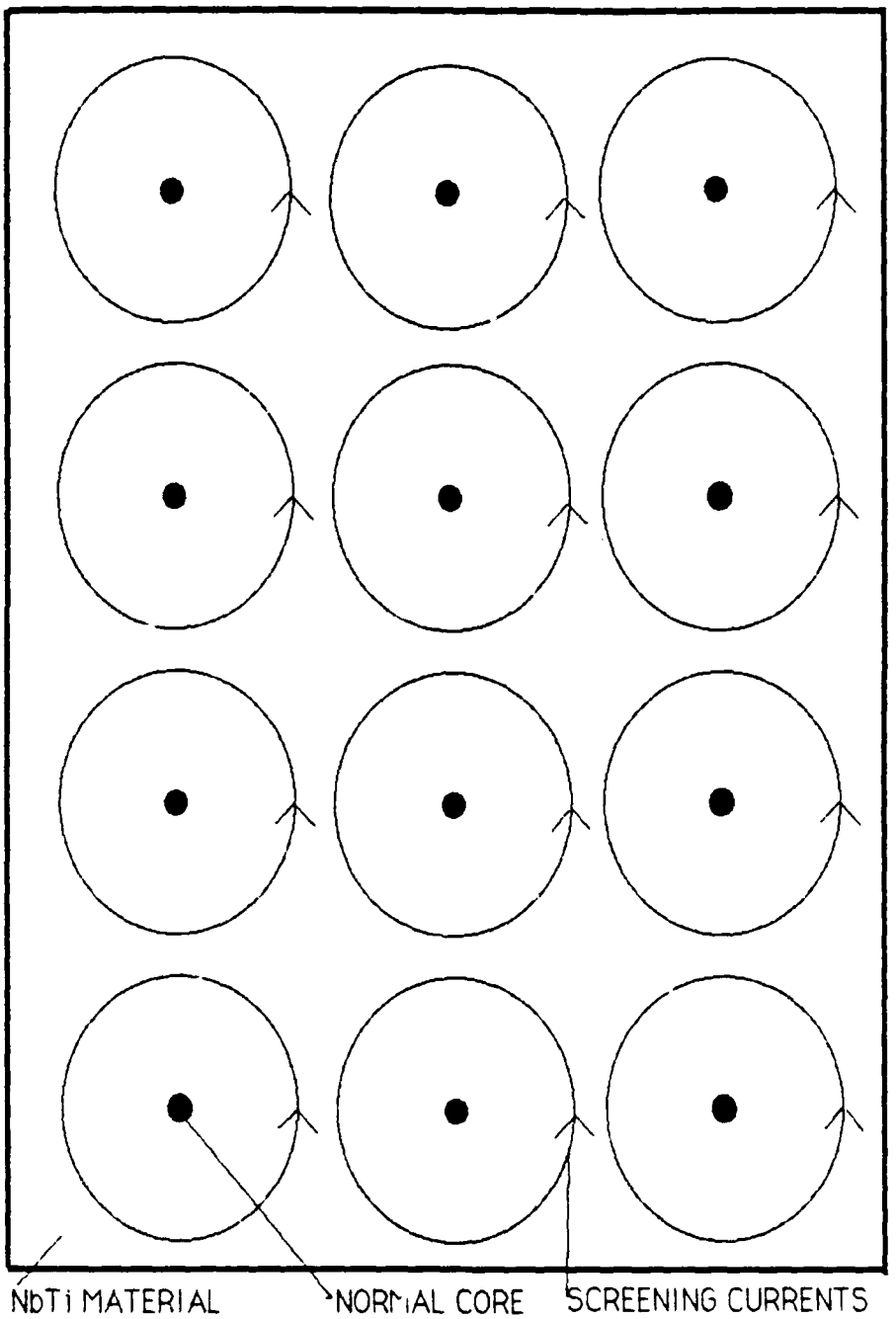

FIGURE 1.5 SCHEMATIC OF VORTEX TUBE PENETRATING NbTi MATERIAL

increase untill the applied field completely overlaps the vortex tubes and complete penetration occurs. This occurs where the applied field equals the upper critical field in Figure 1.4.

increase untill the applied field completely overlaps the vortex tubes and complete penetration occurs. This occurs where the applied field equals the upper critical field in Figure 1.4.

Temperature also effects the critical field. As the temperature of the superconductor is raised to the critical temperature the observed critical field decreases to zero. Figure 1.6 is a graph of the upper critical field verses temperature for NbTi material.

c. CRITICAL CURRENT

The critical current is the maximum current a superconducting material can carry. The critical current is dependent on temperature and applied field. Figure 1.7 is a graph of the interrelation of current density, temperature and magnetic field.

In an ideal superconductor the current in the superconducting wire generates a magnetic self field at the surface of the wire.In an ideal superconductor the critical current is simply the current at which the self-field at the surface equals the critical field. The self field plus the applied field equals the critical field. Therefore, as an external field is applied to the ideal superconductor the critical current is reduced in value.

However, for NbTi superconductors the critical current is much more difficult to determine. Since the upper critical field of NbTi is 12 Tesla, the critical current is limited by flux motion before the critical field is exceeded. The flux tubes experience a Lorentz force which moves the flux tubes at right angles to both the applied current and field. The Lorentz force on a flux tube is shown in Figure 1.8. The flux tube consists of a normal core surrounded by a circulating current that screens the magnetic field in the core from the rest of the superconducting material. When an

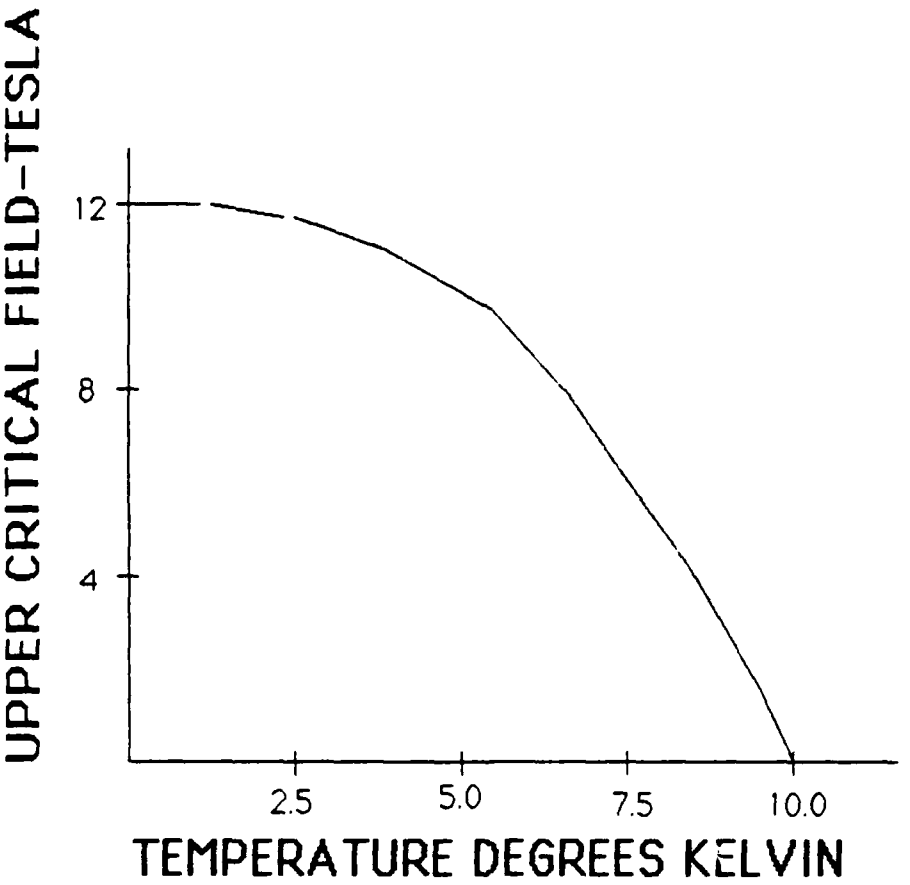

FIGURE 1.6 UPPER CRITICAL FIELD VERSES TEMPERATURE FOR NbTi SUPERCONDUCTOR

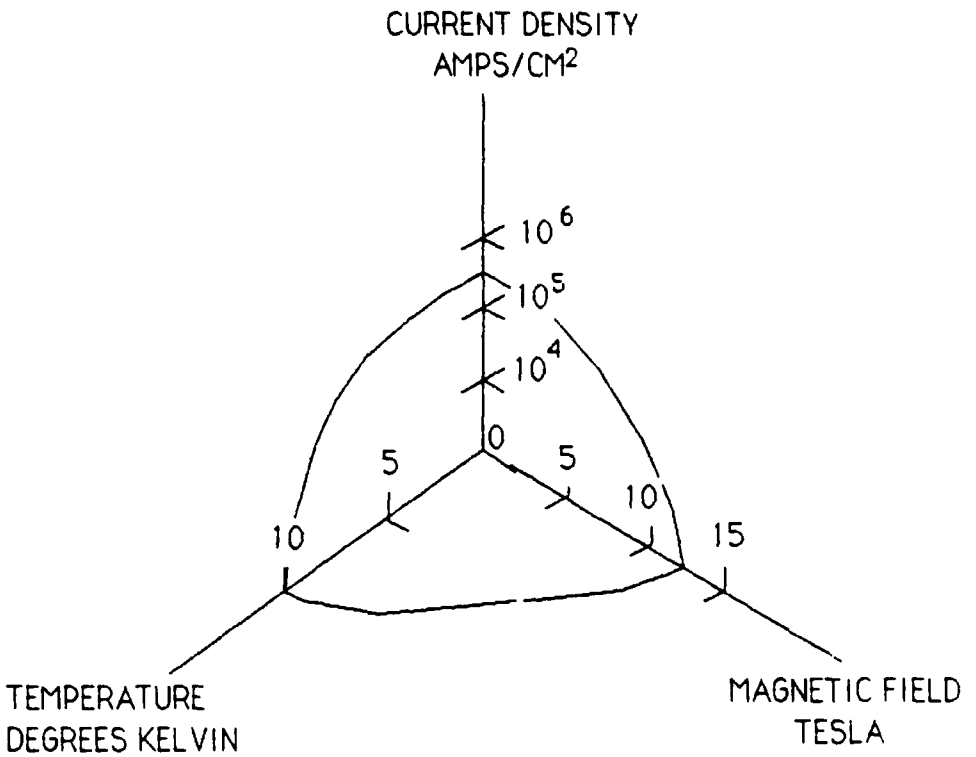

FIGURE 1.7 INTERRELATION OF CURRENT DENSITY, UPPER CRITICAL MAGNETIC FIELD AND CRITICAL TEMPERATURE FOR A NbTi SUPERCONDUCTOR

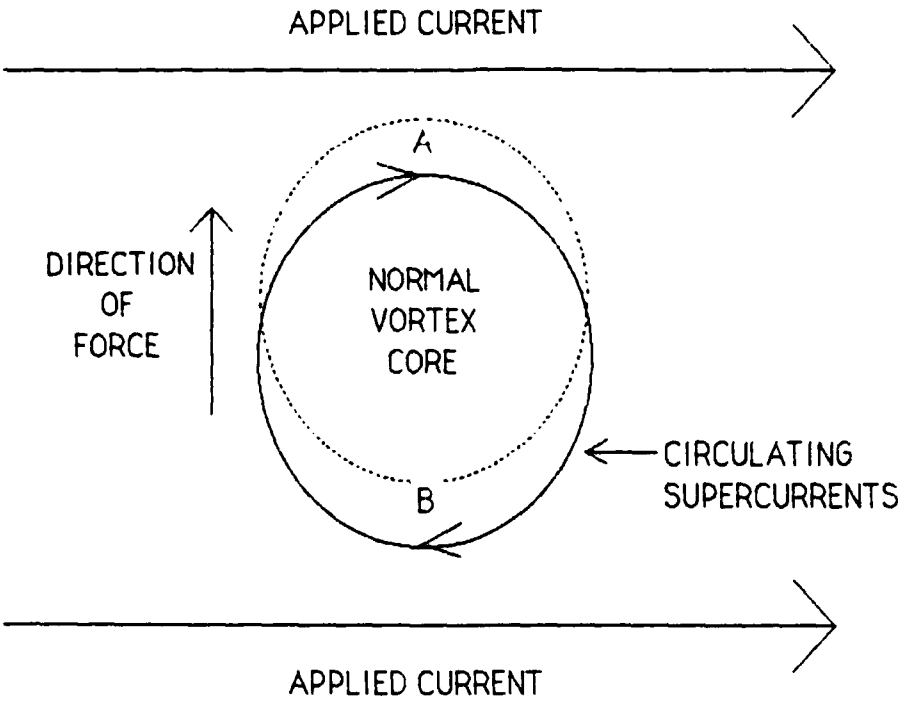

FIGURE 1.8 SCHEMATIC OF FORCE ON VORTEX

externally applied current is added to the circulating supercurrents of a vortex, the combination of the two currents exceeds the critical current of the superconducting material in region A and decreases the current below the critical value in region B. Therefore, region A which was initially superconducting is driven normal while region B,initially part of the normal core is driven superconducting. The Lorentz Force which moves vortices at right angles to the applied field and transport current dissipates energy which heats the superconductor. Also, the moving vortices induce an electric field which results in power dissipation. The heat generated raises the temperature of the superconductor above the critical temperature such that the NbTi is driven normal.

Vortex motion can be stopped by introduction of metallurgical defects into the material. These defects restrain motion of the vortices such that the NbTi can carry the required high current densities. Therefore, the critical current of NbTi is thus determined by the maximum pinning strength.

The critical current of NbTi is an extrinsic property that is dependent on the metallurgical history of the material. The previously discussed critical temperature and upper critical field values could be predicted with certainty because of there intrinsic atomic scale properties. However, the critical current values of NbTi can not be determined with any certainty and must be determined for each sample.

Cold working the impure NbTi materials is necessary to obtain the pinning forces necessary for the required high current densities of a superconducting magnet. Figure 1.9 is a schematic of critical current density verses magnetic field for a cold worked, heat treated, NbTi wire.

1.3 FABRICATION

In this section we will discuss fabrication of NbTi superconductors. The NbTi superconducting magnet must be faricated as a twisted multifilamentary composite. The twisted construction is necessary for

proper operation in the superconducting propulsion system. Stabilization against magnetic and mechanical disturbances is accomplished by dividing the superconductor into fine filaments and surrounding them with either an aluminum or copper stabilizing element. Ac losses are reduced by twisting and transposing the superconducting filaments. The filament is the building block for the NbTi composite. The filament diameter is usually less than 100 micro-meters and each filament has a twist pitch of about one turn per centimeter. As many as 10,000 of these filaments are combined inside a copper or aluminum matrix to make up a strand. The strand is then wound to produce the final coil form.

1.4 STABILITY

The superconducting coil of a shipboard propulsion system is inherently unstable. Magnetic or mechanical disturbances may locally heat the superconductor and drive the entire conductor into the normal state through a thermal runaway process (normally called a quench). This results from a large quantity of heat being liberated such that the superconductor coolant is vaporized at practical current densities. The quench begins when a magnetic or mechanical disturbance heats a small region of the superconductor so that it becomes resistive. Current then passing through this resistive region generates additional heat. This, in turn raises the temperature of more material and leads to more heating untill eventually the entire superconductor is driven normal. The copper or aluminum stabilizing elements prevent thermal runaway from becoming self sustaining. Sufficient stabilization material is used to carry the current should the superconductor be driven normal. In the event of a disturbance, the large amount of stabilizing material can momentarily handle the current while the liquid-helium refrigerant cools the superconductor back down below the critical temperature. A large magnet with a superconducting shunt that prevents thermal runaway is commonly referred to as a cryogenic stabilized magnet.

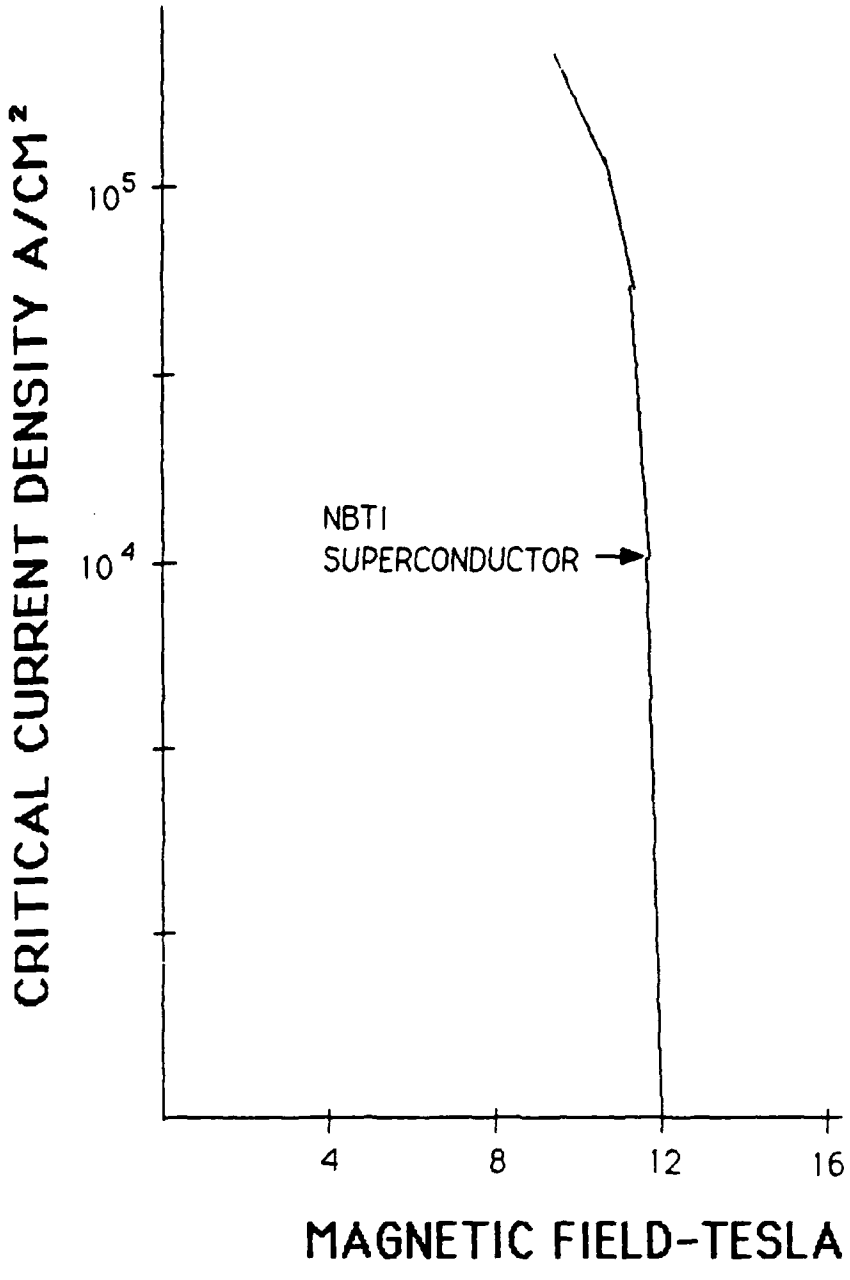

FIGURE 1.9 CRITICAL CURRENT VERSES MAGNETIC FIELD FOR NBTI SUPERCONDUCTOR

The designer of a superconductor propulsion system must decide on either full or limited cryogenic stabilization. With full cryostabilization, enough stabilizer is added so that the superconductor will recover from disturbances that would normally drive the superconductor normal. The major advantage of this stabilization technique is that the superconductor can handle about any type of disturbance expected during normal operation. The major disadvantage of full cryostabilization is that typically 10 to 20 times the superconductor must be added as stabilizing material. This leads to a very large and costly magnet.

With limited cryostabilization only enough normal conducting matrix material is added to stabilize the superconductor against disturbances of a specified limited size. If the maximum disturbance size can be predicted, then limited cryostabilization appears an attractive alternative.

1.5 AC LOSSES

AC superconducting machines produce losses that are unlike the DC superconducting machines that were discussed in the previous sections. Hysteretic loss is the most significant form of an AC loss. Filament size is directly related to hysteretic losses. The smaller the filament diameter, the smaller the hysteretic loss per unit volume. The problem is that filaments cannot be fabricated uniformally below about 1 micrometer in diameter. Therefore, a lower limit is set on the magnitude of the hysteretic losses when designing a superconducting propulsion system.

1.6 MECHANICAL PROPERTIES

The mechanical properties of superconductors must also be considered when designing a superconducting shipboard propulsion system. Superconductors are subjected to substantial stresses. Fabrication stress, thermal-contraction stress, and magnetic stress are the three primary types of stresses. Fabrication stress occurs in construction when the superconducting wire is subjected to bending stress as it is wound into the magnet coil and to uniaxial stress from pretensioning of the wire during

the winding operation. Thermal-contraction stress occurs when different materials of the magnet structure are cooled to cryogenic temperatures. The magnetic stress occurs when the superconducting winding is energized. The Lorentz force acting on a magnet can be very large and is a major issue to the designer of a superconductor propulsion system.

CHAPTER 2
SUPERCONDUCTING COIL DESIGN,CONSTRUCTION,AND EXPERIMENTAL TEST

2.1 INTRODUCTION

The objective of this section is to determine the performance and quench behavior of a Nb-Ti superconducting coil and access the feasibility of application to a superconducting shipboard propulsion system . Several other type 2 superconductors were examined such as Nb3Sn, V3Ga, Nb3(Al-Ge) and Nb3Ge. The critical field intensity of Nb3Sn is higher than the field of intensity of Nb-Ti, but unlike Nb-Ti they are brittle compounds rather than ductile alloys. Also, V3Ga, Nb3(Al-Ge) and Nb3Ge have high critical field intensities that are needed for a high field superconducting magnet. However,a practicle fabrication technique has not yet been demonstrated .In addition, the high temperature superconducting ceramics that operate in the liquid nitrogen cooling range are brittle and difficult to manufacture into coil shapes . Therefore, Nb-Ti (operates in the liquid helium cooling range) was selected as the alloy to be used in the design of the superconducting test coil.

Copper was selected as the stabilizing element to provide protection to the superconductors in the event of a quench. Aluminum is an another possibility and is expected to provide an increase in magnetic stability. However, compared to copper, aluminum matrix material is much more difficult to combine with the Nb-Ti superconductor. Stability of an aluminum-stabilized Nb-Ti superconducting magnet will be discussed in chapter 3. (Waltman , D. J. , McDonald , F. E. , Superczynski , M. J. , 1988)

2.2 SUPERCONDUCTING COIL CONSTRUCTION

a. COIL CONSTRUCTION PROCEDURE The objective in the construction phase is to produce a mechanically rigid composite that is magnetically stable. The Nb-Ti wire is fully potted and reinforced with

fiber glass cloth to produce the rigid composite. This is necessary to prevent relative conductor motion that could lead to frictional heating and a magnetic quench . The disadvantage of the fully potted coil is that large stresses can develop during magnet construction and cool-down to the liquid helium temperature of 4.2K. These stresses represent stored energy which can be released when the magnet is energized . If the strain energy developed by the magnetic hoop force exceeds the failure limit of epoxy, the epoxy will crack and a quench will occur due to the local temperature rise that will develop. A sufficient amount of copper stabilizing material must be used with the Nb-Ti to dissipate the energy stored in the magnetic field of the coil during a quench. The cross sectional view of the test coil used for the experiment(Waltman , D.J.,1988) is shown in Figure 2.1. Heaters, thermocouples, and strain gauges are installed at various winding locations such that the electrical and thermal behavior of the magnet can be measured during the quench period. The dimensions of the coil are 61.21-cm I.D.,68.43-cm O.D., and 15.24-cm length. The coil contains 46 layers of winding and has a total of 7,502 electrical turns of copper stabilized Nb-Ti superconducting wire and a total inductance of 49 henries. The superconducting wire contains 168 filaments of Nb-Ti superconducting wire having a twist pitch of 1.69 cm and has a copper to superconductor cross-sectional area ratio of 2 to 1. The wire is rectangular in cross section, has overall dimensions of 0.660 by 0.914 mm, and is coated with Formar insulation approximately 13-microns thick. Figure 2.2 shows the superconducting magnet winding coil form and potting chamber. A lathe mechanism equipped with a variable speed reversible motor was used to turn the coil to wind the test coil. Tension in the wire is developed by applying reverse torque to the wire supply reel through a controllable hysteresis clutch that is mechanically attached to the supply reel. The clutch is driven by a fractional horsepower motor. A cleansing assembly consisting of a liquid freon jet stream and several felt wiping pads is used to clean the wire during the coil winding process. A diagram of the superconducting coil winding system is shown in Figure 2.3. During the coil construction procedure three layers of 0.089-mm- thick fiber glass cloth is wound onto the coil form mandrel. Each layer of fiber glass cloth

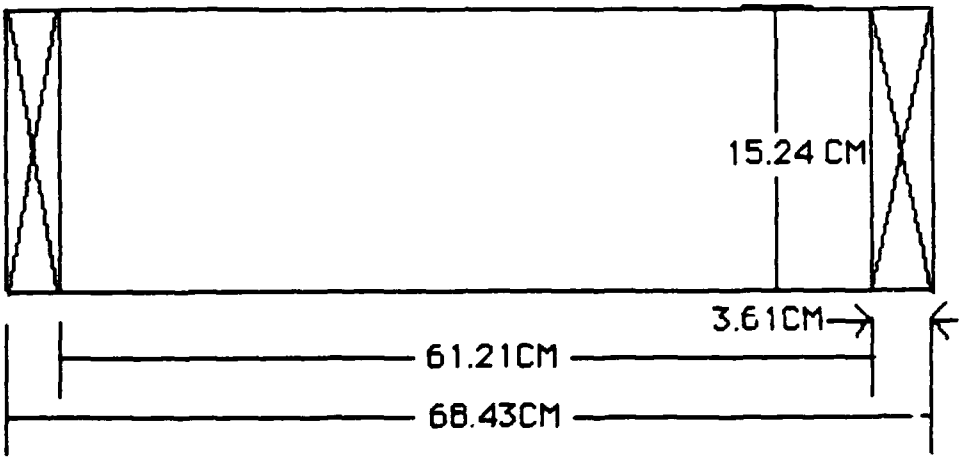

FIGURE 2.1 CROSS SECTIONAL VIEW OF SUPERCONDUCTING TEST COIL(Nb-Ti)

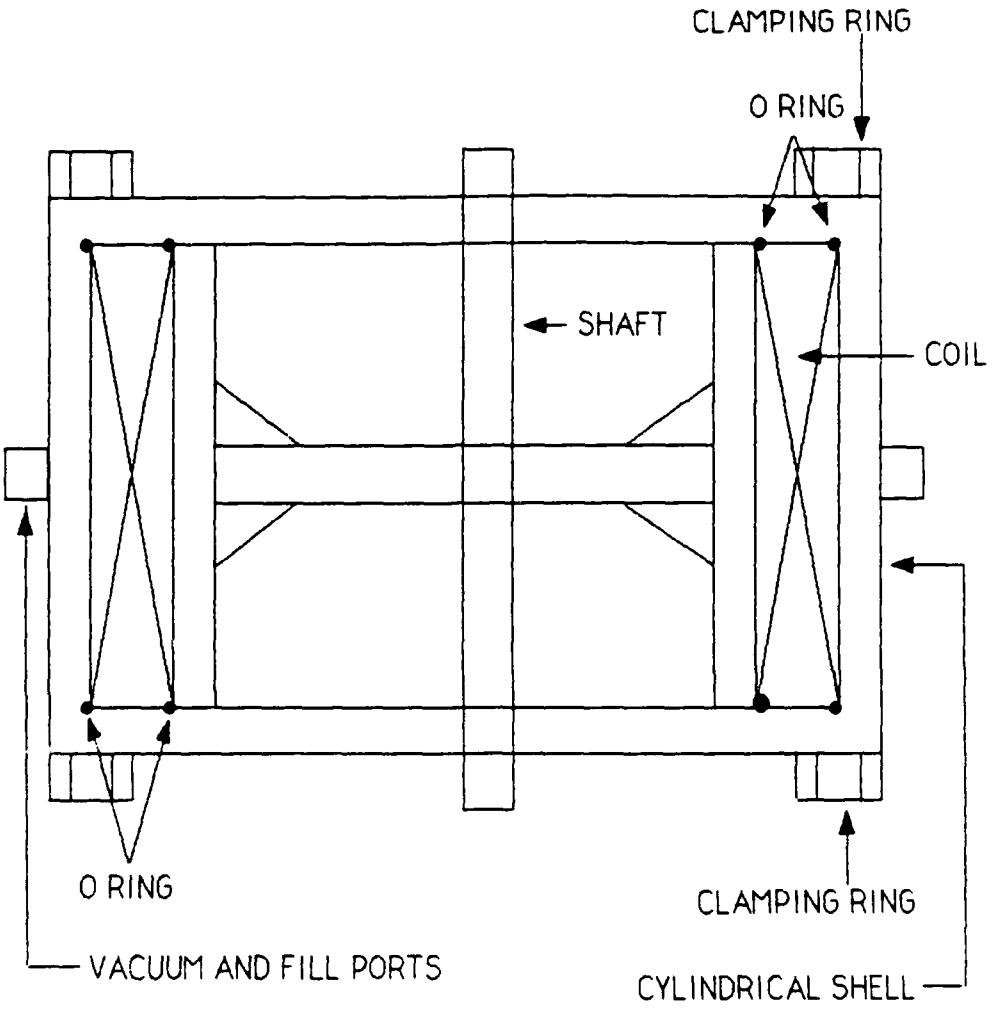

FIGURE 2.2 0.61-METER SUPERCONDUCTING MAGNET WINDING COIL FORM AND POTTING CHAMBER

FIGURE 2.3 SUPERCONDUCTING COIL WINDING SYSTEM

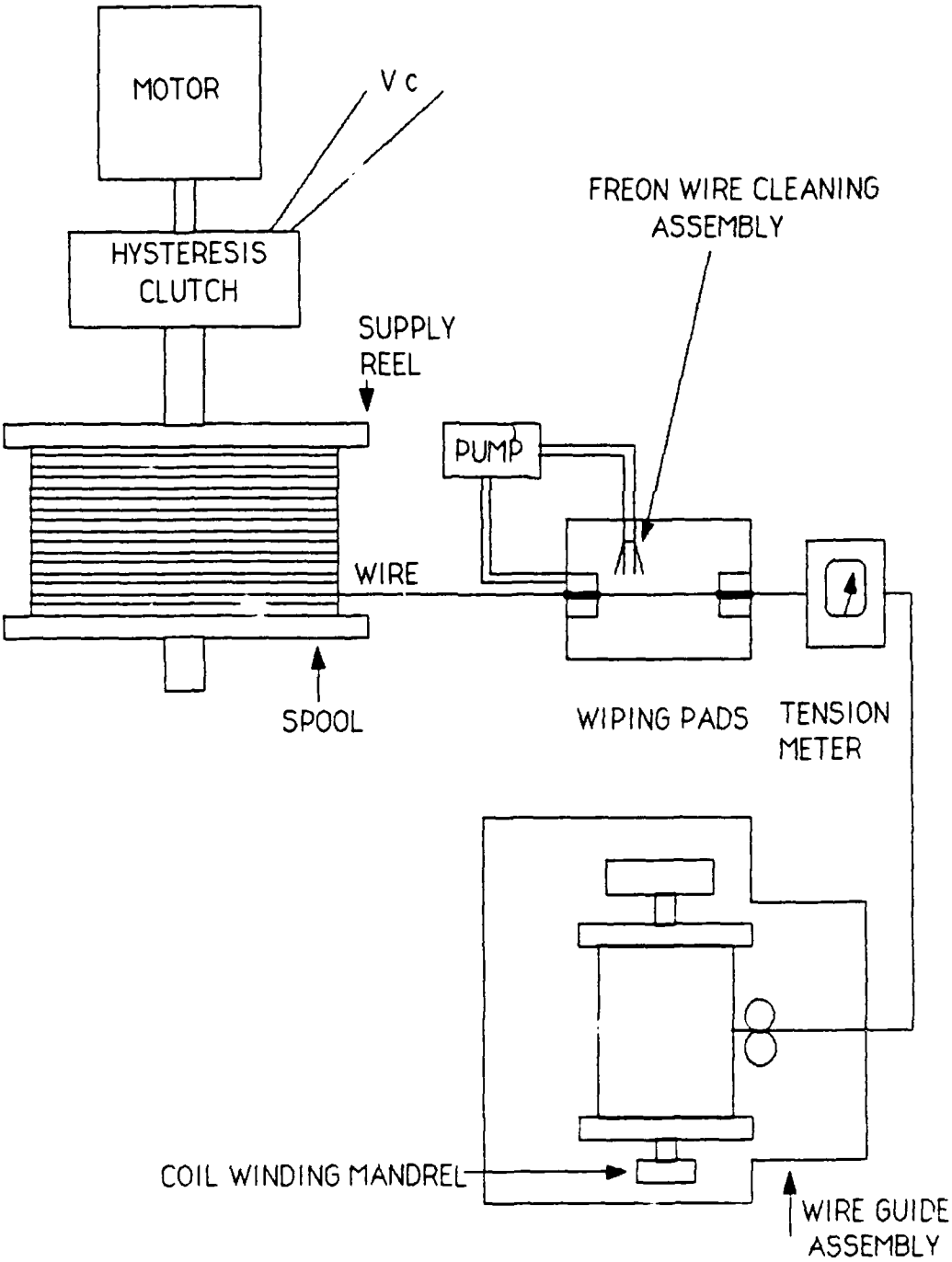

is made with an individual strip of cloth of sufficient length to completely cover the circumference of the mandrel with approximately a 0.635-cm overlap at the ends. The widths of the cloth layers were selected to allow coverage of the sides and outer circumference of the completed winding with a 0.635-cm overlap at the center line of the outer coil surface. This complete coverage of the entire surface of the wound coil is necessary to provide continuous reinforcement of the magnet. After the initial layers of fiber glass cloth were wound on the mandrel, a layer of superconducting wire was wound over the fiber glass base. The input electrical lead and the first electrical turn of the coil are of soldered double wire construction. The last electrical turn and exit lead of the completed winding are also of soldered double wire construction. The soldered double wire construction is to ensure electrical and mechanical integrity and performance for these leads. They are subjected to mechanical abuse during magnet construction and operation. After the first layer of the winding, a layer of 0.089-mm-thick fiber glass cloth was wound onto the winding layer. Then, the next layer of wire was wound over the layer of cloth. This winding procedure was continued with alternate layers of wire and cloth for a total of 46 layers and 7,502 turns. The outer surface of the wound coil was then wrapped with multiple layers of 0.089-mm-thick fiber glass cloth to provide an external hoop force restraint member and protection for the outer layer of superconducting wire. A single length of wire was not sufficient to complete the winding of the coil. The coil winding was spliced at the first turn of layer 42. The wire used to complete the winding was identical to and and manufactured from the same billet as the wire of the first 42 turns. The winding was spliced over one complete turn of the coil with the two wires soldered together on their sides. A one turn splice was selected to allow the ends of two superconducting wire to butt with a minimum void in the coil. The ends of the two wire splice were electrically insulated with varnish to eliminate the possibility of a shorted turn.

b. SUPERCONDUCTING COIL INSTRUMENTATION

Wire heaters, thermocouples and strain gauges were located at various positions about its inner bore and outer surface during the winding of the test coil. Table 2.1 shows a table of test coil instrumentation while Figure 2.4 shows a test coil instrumentation location diagram. The heaters, thermocouples, and strain gauges located on the inner bore of the magnet were installed directly in physical contact with the first layer of superconducting wire. The heaters, thermocouples and strain gauges located on the outer surface of the magnet were placed on the first layer of fiber glass cloth that covers the last layer of wire. One thickness of cloth physically separates the heaters and sensors from the final layer of magnet winding.

Heaters were installed at each of the instrumentation set locations. They were designated H1 through H9. They have dimensions of 25.4 mm in length and 0.127mm in diameter. The current leads for the heaters were made with small diameter copper wires. The wires were twisted together and run, perpendicular to the winding, up along the surfaces of the inner bore (H1, H2, H3) and outer circumference (H7, H8, H9) ,exiting the magnet structure on the same coil end as the current leads of the magnet. In Figure 2.4 the current lead end of the magnet is designated the top of the coil. One copper-constantan (type T) thermocouple, and one gold-chromel (typeK) thermocouple were installed near each heater. The physical locations of each thermocouple is given in Table 2.1. The thermal reference junctions for both the copper-constantan and gold chromel were established at liquid helium temperatures of 4.2K.

Strain gauge sensors were located on the inner and outer circumference of the coil at locations S4, S5, S6, and S10, S11, S12, as shown in figure 2.4. The locations of the strain gauges are also shown in Table 2.1. There were two sensing sections for each strain gauge. One sensing section was orientated parellel to the wire of the coil. The other wire was orientated perpendicular to the wire.

TABLE 2.1 TEST COIL INSTRUMENTATION

Set Number	Clock Location	Instrumentation Axial Dist(CM)	Instumentation Description
H1	3:30	H: 5.56, T:5.87, K:4.92	Inner Bore, 1 Heater, 1 Type T and 1 Type K Thermocouple
H2	12:00	H:6.83, T:7.14, K:6.51	1 Heater, 1Type T and 1Type K Thermocouple
H3	8:15	H:7.30, T:7.46, K:6.98	1 Heater, 1Type T and 1 Type K Thermocouple
S4	2:00	6.83	1 Strain Gauge
S5	10:30	6.98	1 Strain Gauge
S6	5:15	6.98	1 Strain Gauge
H7	12:00	H:7.78, T:8.09, K:7.46	Outer Surf, 1Heater, 1Type T, and 1 Type K Thermocouple
H8	3:30	H:7.78, T:8.09, K:7.46	Outer Surf, 1 Heater, 1 Type T and 1 Type K Thermocouple
H9	8:30	H:7.62, T:7.93, K:7.30	1Heater, 1 Type T and 1Type K Thermocouple
S10	2:00	7.62	1 Strain Gauge
S11	6:00	7.62	1 Strain Gauge
S12	11:00	7:30	1 Strain Gauge

* See Table 2.1

Type T-copper/ constant thermocouple; type K-gold chromel thermocouple

***H=heater location in cm; J= type thermocouple location in cm; type K thermocouple location in cm. +Top of coil is defined as the coil end at which the current leads enter and exit the coil.

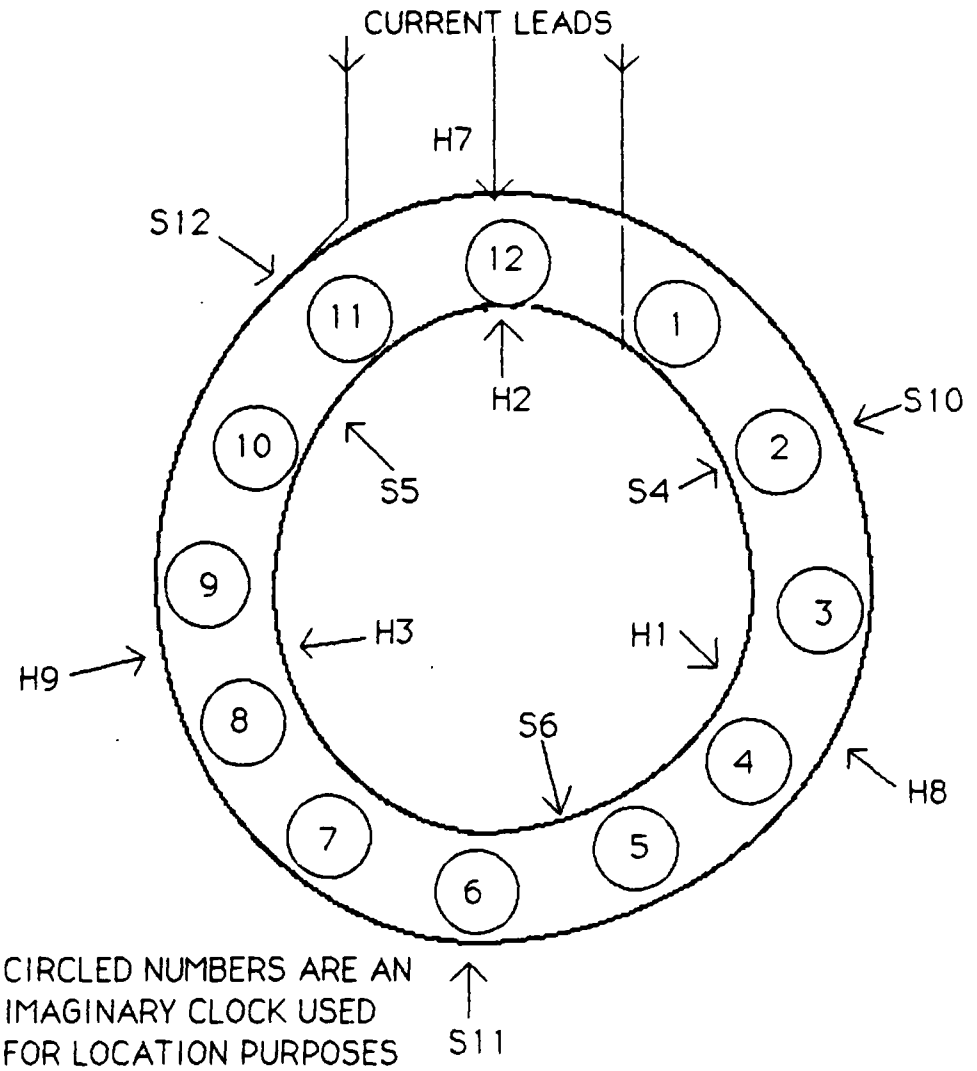

TOP VIEW

FIGURE 2.4 SUPERCONDUCTING COIL INSTRUMENTATION LOCATION DIAGRAM

c. TEST COIL POTTING PROCEDURE

Potting of the superconducting coil was performed after winding of the superconducting test coil. Figure 2.2 shows the cylindrical shell of the potting chamber while Figure 2.5 shows the test coil potting chamber assembly. Figure 2.6 shows the coil and potting chamber that was used to maintain the coil at a temperature of 65 degrees Celsius during its potting process. The epoxy used to impregnate the coil consists of Ciba 6004 epoxy resin and Lindride 12 and Lindride 16 hardner mixed in equal parts. The proportions of resin and hardener are100 parts to 85 parts by weight, respectively. The epoxy components were initially heated to 65 degrees Celsius. The solution was degassed to a pressure of 40 microns and then piped into a coil potting chamber which has been evacuated to a pressure of approximately 10 microns. Once the epoxy was transferred into the assembly, the pressure was increased to 100 psi by using nitrogen gas to force the impregnant into the winding coil. The potting conditions of 65 degrees Celsius and 100 psi were maintained for a period of 20 hours to cure the epoxy. Figure 2.7 shows a picture of the test coil after the excess epoxy has been removed.

A cylindrical retaining ring was fitted over the outer surface of the test coil to provide additional mechanical restraint to the composite of the coil. The ring must withstand the action of the large magnetic forces produced in the magnets winding. A schematic of the retaining ring is shown in Figure 2.8. Figure 2.9 shows a schematic of a circular disc fabricated from 0.635-cm thick aluninum alloy. This device was attached to the bottom end of the outside cylindrical ring. Figure 2.10 shows a schematic of a circular disc that is attached to the top end of the cylindrical retaining ring. This disc was fabricated from a 0.635-cm-thick, laminated, fiber glass sheet. In addition, the disc provides a mounting platform for the instrumentation terminal boards used for connecting the electrical leads of the coil heaters and sensors

FIGURE 2.5
TEST COIL POTTING CHAMBER ASSEMBLY

FIGURE 2.6
COIL AND POTTING CHAMBER THAT WAS
USED TO MAINTAIN THE COIL AT A TEMPERATURE
OF 65 DEGREES CELSIUS DURING THE POTTING PROCESS

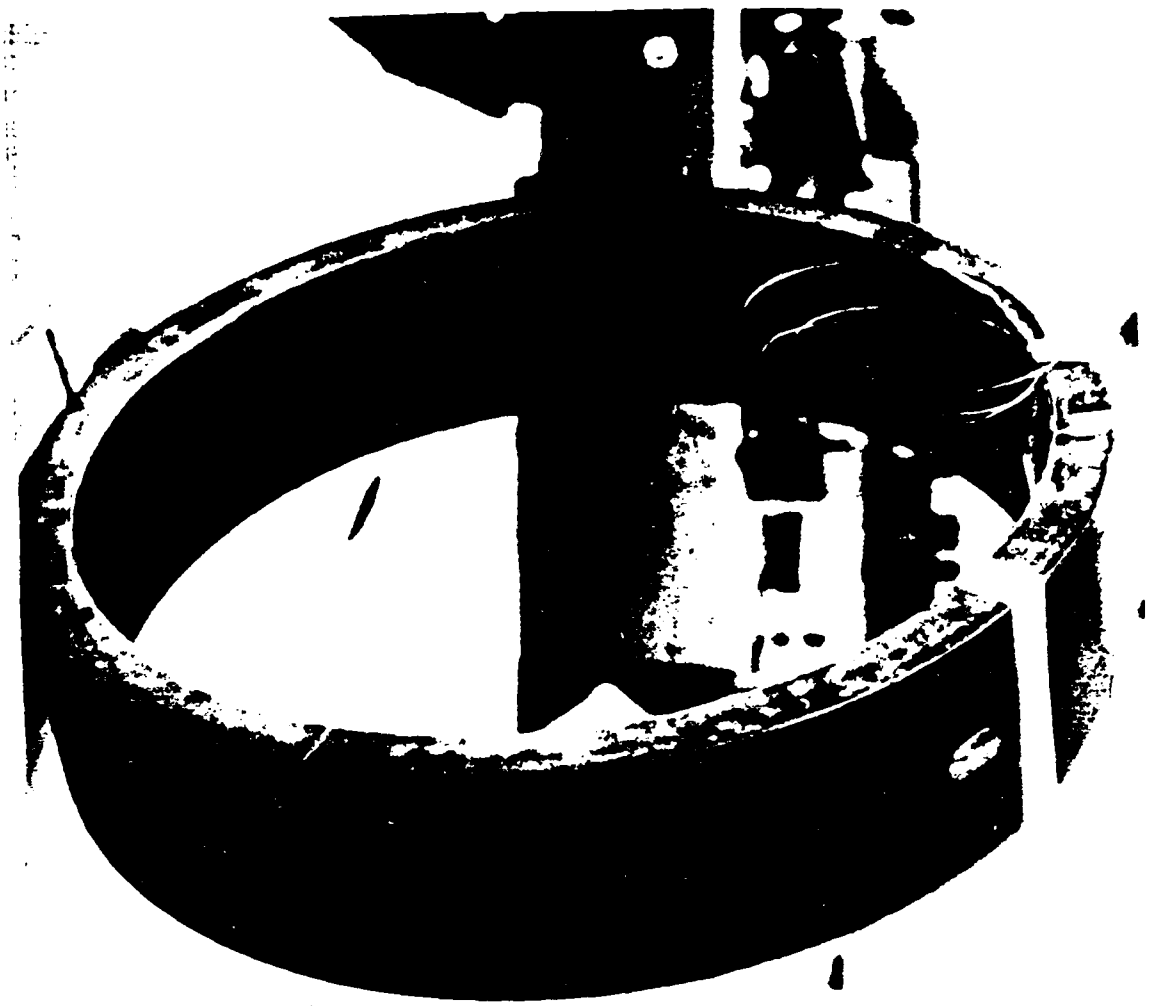

FIGURE 2.7
PICTURE OF TEST COIL AFTER EXCESS
EPOXY HAS BEEN REMOVED

FIGURE 2.8
SUPERCONDUCTING TEST COIL
CYLINDRICAL RETAINING RING

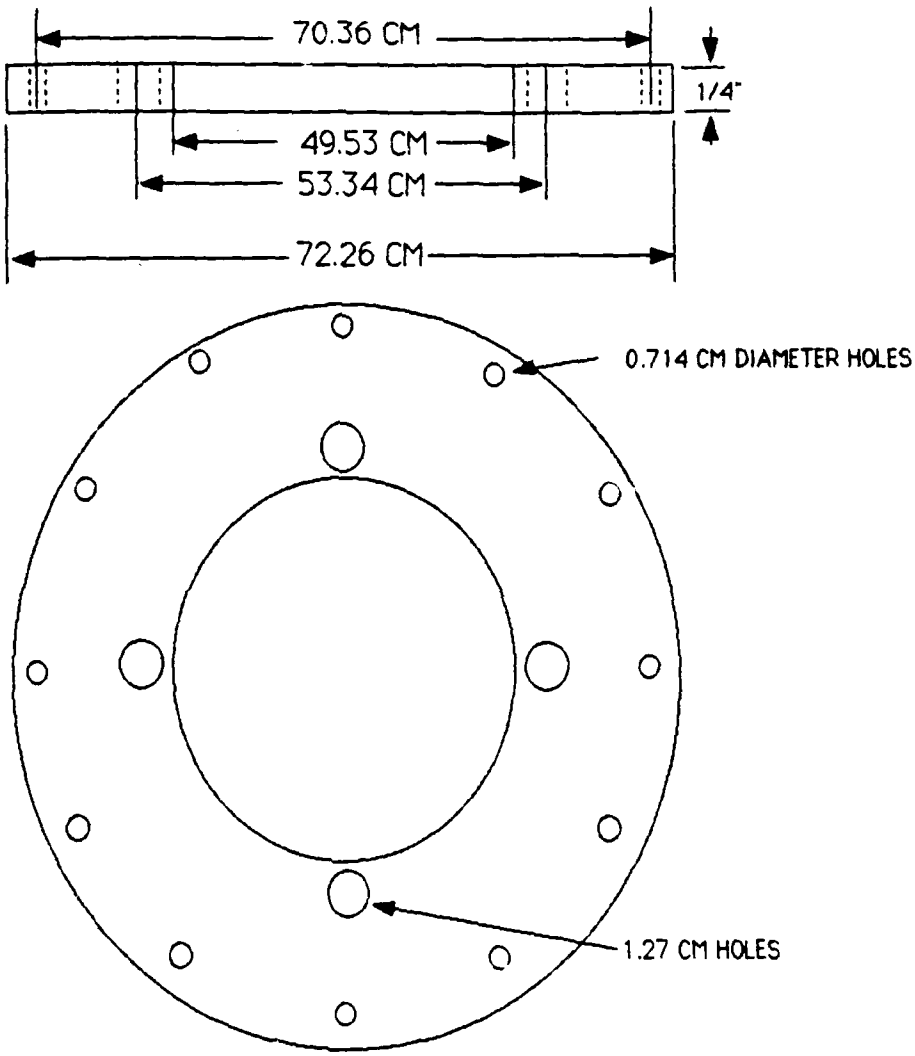

6061 ALUMINUM ALLOY

FIGURE 2.9 LOWER COIL SUPPORT DISK

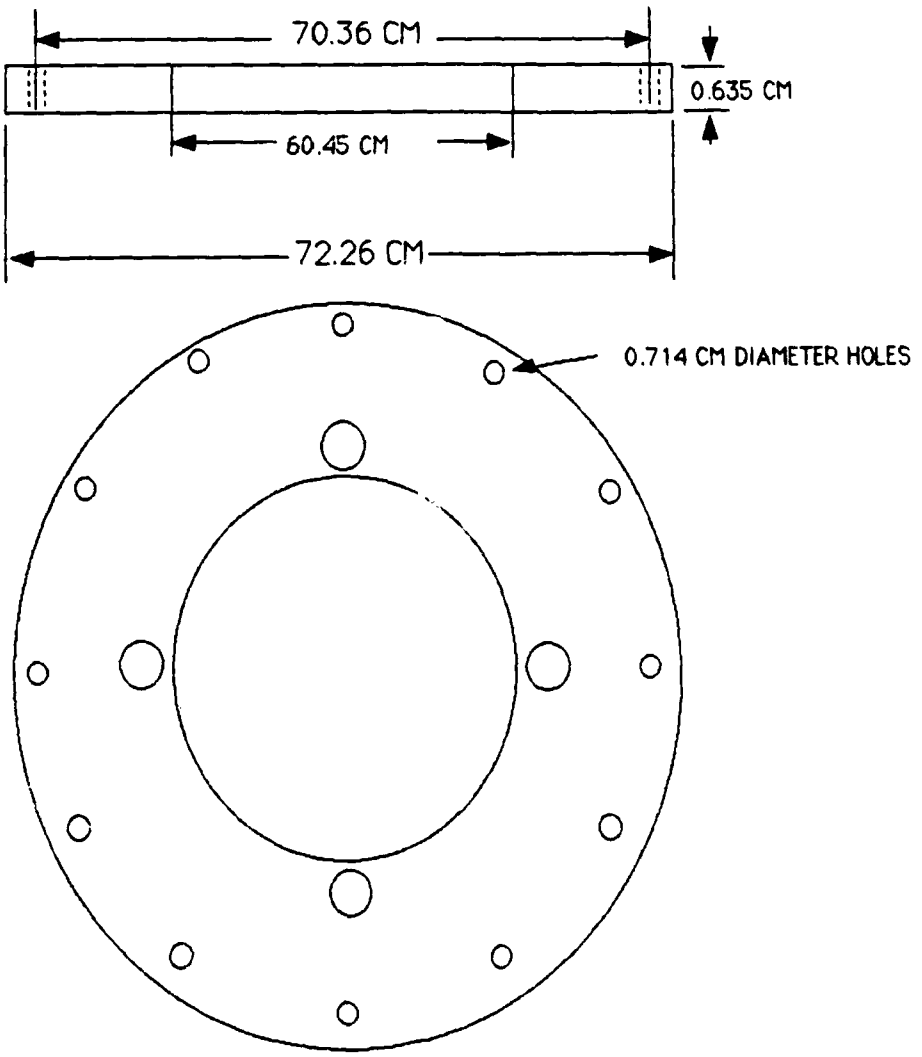

LAMINATED FIBER GLASS

FIGURE 2.10 UPPER COIL DISK

to the control and data acquisition cables of the laboratory test equipment. Figure 2.11 shows the completed test coil assembly.

The current leads of the test coil winding (soldered double superconducting wires) were soldered in parellel with a 1.59-cm-wide length of copper braid. This parallel combination, 0.91-m in length for each lead, starts at the point where the winding leads physically exit the magnet composite and terminates above the coil at a pair of vapor cooled leads. The purpose of the braided material is to improve current transfer from the ventilated copper rod vapor-coiled current leads to the superconducting magnet wire.

2.3 LABORATORY MEASUREMENTS

A superconducting magnet power supply having a maximum output current capacity of 180 amperes is used to energize the test coil in the dewar assembly of Figure 2.11. The magnet load line for the 0.61-m test coil and its conductor short sample characteristics are shown in Figure 2.12. From the figure the maximum critical point is shown as 6.5 tesla and 190 amperes.

A pulse generator and current amplifier were used to deliver a current pulse of known energy to the heater selected to initiate a quench of the magnet. The system used for the experiments consists of a multiple-channel strip chart recorder used to measure and record the magnet operating current and the winding temperatures of the magnet.

Table 2.2 shows the test runs used to measure the performance and quench behavior of the 0.61-m superconducting test coil. Preliminary tests were conducted at operating currents of 30 and 75 amperes to verify magnet and data acquisition system operation.

During run no. 1, the magnet suffered damage to its winding and quenched when energized to a current of 30 amperes as indicated in Table 2.2. The magnet coil was found to contain several resistive

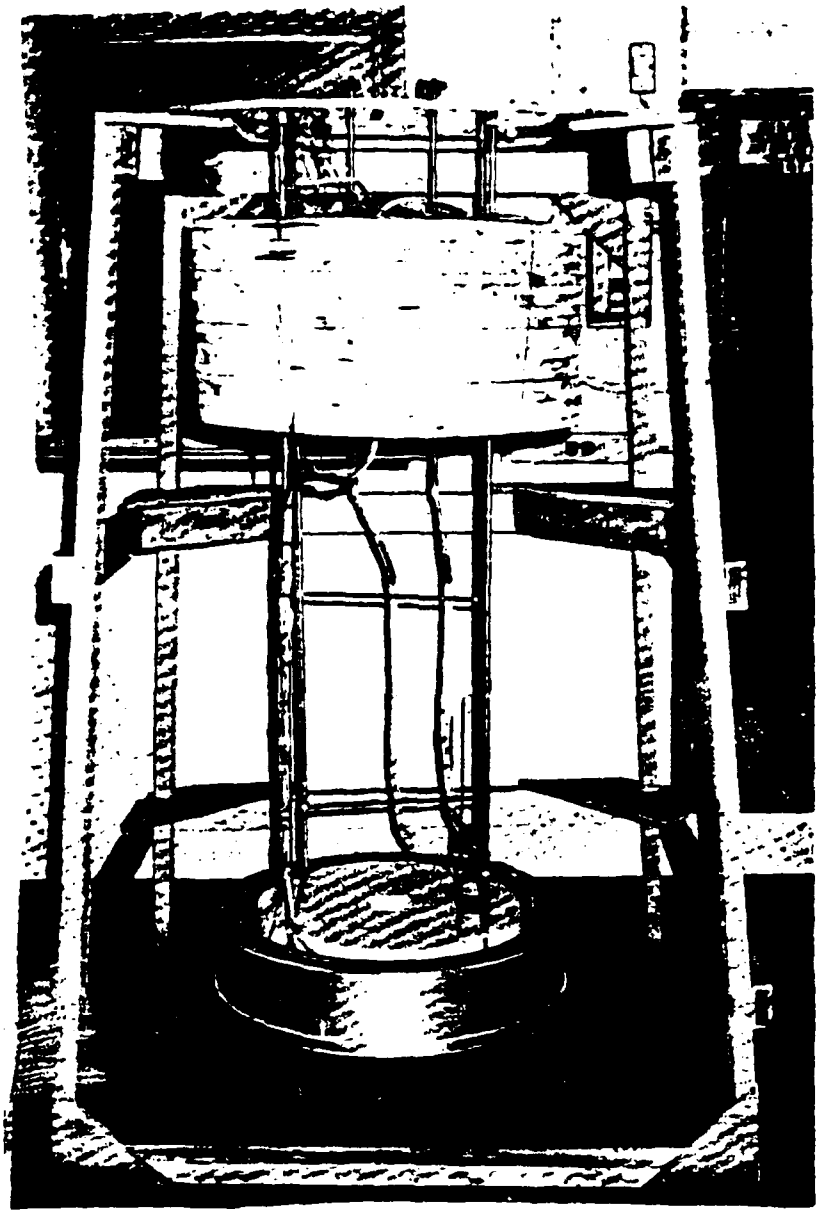

FIGURE 2.11
COMPLETED TEST COIL AND SUPPORT SYSTEM

FIGURE 2.12 SUPERCONDUCTING MAGNET LOAD LINE AND CONDUCTOR SHORT SAMPLE

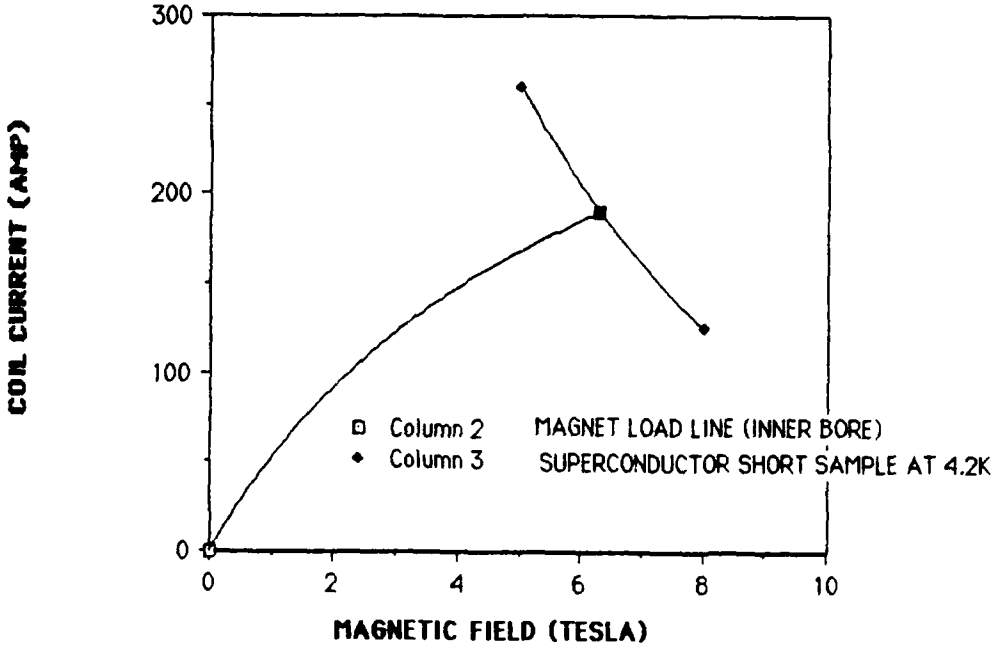

TABLE 2.2 SUPERCONDUCTING MAGNET SUMMARY OF RESULTS

Run No.	Coil Current Amps	I/Ic	Store Energy (Joules)	Heater Location No.	Energy To Quench (Joules)	Max Temp Rise (K)	Time Constant (sec)	Max. Coil Voltage (kV)
1	100	0.3	245,000	H2			1.5	2.7
2	100	0.3	245,000	H1	2.5E-3	45	1.5	2.7
3	120	0.4	353,000	H1	1.2E-3	54	1.3	3.9
4	129	0.45	408,000	H1	1.1E-3	62	1.14	5.2
5	135	0.5	447,000	H3	6.1E-4	88	1.04	5.4
6	150	0.6	551,000	H3	4.0E-4	99	0.92	6.6

Run No.	Comments
1	Heater to thermocouple short occured such that magnet suffered damage.
2	New Heater H1 installed. However, poor thermocouple to Superconducting test coil contact occured.
3	Bad results due to poor thermocouple contact.
4	This run had heater failure, magnet damage and poor thermocouple contact.
5	Improved thermocouple contact.
6	Operating current of 150 Amps is 80% of maximum magnet load line current.

winding shorts at various locations in the first two winding layers of the magnet. The shorts were the result of wire insulation damage that apparentely occured during superconducting coil construction. After repairing the system, runs 2, 3, and 4 were performed. After run 4 the winding again develop a short. The winding short was located in the first layer of winding at the location of heater H1. A failure of the power transistor in the pulse amplifier connected to heater H1 caused a high value of current to flow through the heater wire, causing it to overheat and burn out. This, burned the insulation of the superconducting wire, and an electrical short developed between two adjacent turns at the heater location. The coil was repaired by electrically removing the shorted turn from the winding. During the first coil repair, it was observed that heaters installed at locations H1 and H2 had pulled away from the surface of the inner bore. The poor thermal contact condition was corrected and the magnet was then successfully operated and purposely quenched using heater H3 for test runs 5 and 6 at operating currents of 135 and 150 amperes, respectively. The evaluation was completed with test run 6. The magnet operating current of 150 amperes represents a value along the load line that is 80% of critical current and field. This is the normal operating design point for a potted superconducting magnet. A plot of the measured coil currents for magnet quenches for runs 1 through 6 is shown in Figure 2.13.

2.4 LABORATORY MEASUREMENT RESULTS

The experimental results of the superconducting coil are shown in Table 2.2. The time constants decrease as the operating current increases. The time constant is the time for the operating current to drop to 36.79% of its initial value. Higher operating currents correspond to higher values of stored energy. The results are as expected since almost all of the stored energy in the magnetic field is dissipated in the copper matrix material of the magnet's superconducting wire. The resistance in the winding increases as the level of stored energy increases. This results in a shorter current decay time constant. Table 2.2 also shows the increase

FIGURE 2.13 MEASURED COIL CURRENT FOR QUENCHES INITIATED AT VARIOUS OPERATING CURRENTS

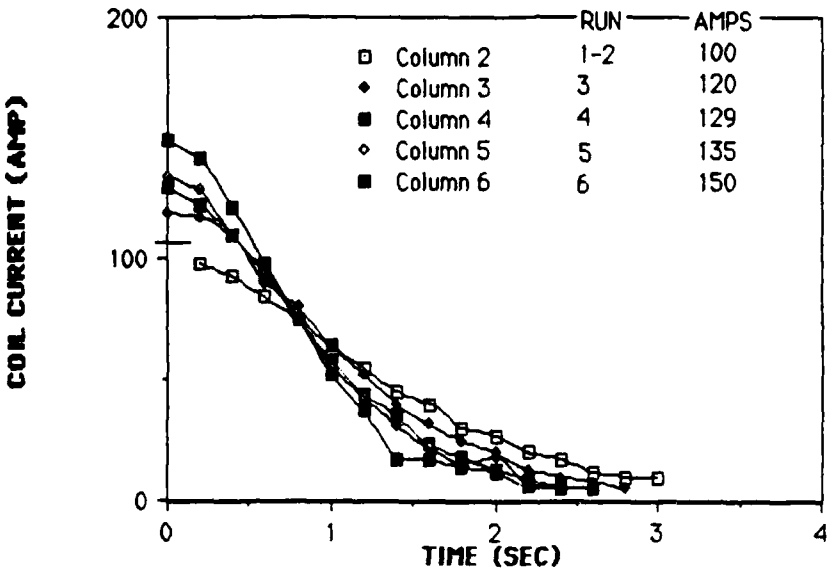

in measured coil winding temperature for increasing levels of magnet stored energy. During runs 2, 3, and 4 the thermocouples were in poor thermal contact with the windings and this abnormal condition was reflected in the temperature measurements. However, thermal contact was satisfactory during runs 5 and 6. The design limit for potted superconducting coils is normally 100 degrees kelvin. The superconducting test coil experienced a maximum temperature rise of 99 degrees kelvin when quenched at an operating current of 150 amperes.

2.5 COMPUTER PROGRAM RESULTS

A computer program was developed by Robert Lari of the Argonne National Laboratory to analytically determine the quench behavior of the 0.61 meter superconducting test coil. Table 2.3 is a summary of the computer program results for the 0.61 meter superconducting test coil. Figure 2.14 is a plot of the superconducting currents during a computer simulated quench. These results were obtained for a quench initiated at the inner bore of the coil at each of the operating currents of Tablle 2.2 and Figure 2.14. A comparison of the computer quench results of Table 2.3 with the measured results of Table 2.2 shows that the time constant of the current decay is less for the computed results for each of the operating currents. For all runs, the peak internal voltage developed within the windings is greater for the simulated results than for the measured results. Figure 2.15 and Figure 2.16 show quench plots of both the measured magnet currents and computerized magnet currents during conditions of 100 and 150 amperes, respectively. As can be seen from Figures 16 and Figures17 the time for the current to decay from its initial value to a 36.78 % value is 0.12 seconds less for the Quench computer program than the measured results. An operating current of 100 amperes was used to quench the coil. When the quench current was increased to 150 amperes the quench current decay was found to be 0.16

FIGURE 2.14 COIL QUENCH COMPUTER RESULTS

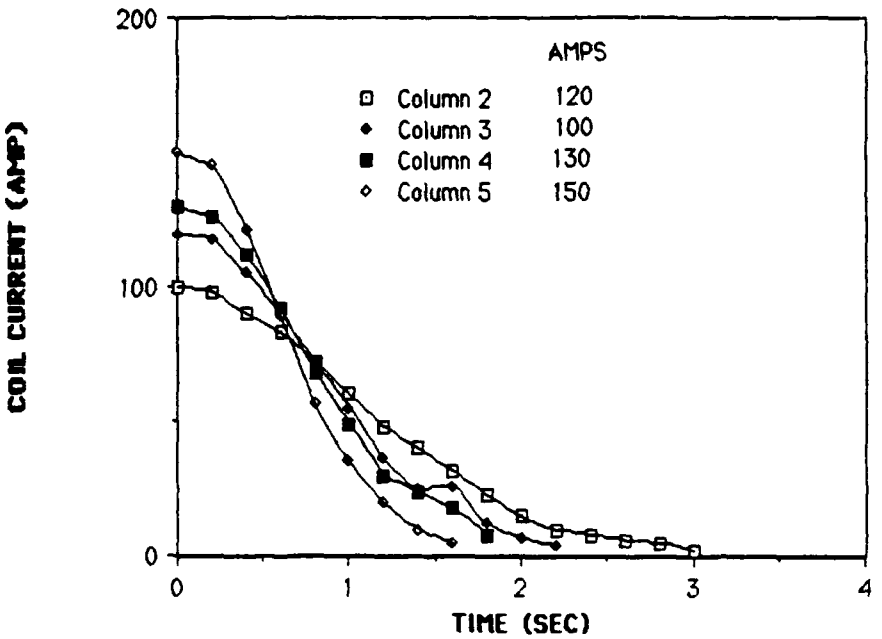

FIGURE 2.15 MEASURED VERSES QUENCH COMPUTER PROGRAM RESULTS AT 100 AMPS

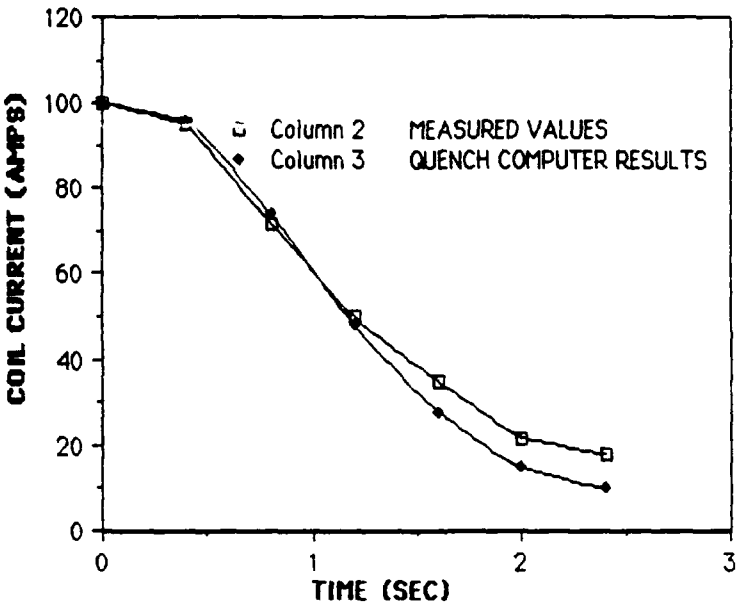

FIGURE 2.16 COMPARISON OF MEASURED AND QUENCH RESULTS AT 150 AMPS

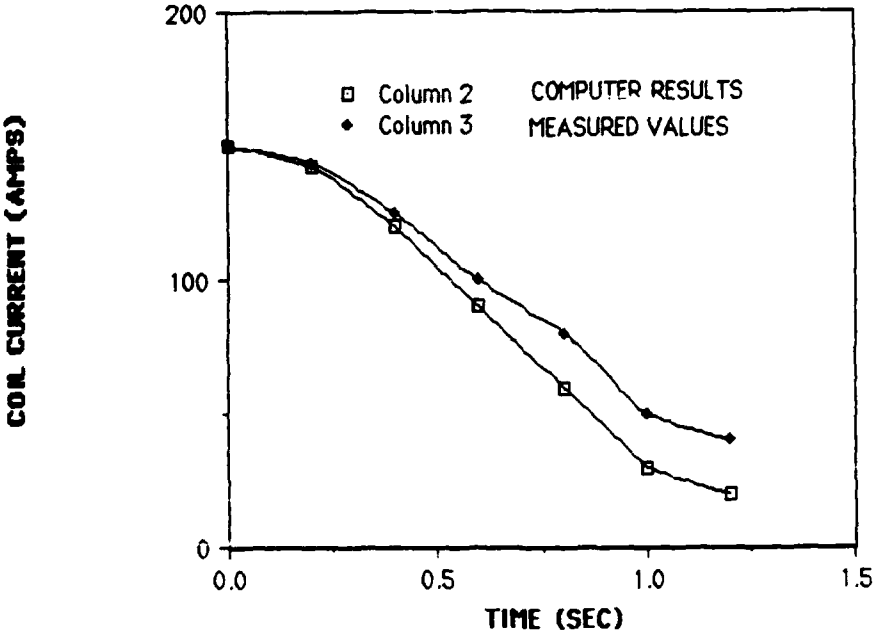

TABLE 2.3 SUMMARY OF 0.61 METER SUPERCONDUCTIVE MAGNET QUENCH COMPUTER PROGRAM RESULTS

Coil current (Amps)	Stored Energy (Joules)	Max Temp Rise (K)	Time Const (Sec)	Max.Coil Voltage(V)
100	245,000	75.6	1.4	3,051
130	414,000	89.5	1.0	5,948
150	551,000	100.0	0.82	8,556

seconds less than that for the measured current decay. The developed internal winding voltage for the Quench computer program is considered theworst case condition. The results of the computer simulation were significantly different than the measured values because the mutual inductances of the aluminum reinforcing ring, the lower retaining ring, and the winding of the test coil ring were not included in the computer simulation. Thermocouple contact was satisfactory during runs 5 and 6 as is reflected in Tables 2.2 and 2.3. Therefore, the measured temperature rise was in close agreement with the temperature rise predicted by the Quench computer program. In addition, the measured and predicted hot spot temperatures are within the design safety limit of 100 degrees Kelvin for potted superconducting magnets.

2.6 CONCLUSIONS AND RECOMMENDATIONS

The superconducting test coil experiment produced some interesting results. First, the strength of the impregnated coil appears to be more significant than the hot spot developed during a quench. Next the magnet developed several self quenches.which appear to be due to insulation breakdown and instrumentation problems during magnet constuction. However, quenching of the magnet could be a major obstacle during full - scale testing in an adverse environment such as a superconducting shipboard propulsion system Therefore it is .recommended that experiments be conducted with NbTi wire with aluminum stabilizing elements since an improvement in magnet stability is expected compared to copper - stabilized NbTi wire.

CHAPTER 3
STABILITY MEASUREMENTS OF A NB-TI/AL SUPERCONDUCING MAGNET

3.1 INTRODUCTION

In Chapter 2 stability measurements were conducted with a copper-stabilized Nb-Ti magnet. For a shipboard superconducting propulsion system operating in an adverse environment, stability appears to be the major issue. Aluminum-stabilized Nb-Ti superconductors are expected to have an improvement in stability over copper-stabilized Nb-Ti superconductors. The aluminum stabilizer has improved thermal conductivity, heat capacity, and electrical conductivity at 4.2 degrees Kelvin compared with the copper stabilizer. Therefore, in this chapter, the stability of Nb-Ti/Al will be compared with the stability of Nb-Ti/Cu.

3.2 ALUMINUM-STABILIZED SUPERCONDUCTING COIL CONSTRUCTION

The objective during the construction phase is to produce a mechanically rigid Nb-Ti/Al superconducting coil. The most difficult part of the coil construction phase is the fabrication of the aluminum matrix Nb-Ti superconductor. Figure 3.1 represents a schematic of a NbTi/Al superconducting wire fabricating process. Figure 3.2 represents a cross-sectional view of aluminum- stabilized, multifilamentary wire. The conventional technique used for preparing the multifilament NbTi superconductor embedded in an aluminum alloy is presented below. First the Al billet was drilled with 121 holes. The Al 1100 matrix consists of a diameter of 76-mm and a length of 24-mm. Next, 4.8 mm diameter Nb-53Ti rods were inserted into the holes of the billet. The billet was then extruded to an extrusion ratio of 10. This composite was then inserteded into a high purity aluminum tube. The NbTi-Al core and high purity aluminum tube were next assembled in a copper tube of 31.8-mm outside

FIGURE 3.1 Nb-Ti/Al SUPERCONDUCTING WIRE FABRICATION PROCESS

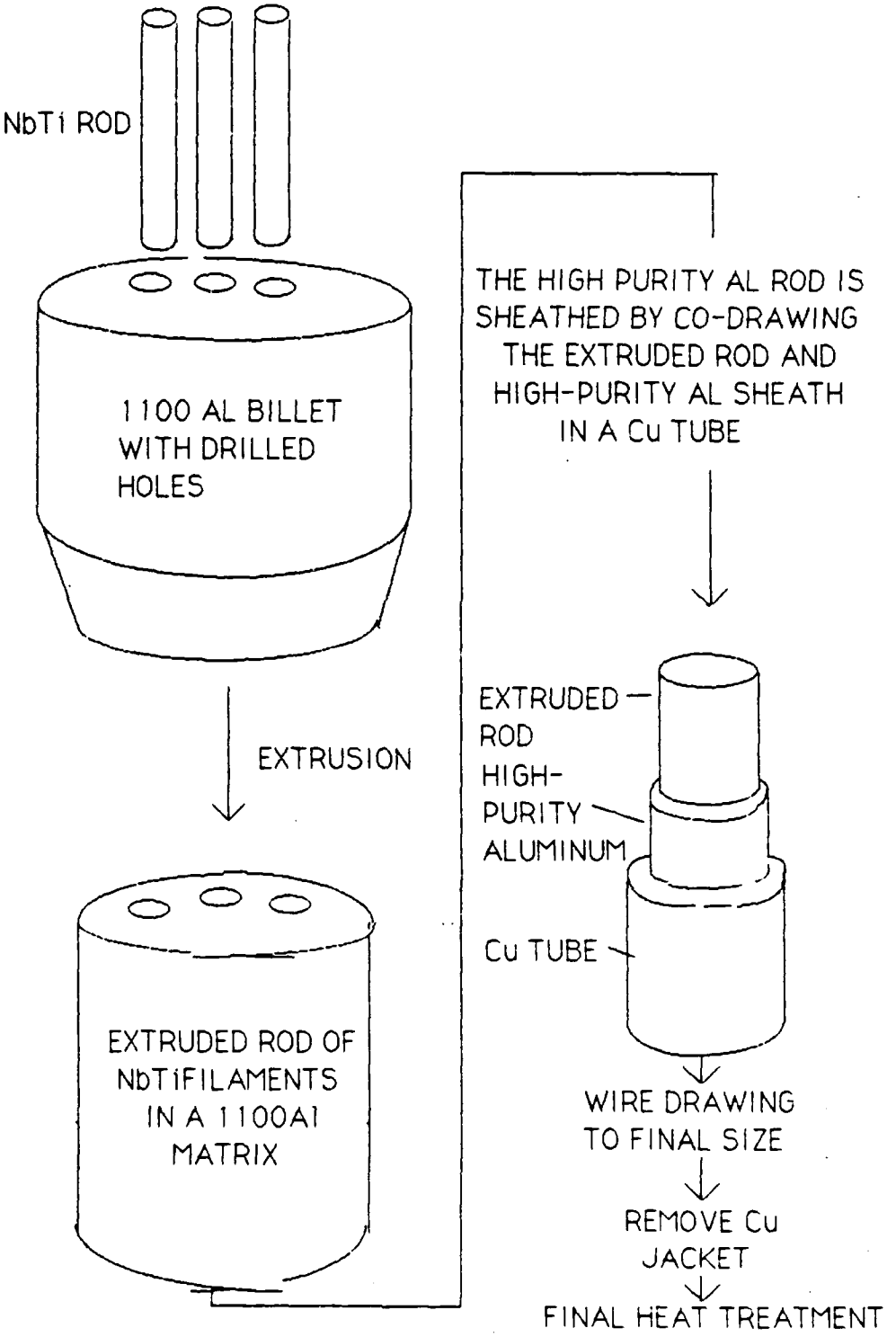

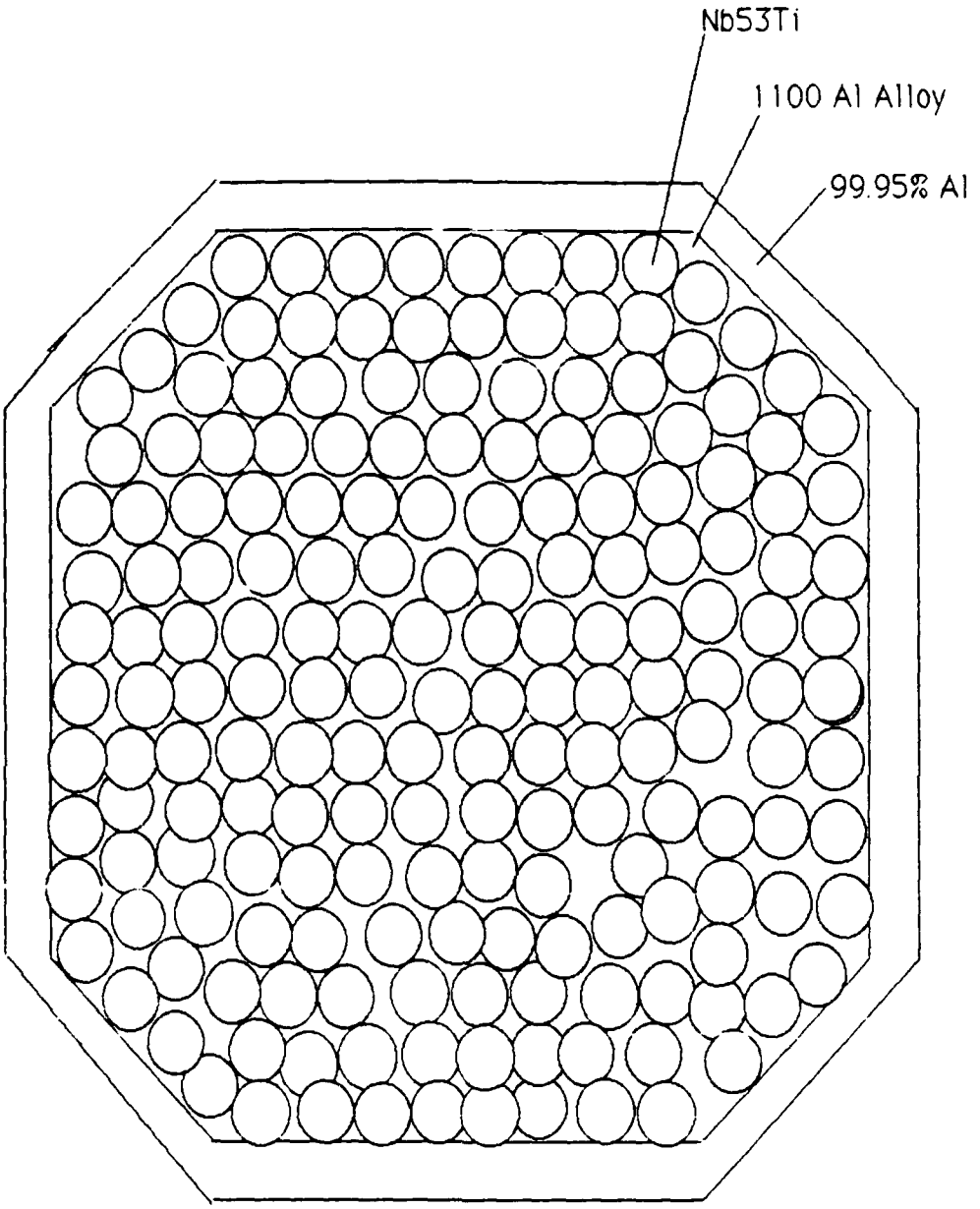

FIGURE 3.2 CROSS-SECTIONAL VIEW
OF Nb-Ti/Al SUPERCONDUCTING WIRE

diameter and 25.4-mm inside diameter. The composite was then drawn down to its final size of 0.91-mm outside diameter. The outer copper sheath was stripped from the wire using nitric acid. Heat treatment of the composite wire was performed at a temperature of 375 degrees Celsius prior to extruding to a rectangular cross-section of 0.635 mm by 0.889 mm. The wire as received from the manufacturer was not insulated. Therefore, the wire was varnished by hand to form an insulated coating.

The NbTi/Al test magnet and heater location is shown in Figure 3.3. Mechanical and electrical integrity of the coil current leads was required to compensate for abuse during handling and experimental setup. This was accomplished by soldering NbTi/Cu with the current leads, first turns, and last turns of the NbTi/Al coil. The NbTi/Al coil has 47 electrical turns and four layers. A constantan wire heater was embedded in each coil between layers 2 and 3.

3.3 EXPERIMENTAL METHOD

The NbTi/Al coil was placed in the inner bore of a background magnet as shown in Figure 3.4. The figure shows the test coil positioned coincentrically at the midlength of the inner bore of the background magnet. Prior to performing the experiment, the NbTi/Al coil and background magnet was placed in a liquid helium dewar and cooled to 4.2 degrees Kelvin. Figure 3.5 shows the instrumentation and power supply connection diagram.

During the experiment, the energy required to quench the NbTi/Al magnet was measured. Various levels of fixed field strength and various values of test operating current were used to determine the energy to quench the magnet. The pulse generator and power amplifier shown in Figure 3.5 was used to deliver a pulse of energy to the resistor heator embedded in the test coil. The dummy resistor shown in Figure 3.5 was used to measure the pulse characteristics prior to applying the pulse to the heator. A pulse width of 100 to 300 microseconds was applyed to the

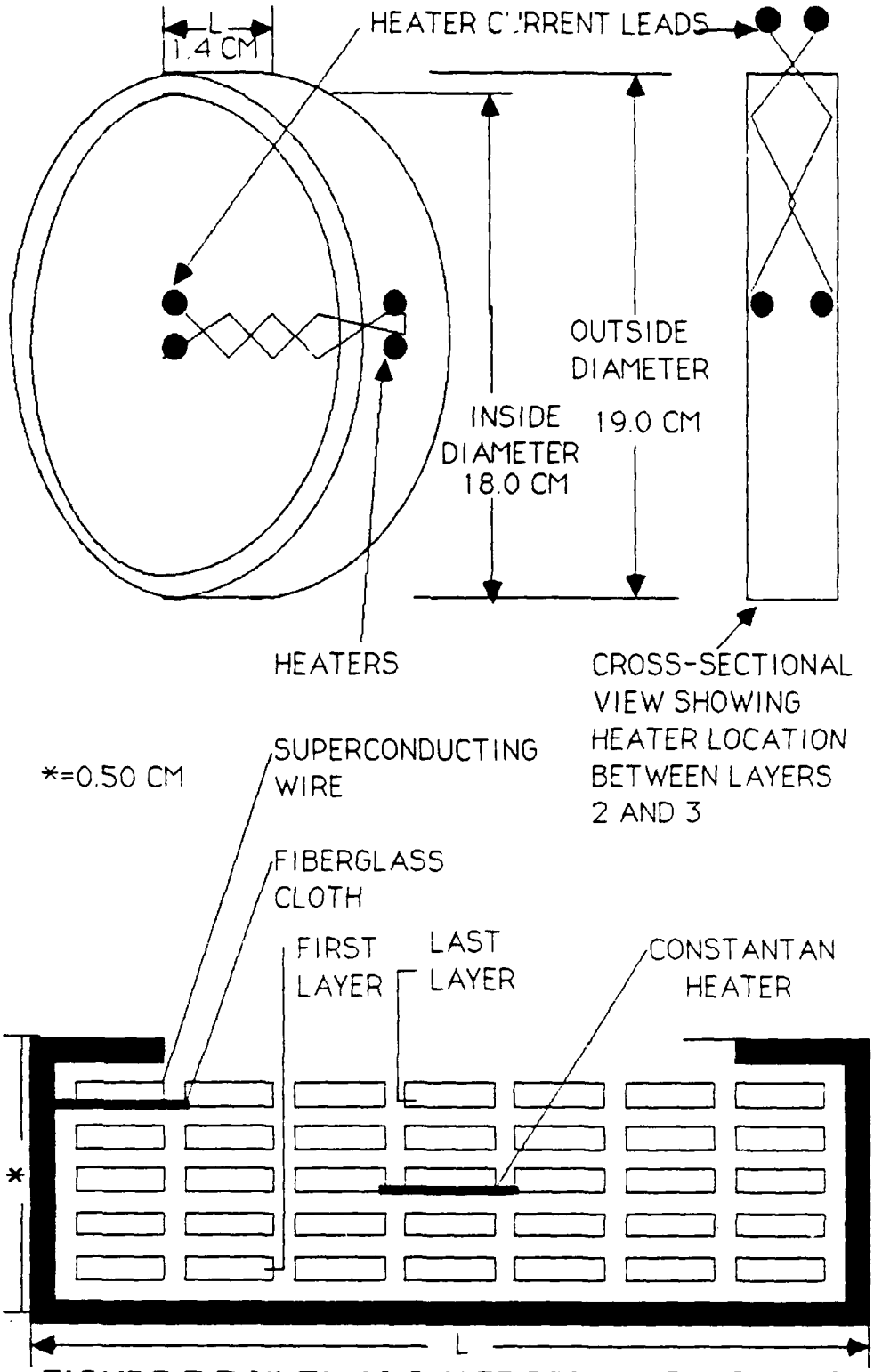

FIGURE 3.3 NbTi/Al SUPERCONDUCTING TEST COIL CONSTRUCTION AND HEATER LOCATION

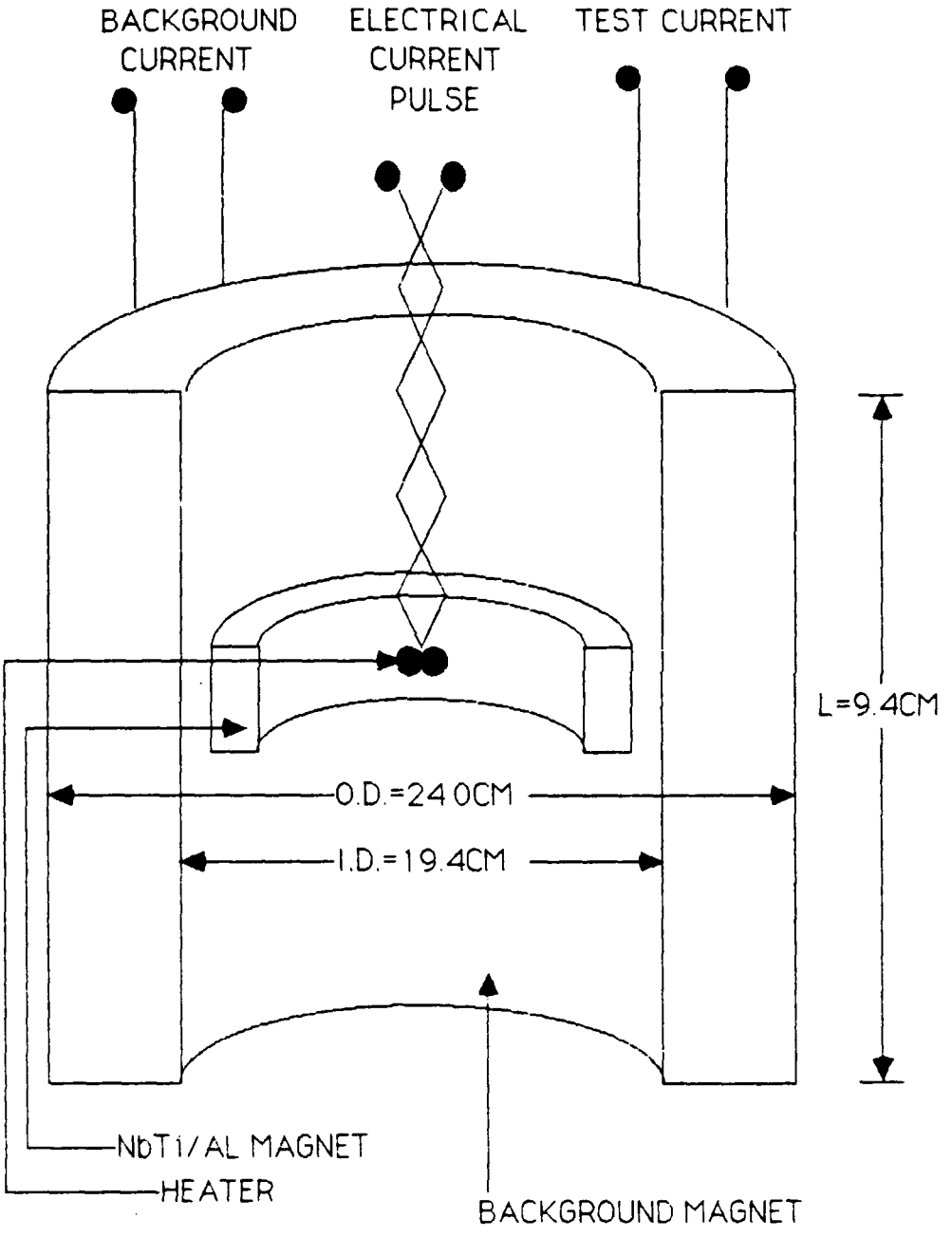

FIGURE 3.4 NbTi/AL SUPERCONDUCTING MAGNET ASSEMBLY FOR ENERGY TO QUENCH MEASUREMENTS

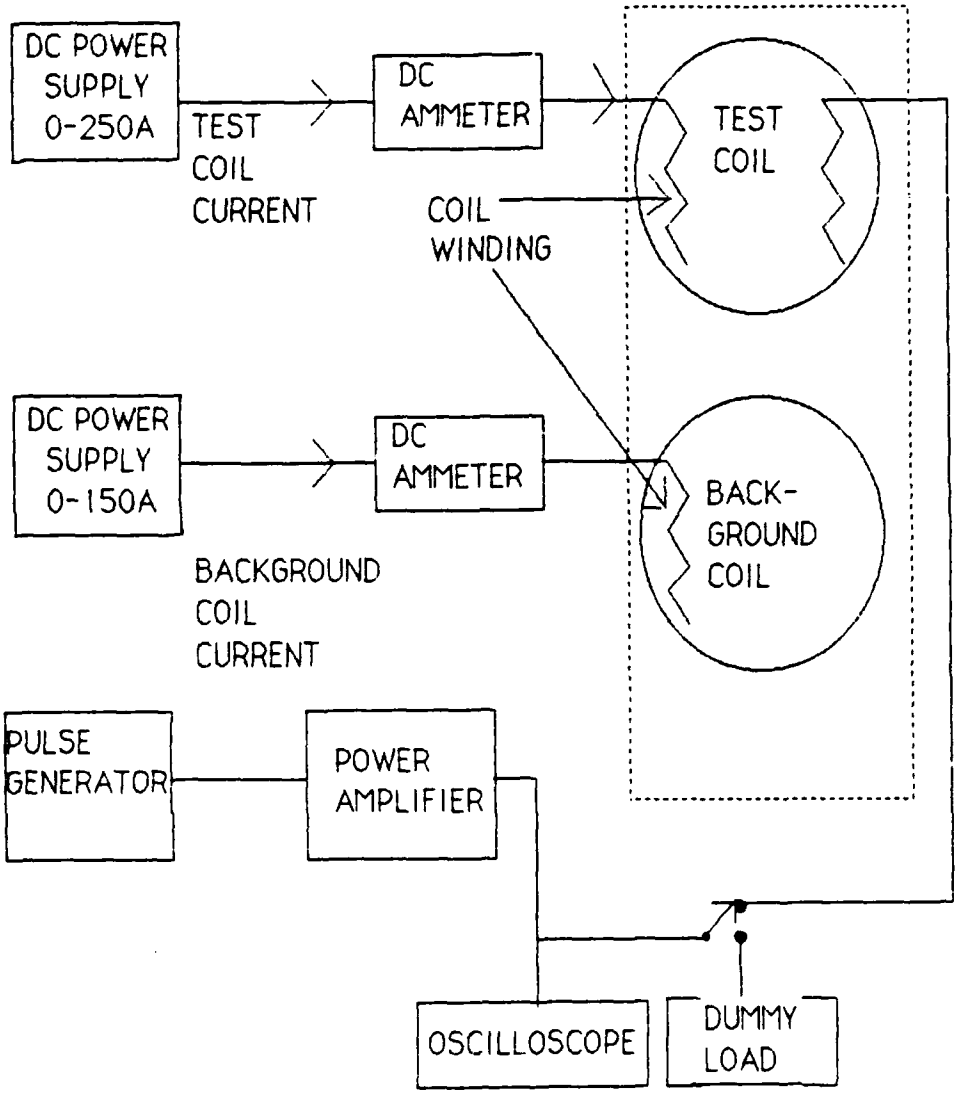

FIGURE 3.5 EXPERIMENT INSTRUMENTATION AND POWER SUPPLY CONNECTION DIAGRAM

FIGURE 3.6 ENERGY TO QUENCH VERSES OPERATING CURRENT/CRITICAL CURRENT FOR NbTi/Al AND NbTi/Cu COILS

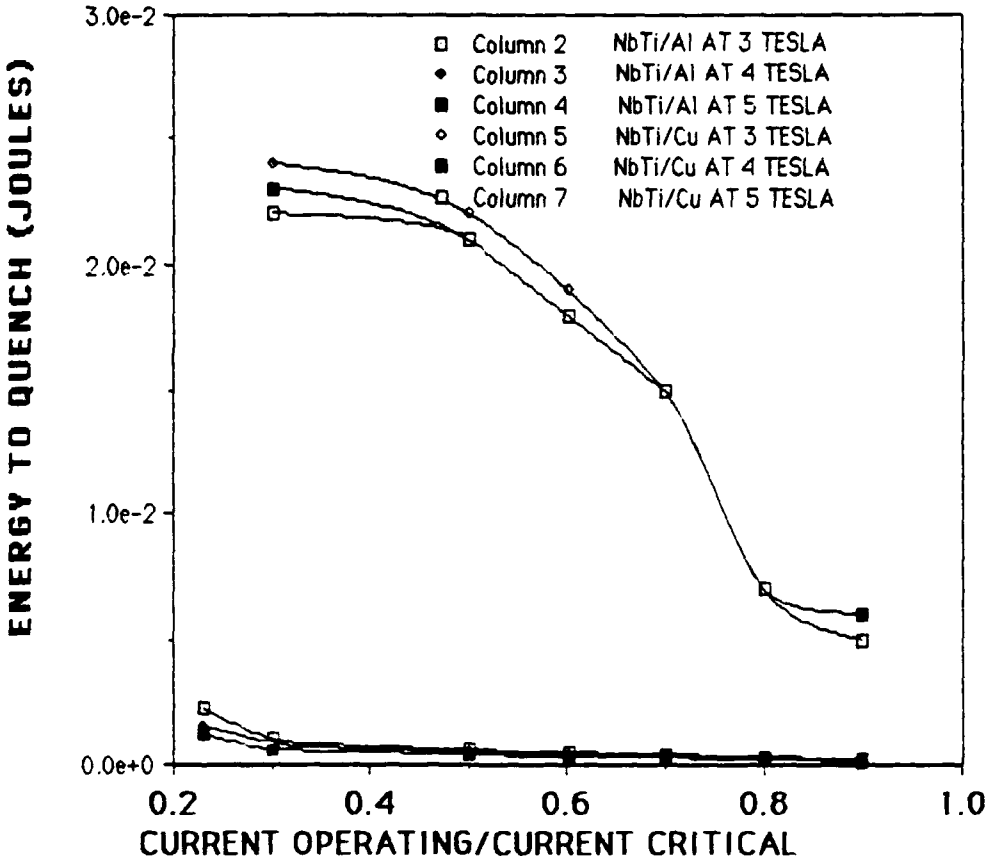

the coil. The pulse amplitude was initially set to a value estimated to be less than the value needed to quench the magnet. The quench value was then recorded when the amplitude was increased in small increments to the quench threshold.

3.4 DISCUSSION OF RESULTS

Figure 3.6 compares the minimum energy that is required to quench the NbTi/Al coil with the minimum energy that is required to quench the NbTi/Cu coil of Chapter 2. The energy required to quench the NbTi/Al coil is approximately 30 times greater than the energy required to quench the NbTi/Cu coil. However, the shape of the curve for the NbTi/Al coil was not as expected at an operating current/critical current of greator than 0.9. The curve for the NbTi/Al coil was expected to show a sharp decrease in magnitude as the operating current approached the critical current. The nonuniformity of the NbTi/Al coil is a possible cause of the unpredicted behavior. .It is recommended that further experiments be conducted before NbTi/Al coils be tested in a superconducting electric propulsion system.

CHAPTER 4
PROPULSION SYSTEM CONVERSION OF DD963 DESTROYER FROM MECHANICAL TO SUPERCONDUCTING ELECTRIC DRIVE

4.1 INTRODUCTION

The objective of Chapter 4 is to assess the feasibility of converting the propulsion system of a DD963 Class destroyer from mechanical to superconducting electric drive. (Christensen, Grigg, Keamy, Stiglich, 1987) The anticipated benefits from this conversion are an increase in survivability, available deck area, maintainability, propeller efficiency, speed, and endurance range along with a decrease in displacement and self-radiated noise without compromising existing mission capabilities.This chapter will only investigate the impact on the ship caused by converting from mechanical to electrical drive; specific use of anyweight, space, or power "savings" will not be addressed. After successful installation and evaluation of this conversion, a follow-on study could be made to determine how to most effectively use the"gains" realized by this modification.

4.2 DD-963 SUPERCONDUCTING PROPULSION PLANT REQUIREMENTS

The superconducting electric drive DD963 must meet or exceed existing operational performance and all mission requirements. These include:

SURVIVABILITY - With the use of a superconducting electric propulsion system, the weight and volume of shafting and mechanical couplings between the prime mover and proeller can be greatly reduced. The replacement of long shafting runs with parallel electric cabling and

the adoption of an integrated electrical distribution system will significantly reduce the threat of battle damage.

USABLE DECK AREA - The ability to transmit power from the prime mover to the propeller through electrical cables rather than direct mechanical coupling will provide much greater flexibility in the number and location of supporting propulsion equipment. The ability to cross connect prime movers and shafts coupled with the adoption of an integrated electrical distribution system may result in a reduction in the number of required propulsion gas turbines. Both of these features should significantly reduce the required area for the engineering system and provide additional usable deck area for other mission requirements.

RANGE - The ability to cross connect prime movers with the propulsion drive train allows the use of only one gas turbine at slow speeds (cruising speed and below.) This would allow each prime mover to operate at a more economical loading and hence at a lower overall fuel consumption rate which would increase the endurance range.

DISPLACEMENT - The replacement of the reduction gears and segments of shafting with lighter electric drive components would decrease the displacement of the ship. Additionally, replacement of the controllable pitch propellers with conventional fixed pitch propellers would not only eliminate the elaborate hydraulic control system required with CRP propellers but also be more efficient.

SPEED - The replacement of reduction gears with superconducting machinery, the elimination of segments of the shafting, and the installation of a lighter and more efficient propeller are expected to have minimal impact on the speed of the ship.

NOISE - The replacement of mechanical reduction gears with electric machines will significantly reduce the self-radiated noise signature of the ship.

MAINTAINABILITY - The electrical drive system is expected to be more maintainable than the existing mechanical drive system. Manning requirements are expected to remain constant since the increase in electrical equipment will be offset by the decrease in mechanical components.

4.3 CONVERSION DESIGN METHODOLOGY

a. DESIGN PHILOSOPHY

This conversion will involve extensive modifications to the existing DD963 propulsion spaces, electrical distribution, shaft alleys, shafts, and propellers (SWBS 100, 200, 300, and 500.) Overall ship performance and mission capability will be the determining factor, not cost, for all options explored. Current NAVSEA (NAVAL SEA SYSTEM COMMAND) design standards combined with good engineering practice will be used throughout all stages of the design to ensure that the ship meets, or exceeds, all existing space and energy requirements.

b. ELECTRICAL

The conversion from mechanical drive to electric drive is considered possible only due to the recent developments in superconducting machinery which are both lighter and more efficient than conventional electric machinery. Superconducting alternating current (AC) generators and direct current (DC) homopolar motors were selected as replacement components for the mechanically driven reduction gears of the DD963. Although AC/AC, DC/DC, and AC/DC (hybrid) configurations were considered, AC/DC (hybrid) system was selected primarily because of its compatibility with high speed gas turbines. The benefits of shifting from mechanical to electrical propulsion drive can best be optimized by placing an integrated electrical distribution system into the conversion design. This allows both the ship's service and propulsion power to connect into a common distribution system. From this common bus, the ship's propulsion power is fed to electrical propulsion motors while the ship's service power is fed to

a separate ship's service bus. However, to incorporate an integrated electrical distribution system into the design, all generators must be electrically compatible. The best choice would be to maintain the integrated electrical distribution bus at 60 hz AC since it would be compatible with the existing ship's service system and install AC/DC converters locally on the propulsion motors if required.

Figure 4.1 presents a block diagram of the integrated electrical distribution system. Three upgraded 26,250 HP LM-2500 gas turbines are connected to superconducting AC synchronous propulsion generators. Two 40,000 HP superconducting motors are connected to shortened propeller shafts. A crossover switch is used to operate both superconducting motors during the failure of individual busses.

Two pole AC synchronous superconducting generators are selected as the most compatible with 3600 rpm gas turbines and an integrated electrical distribution system. Currently, the DD963 has fourLM-2500 gas turbines currently limited to 20,000 HP each. By replacing the reduction gears with electrical generators and installing theLM-2500 upgrade package during the conversion, their output can be increased to 26,250 HP each. However, the upgrade of the existing LM-2500's will provide excessive power (105,000 HP) versus the current 80,000 SHP. With the adoption of an integrated electrical distribution system, three upgraded LM-2500's would be sufficient since the ship could still provide sufficient powering to meet all existing performance requirements. Additionally, the removal of one of the existing gas turbines would provide additional space and weight for future shipboard systems upgrades. Despite the requirement for power conversion from AC, superconducting DC homopolar motors were selected as the propulsion motors because of their excellent speed control characteristics which is essential during maneuvering situations.

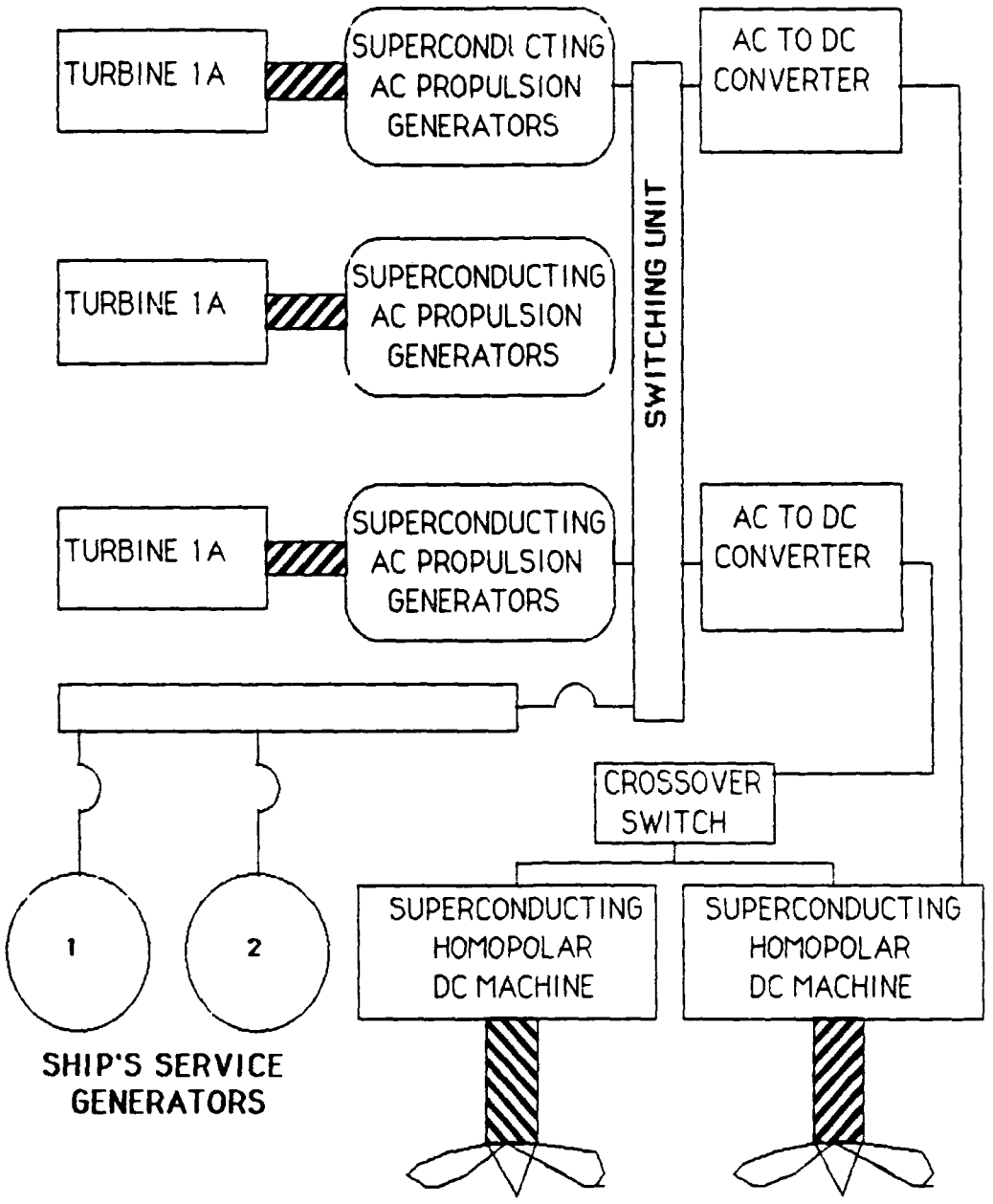

FIGURE 4.1 INTEGRATED ELECTRIC DISTRIBUTION SYSTEM FOR THREE GAS TURBINES

With the adoption of the integrated electrical distribution system,the installation of ship alt DD963-452K (all electric auxiliaries) was considered cost effective. The increase of 1865.3 KW in ship's service electrical loads was not considered significant compared to the weight savings of 45.1 tons and the elimination of three waste heat boilers (MIT 13A vault data).

The DD963 currently has three 2,000 KW ship's service generators; two of which are normally always operational with the third in standby. With the adoption of an integrated electrical distribution system, the propulsion generators will be able to supply power for all ship's service needs underway except during high speed runs. The current maximum ship's service load, adjusted for the installation of ship alt DD963-452K, is 4,273 KW. Since the ship's service generators will most likely only be operational during special operations (i.e. at anchor, inport steaming, restricted maneuvering, and battle (readiness conditions) two ship's service generators are sufficient to meet all of the ship's service operational requirements.

The reduction in both propulsion and electrical equipment will not degrade the mission capabilities of the vessel; system redundancy is improved by providing five separate power sources and integrating them into a simple parallel system. The result is a system which has five electrical generators, each of which can be used to power either or both propulsion shafts and all ship's service electrical loads. In support of the superconducting equipment, four cryogenic compressors, each with two independent paths which can be cross-connected, were installed: one in each of the main enginerooms and two in the shaft alley.

The conversion from mechanical to electrical drive is expected to have little effect on the existing remote control stations located on the bridge. Although they will be modified slightly to accommodate the new system, all remote control stations will maintain their present "look and feel" and so should pose no problems to currently qualified operators.

Section 4.6 provides a detailed description of a proposed cryogenic system to support the above superconducting machinery configuration.

c. NAVAL ARCHITECTURE

Figures 4.2a-e present general arrangements for the integrated electric drive conversion as compared to the conventional DD963. The proposed arrangements for this conversion take advantage of the flexibility afforded by the electric drive system which reduces machinery weight and volume while increasing damage control survivability and redundancy.

The placement of two 40,000 SHP superconducting electric drive motors in the shaft alley minimizes shaft weight and separates the electric drive motors from the enginerooms. This arrangement improves damage control capabilities by reducing propulsion shaft vulnerability and making it possible for both shafts to operate with one engineroom totally disabled. The existing propulsion shaft seals will be moved aft two feet and the fuel tank top beneath the shafts in the shaft alley must be recessed to make room for the drive motors (11.7 ft length and 6.4 ft diameter.) These modifications are very straight forward and should pose no technical difficulties since there will be negligible impact on other shipboard systems and the areas will be readily accessible during conversion.

The removal of both a main propulsion and a ship's service gas turbine is made possible by the installation of the upgrade package to the existing LM 2500 gas turbines, which will increase their power rating to 26,250 SHP, and integrating the electric drive system with the ship's service electrical distribution system. Due to the change to an integrated electrical distribution system, the implementation of ship alt DD963-452K (all electrical auxiliaries) was considered very beneficial. The net impact of this ship alt was the elimination of three waste heat boilers at a savings of 45.3 tons and a gain of 480 ft2 of deck area.

FIGURE 4.2A
963 GENERAL MACHINERY ARRANGEMENT
NO.1 ENGINE ROOM

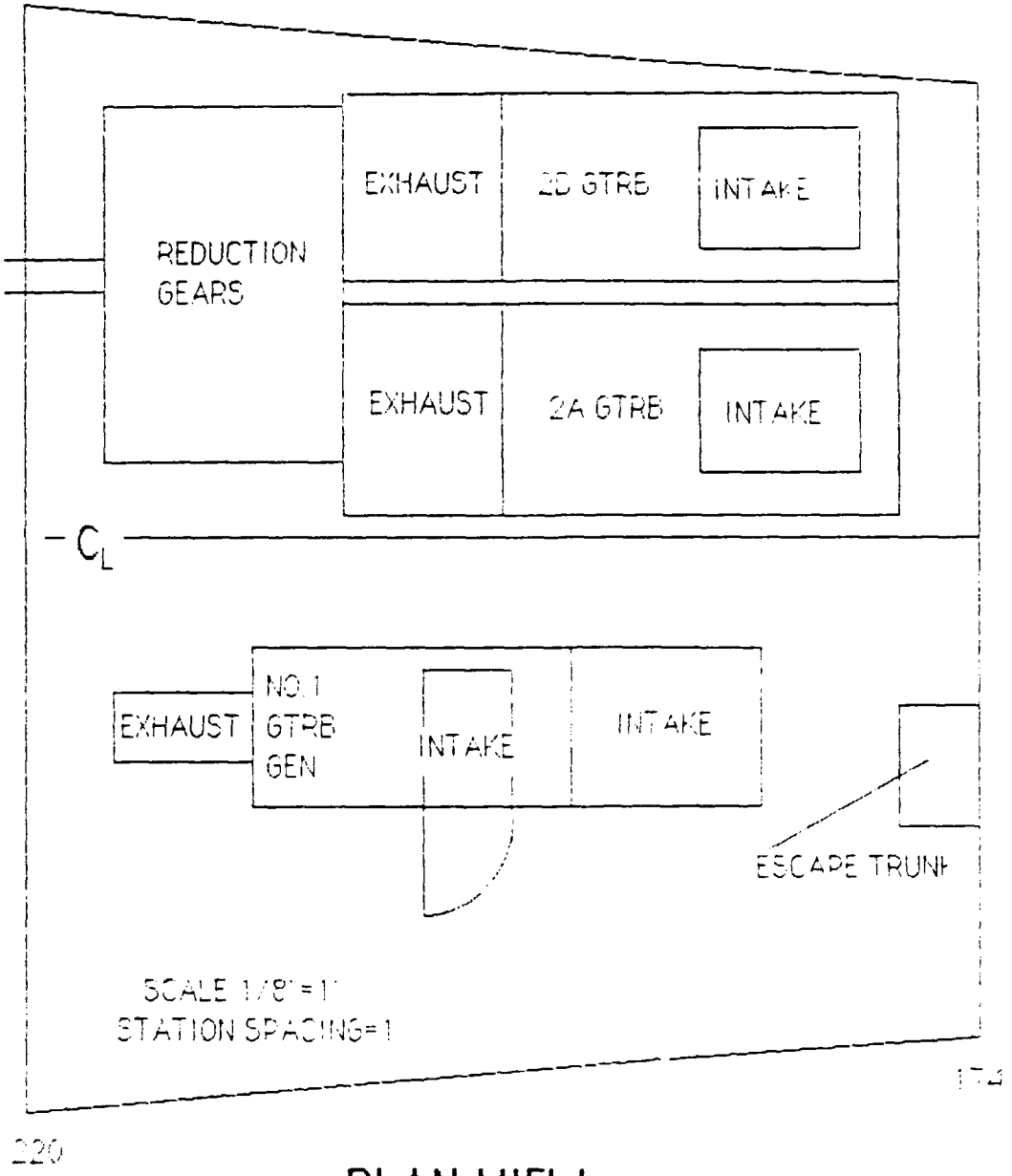

PLAN VIEW

FIGURE 4.2B
963 GENERAL MACHINERY ARRANGEMENT
NO.1 ENGINE ROOM

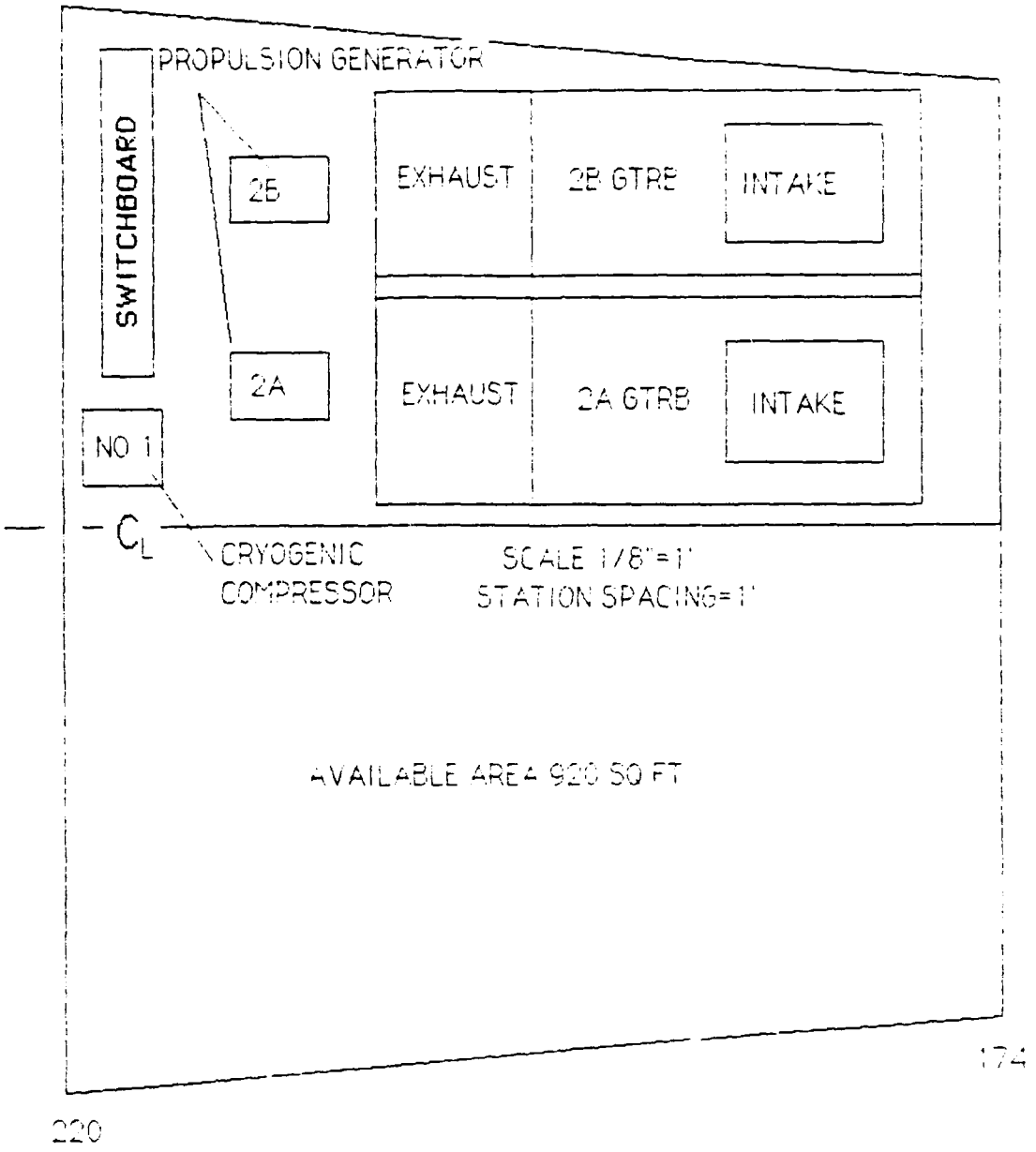

PLAN VIEW

FIGURE 4.2C

963 GENERAL MACHINERY ARRANGEMENT

NO.2 ENGINE ROOM

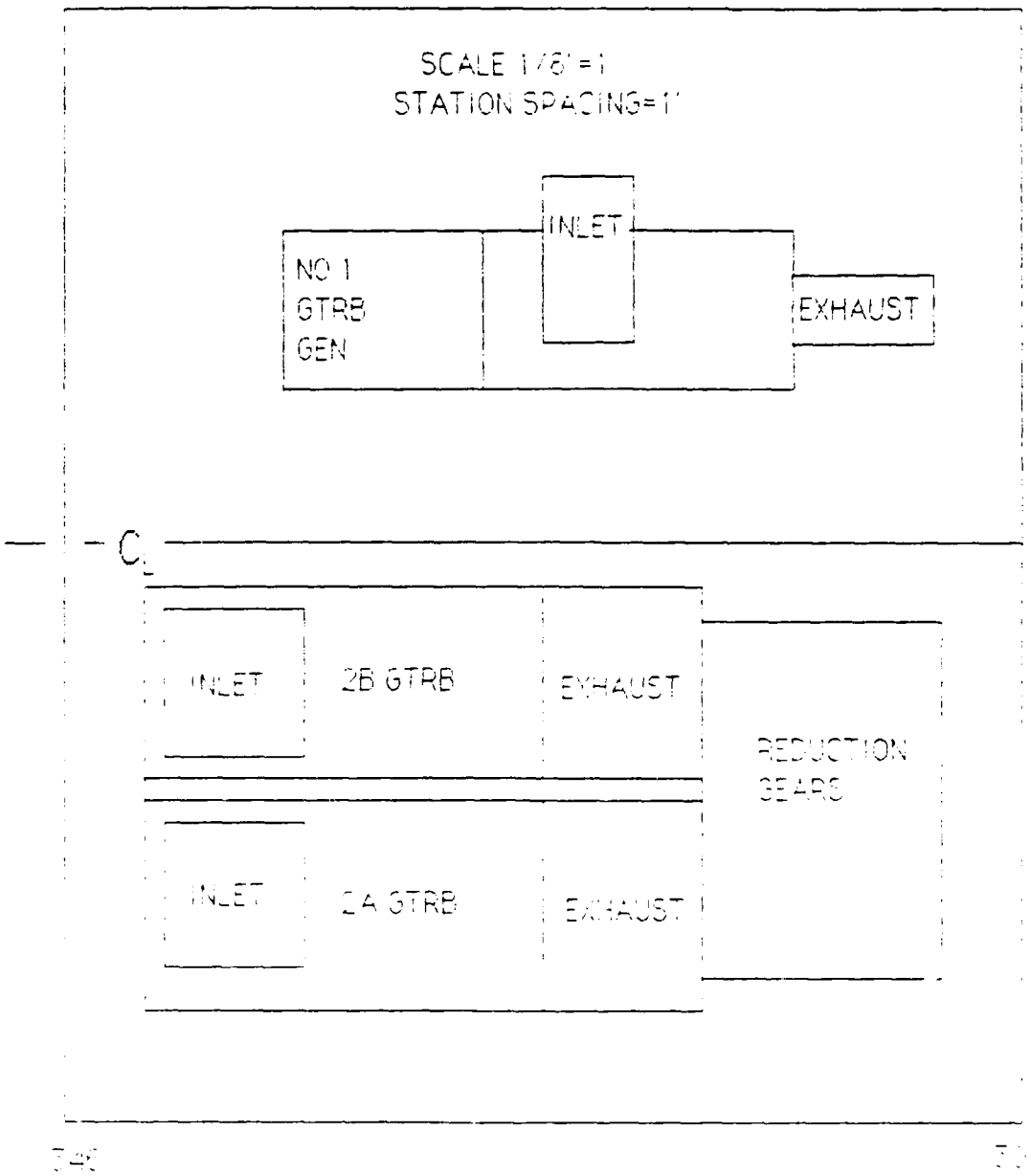

PLAN VIEW

FIGURE 4.2D

963 GENERAL MACHINERY ARRANGEMENT

NO.2 ENGINE ROOM

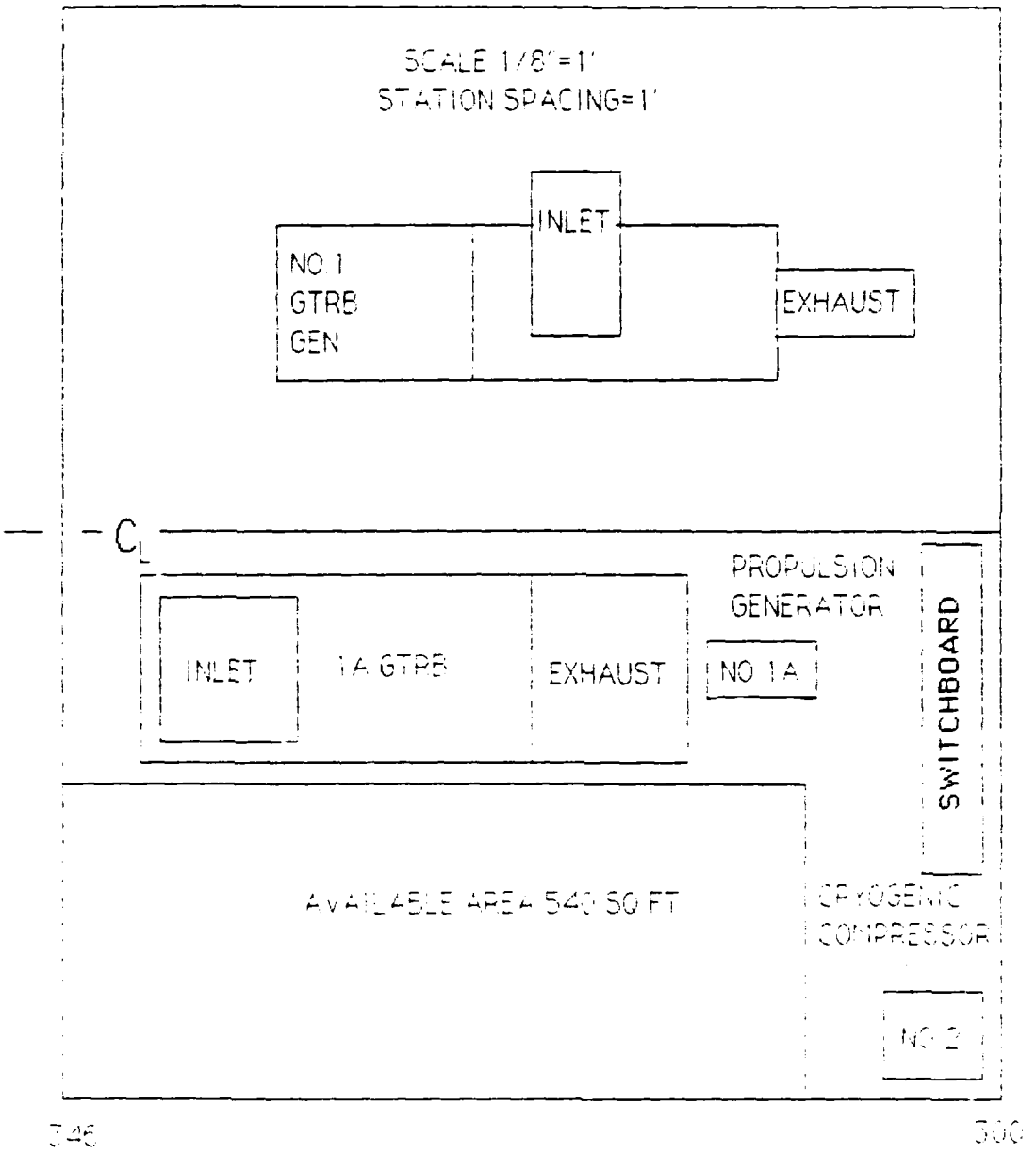

PLAN VIEW

FIGURE 4.2E

DD- 963 SHAFT ALLEY MODIFICATIONS

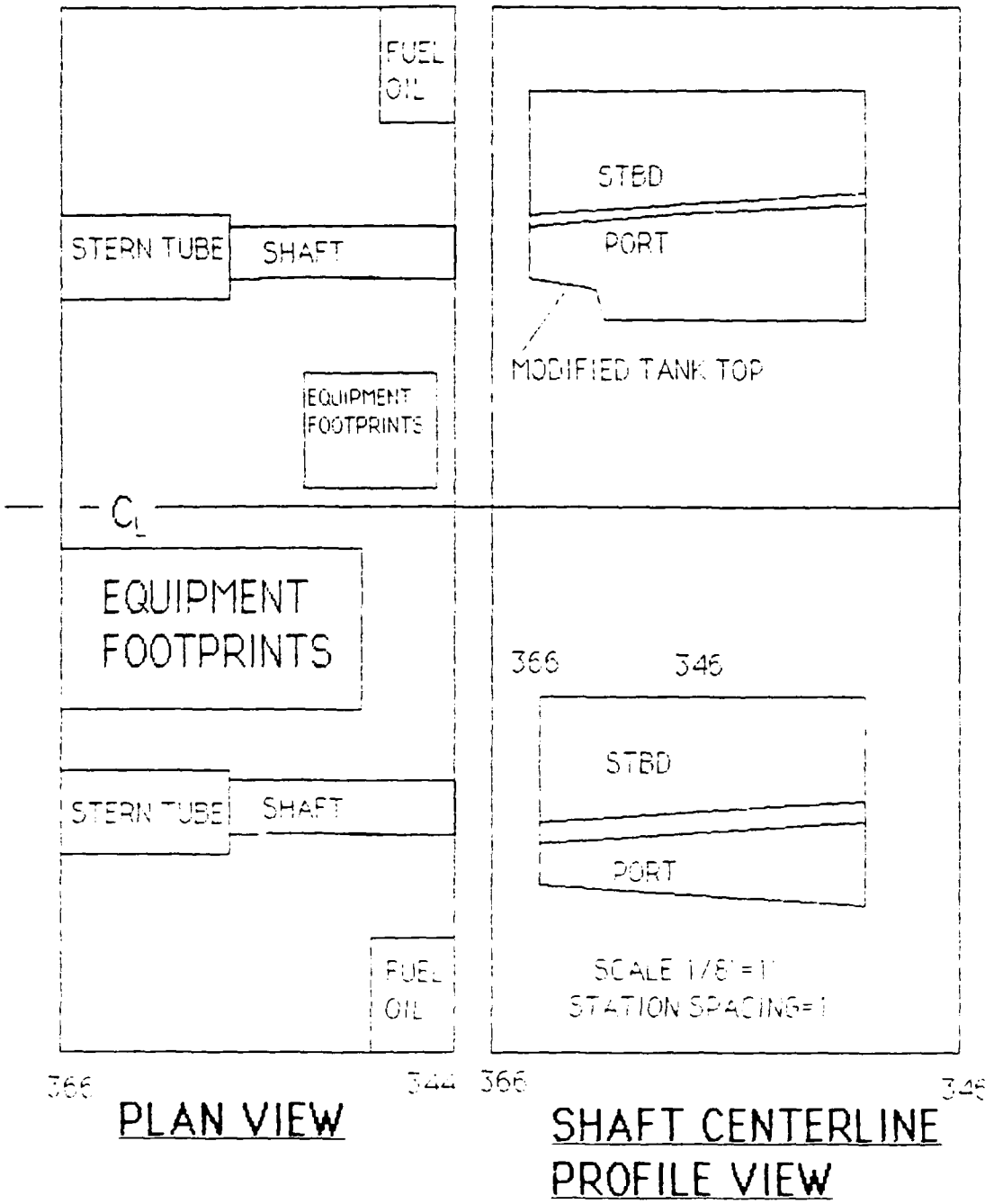

The decision was made to remove number 1B gas turbine and number 1 ship's service generator, located in the after and forward enginerooms respectively. This would balance the weight removal of a large segment of the shaft and replacement of the CRP propellers with lighter fixed pitch ones and provide large versatile compartments for conversion to alternate uses. These modifications resulted in a 0.24 degree angle of heel to port and a trim of 0.12 feet by the bow. Both of these are well within the contractor design limits of 0.25 degrees and 1.0 foot respectively. To maximize the amount of deck space to be made available for other ship's functions on the starboard side of the forward engineroom (960 ft2), some of the existing auxiliary support equipment (i.e. lubrication oil purifiers, starting air flasks, escape trunk and switchboard) would have to be moved to the port side. The impact of moving these supporting equipment is minimal since the shift would involve only the shifting of foundations and modifying existing piping and cabling runs. The removal of one of the aft propulsion gas turbines would allow a reduction in the existing intake and exhaust ducting through the decks above the after engineroom. Therefore, the net result of this conversion would be a space savings of 4,954 ft2 and a weight savings of 227.1 tons.

4.4 COST ANALYSIS

Using the simplified Cost Model presented in M.I.T. course 13.411, an economic comparison of the cost of converting a DD963 from mechanical to electric drive was conducted (Table 4.1). A final total cost prediction was then made based on an estimate for the operating fuel cost savings during an additional 20 year service life.

Since only weight groups 100, 200, 300, and 500 were significantly affected by this conversion, only the net weight changes for each of these weight groups were factored into this cost analysis. Based on the removal of 433.9 tons and the addition of 228.9 tons, the total cost for the conversion was estimated to be $118.8 million. An operating profile of

TABLE 4.1 COST CALCULATIONS

DD963 BASELINE CONFIGURATION

WEIGHT GROUP	REMOVED WEIGHT	ADDED WT (LT)	TOTAL WT REMOVED + ADDED(LT)	COST MODEL FACTOR (M$/100LT)	COST (M$)
STRUCTURE (100)	65	6	71	2.0	1.42
PROPULSION (200)	272	167.8	439.8	13.2	58.054
ELECTRICAL (300)	51.5	55.1	106.6	17.9	19.081
AUXILIARY (500)	45.4	-	45.4	9.0	4.086
TOTAL	433.9	228.9	662.8	-	82.641

GFE COST

WITH THE SIMPLIFIED COST MODEL, GFE IS ASSUMED TO BE ROUGHLY EQUAL TO SHIPBUILDER COST OF THE ADDED MACHINERY.

WEIGHT GROUP		TOTAL WT ADDED ADDED(LT)	COST MODEL FACTOR (M$/100LT)	COST (M$)
STRUCTURE (100)		6	2.0	0.12
PROPULSION (200)		167.8	13.2	22.15
ELECTRICAL (300)		55.1	17.9	9.863
TOTAL		228.9	-	32.133

TABLE 4.1 COST CALCULATIONS

DD963 BASELINE CONFIGURATION

CONTINUED

TOTAL COST
TOTAL COST OF THE REMOVED/ADDED MACHINERY EQUALS SHIPBUILDER COST PLUS GOVERNMENT FURNISHED MATERIAL (GFM) COST
86.641+32.133= $118.774 MILLION
FUEL (FULL POWER)=[(SFC)(SHP)*(7.23BBLS/TON)*(DAYS) UNDERWAY)*(24HR/DAY)*(%TIME)]/2240
FUEL (FULL POWER)=[(.42)(8000)*(7.23BBLS/TON)*(109DAYS) UNDERWAY)*(24HR/DAY)*(.06%TIME)]/2240=17022BBLS
FUEL (ENDURANCE)=[(.96)(1600)*(7.23BBLS/TON)*(109DAYS) UNDERWAY)*(24HR/DAY)*(.06%TIME)]/2240=12969BBLS
FUEL (ELECTRICAL)=[(.96)(1600)*(7.23BBLS/TON)*(109DAYS) UNDERWAY)*(24HR/DAY)*(1.0)]/2240=12969BBLS
TOTAL FUEL=17022+53580+12969=83571 BBLS

30% underway time per year was chosen as characteristic for the DD963. While underway, 94% of the time is considered to be at endurance speed and 6% of the time at full power (St. John, 1978). At full power, the fuel consumption for both mechanical and electric drive was calculated based on a specific fuel consumption (SFC) of 0.42 lbs/hp-hr. At endurance speeds, the SFC for mechanical drive is 0.64 lbs/hp-hr and for electric drive 0.50 lbs/hp-hr. The SFC for the ship's service electrical power generators was estimated to be 0.96 lbs/KW-hr for the mechanical drive system and 0.67 lbs/KW-hr for the electrical drive ship (St. John,1978; Carmichael, 1987.) This difference is due to with a mechanical drive system, at least one gas turbine per shaft must be operational and hence cannot always be run at its most economical loading. An integrated electrical drive system provides lower SFC due the greater flexibility in the selection of which propulsion or ship's service generators required to be on the line. The current 24 hour electrical load average for ship's service requirements is 1600 KW/hr and is expected to increase to 2,839 KW/hr after the conversion. The required endurance horsepower is three percent lower for the electrically driven ship due to its reduced displacement and greater efficiency propeller (fixed pitch vs. CRPP.) Fuel costs were based on $50/barrel in 1987 dollars (Carmichael, 1987). Using these estimates, the fuel consumed per year for the mechanical drive system was computed to be 85,571 bbls and 73,689 bbls for the electric drive variant. This represents a 13.9 percent reduction in fuel costs which equates to a $0.59 million annual savings. Over the remaining 20 year service life span of the DD963, the cost of fuel for the mechanical drive system was $85.6 million while the electric drive would cost only $73.7 million. Therefore, the electric drive ship could save $11.9 million in direct fuel cost savings. In summary, the total cost for the conversion of a DD963 from mechanical drive to electric drive, factoring in an estimate for the fuel savings over a 20 year service life, would be $106.9 million.

4.5 COMPARATIVE ANALYSIS WITH CURRENT DD963

a. SHIP BALANCE

1. WEIGHT

The weight for the electric drive design was computed based on the most current weight report figures for the DD963 (MIT 13A vault). By considering only weight additions and deletions to the baseline ship, the SWBS weights for the electric drive variant were estimated. Table 4.2 provides a comparative weight change summary while Table 4.3 represents weight calculations

SWBSBASELINE	ELECT DRIVE	CHANGE	
100 3075.5	3016.5	-1.92%	
200 761.9	657.7	-13.77%	
300 285.2	288.8	+1.26%	
400 355.7	355.7	---	
500 736.6	691.2	-6.16%	
600 479.1	479.1	---	
700 153.8	153.8	---	
MARGIN	83.0	66.3	-20.12%
LOADS	1989.9	1984.5	-0.27%
FLDISP	8014.7	7787.6	-2.83%

Table 4.2 Weight Change Summary (in tons)

TABLE 4.3 WEIGHT CALCULATIONS

DD963 BASELINE CONFIGURATION

SWBS	COMPONENT	WT	VCG	LCG	TCG
100	HULL STRUCTURES	3075.5	24.0	269.6	0.00
	FWD M.E.FOUNDATION BEDPLATE	5.2	16.5	190.0	10.00
	FWD M.E. PED. FOUNDATION	1.9	12.7	185.7	9.60
	FWD REDUCTION GEAR FOUNDATION	6.9	11.6	210.5	10.11
	FWD HIGH IMPEDANCE UNIT	10.7	10.7	209.3	10.10
	AFT REDUCTION GEAR FOUNDATION	6.9	11.1	311.3	-11.00
	AFT HIGH IMPEDANCE UNIT	10.7	9.8	310.1	-11.00
	AFT M.E.FOUNDATION BEDPLATE	5.2			
	AFT M.E. PED. FOUNDATION	3.1			
	PROPULSION MTR FOUNDATION (P)	0.0			
	PROPULSION MTR FOUNDATION (S)	0.0			
	PROP GEN FOUNDATION 1A (S)	0.0			
	PROP GEN FOUNDATION 1B (S)	0.0			
	PROP GEN FOUNDATION 2A (P)	0.0			
	PROP GEN FOUNDATION 2B (P)	0.0			
	AFT OUTBOARD UPTAKES	32.6	52.7	354.0	-15.00
200	PROPULSION PLANT	761.9	22.6	309.4	-0.01
	GAS TURBINE 1A (S)	19.9	20.8	191.0	5.25
	GAS TURBINE 1B (S)	19.9	20.8	191.0	14.80
	PROPULSION MOTOR (P)	0.0			
	PROPULSION MOTOR (S)	0.0			
	COOLING SYSTEMS 1	0.0			
	COOLING SYSTEMS 2	0.0			
	COOLING SYSTEMS 3	0.0			
	COOLING SYSTEMS 4	0.0			
	REDUCTION GEAR (P)	71.4	15.5	211.5	10.00
	REDUCTION GEAR (S)	71.4	15.0	312.8	-11.00
	FWD SECTION OF SHAFT RMVD (P)	27.7	14.5	287.0	11.50
	FWD SECTION OF SHAFT RMVD (S)	1.7	9.5	339.5	-11.50
	LINESHAFT BEARING 1 (P)	1.2	13.0	247.5	10.50

LINESHAFT BEARING 2 (P)	1.2	11.5	280.3	10.90
LINESHAFT BEARING 3 (P)	1.2	10.0	313.5	11.10
LINESHAFT BEARING 4 (P)	1.5	8.0	353.5	11.50
LINESHAFT BEARING 5 (S)	1.5	10.9	353.6	-11.40
CRP PROPELLERS	43.5	1.4	496.0	0.00
CRP SUPPORT SYSTEM	15.2	10.0	310.4	0.71
CONVENTIONAL PROPELLERS	0.0			
FWD PORT COMBUSTION AIR	14.6	52.7	200.0	15.00

SWBS	COMPONENT	WT	VCG	LCG	TCG
300	ELECTRIC PLANT, GENERAL	285.2	28.1	299.1	-0.04
	FWD SS GENERATOR	44.5	17.3	206.5	-11.00
	PROPULSION GENERATOR 2A (P)	0.0			
	PROPULSION GENERATOR 2B (P)	0.0			
	PROPULSION GENERATOR 1A (S)	0.0			
	PROPULSION GENERATOR 1B (S)	0.0			
	TRANSMISSION LINES MOTOR	0.0			
	TRANSMISSION LINES GEN	0.0			
	SWITCHING GEAR		0.0		
	MISC SUPPORT FOR GENERATORS	7.0	17.5	206.0	-21.00
	EXCITERS		0.0		
	SILICON CONTROL RECTIFIERS	0.0			

500	AUXILIARY SYSTEMS, GENERAL	736.6	26.4	288.8	-0.01
	S/A DD963-452K	45.4	12.1	26.3	9.61

SUMMARY

100	HULL STRUCTURES	3075.5	24.0	269.8	0.00
200	PROPULSION PLANT	761.9	22.6	309.4	-0.01
300	ELECTRIC PLANT, GENERAL	285.2	28.1	299.1	-0.04
400	COMMAND+SURVEILLANCE	355.7	25.2	162.6	-0.03

500 AUXILIARY SYSTEMS, GENERAL	736.6	28.4	288.8	-0.01
600 OUTFIT+FURNISHING,GENERAL	479.1	32.3	280.1	-0.02
700 ARMAMENT	153.8	36.1	240.2	-0.07
MOD MODERNIZATION PACKAGE	94.0	48.8	245.8	-0.12

LIGHT SHIP (WITHOUT MARGIN)	5941.8	26.0	271.9	-0.01
D + B WEIGHT MARGIN	83.0	48.8	245.8	0.00
LIGHT SHIP (WITH MARGIN)	6024.8	26.3	271.5	-0.01
F00 LOADS (BASIC)	1975.9	10.0	275.0	0.00
MODERNIZED LOADS	14.0	48.8	245.8	0.00
BASELINE F.L. DISPLACEMENT	8014.7	22.34	272.4	-0.01

2. STABILITY

Using the Hydrostatic Analysis Module of the Advanced Surface Ship Evaluation Tool (ASSET), the intact and damaged stability of the electric drive conversion was compared to the existing ship (Figure 4.3). The results of this comparison, summarized below, (Tables 4.4, 4.5, and 4.6) show that the range of stability, maximum righting arm, and GM/B all improved slightly as a result of this conversion. The converted ship is balanced with a 0.24 degree port list and 0.12 foot trim by the bow. Symmetrical flooding and constant permeabilities were assumed for damaged stability calculations. Since the LGC and KG were maintained relatively constant through selective arrangement choices and leaving the hull form and watertight bulkheads intact, a complete stability analysis is considered redundant and the comparison presented is sufficient to fully demonstrate the feasibility of this conversion. As a result of the conversion, 19.0 tons could be added at a TCG of 15 feet to starboard in the available spaces and the ship would not exceed a 0.25 degree starboard list. Installing additional weights would require balancing the ship with either ballast or other arrangement modifications and its impact on intact and damaged stability would have to be verified.

	BASELINE	ELECTRIC DRIVE
MAX RIGHTING ARM	4.7 FT @ 58 deg	4.9 FT @ 60 deg
RANGE OF STABILITY	>90 deg	>90 deg

Table 4.4 Intact Static Stability - High Speed Turn

	BASELINE	ELECTRIC DRIVE
MAX RIGHTING ARM	4.7 FT @ 58 deg	4.9 FT @ 60 deg
RANGE OF STABILITY	15 to >90 deg	15 to >90 deg

Table 4.5 Intact Static Stability - Wind Heeling

	BASELINE	ELECTRIC DRIVE
MAX RIGHTING ARM	4.8 FT @ 45 deg	5.0 FT @ 45 deg
RANGE OF STABILITY	15 to >90 deg	15 to >90 deg

Table 4.6 Damaged Stability Summary - Wind Heeling (compartments 3,4 & 5 flooded)

3. SPACE

The reduction of propulsion plant size provides 4,954 ft2 of usable deck space throughout the ship for conversion to other uses. The size and location of this space is summarized in Table 4.7as follows:

COMPARTMENTS	DIMENSIONS	AREA
AFTER ENGINEROOM & UPTAKES		
Second deck	36 x 15 ft	540 ft^2
First deck	46 x 13 ft	
27 x 6 ft	760 ft^2	
Main deck	46 x 9 ft	414 ft^2
01 Level	46 x 8 ft	368 ft^2
02 Level	46 x 6 ft	276 ft^2
03 Level	46 x 6 ft	276 ft^2
04 Level	8 x 12 ft	96 ft^2
FORWARD ENGINEROOM		
Second deck	46 x 20 ft	920 ft^2
First deck	46 x 17 ft	782 ft^2
MISCELLANEOUS		
#3 Waste Heat Boiler	27 x 6 ft	162 ft^2

TOTAL USABLE DECK AREA GAINED = 4,954 ft^2

Table 4.7 Usable Deck Area Summary

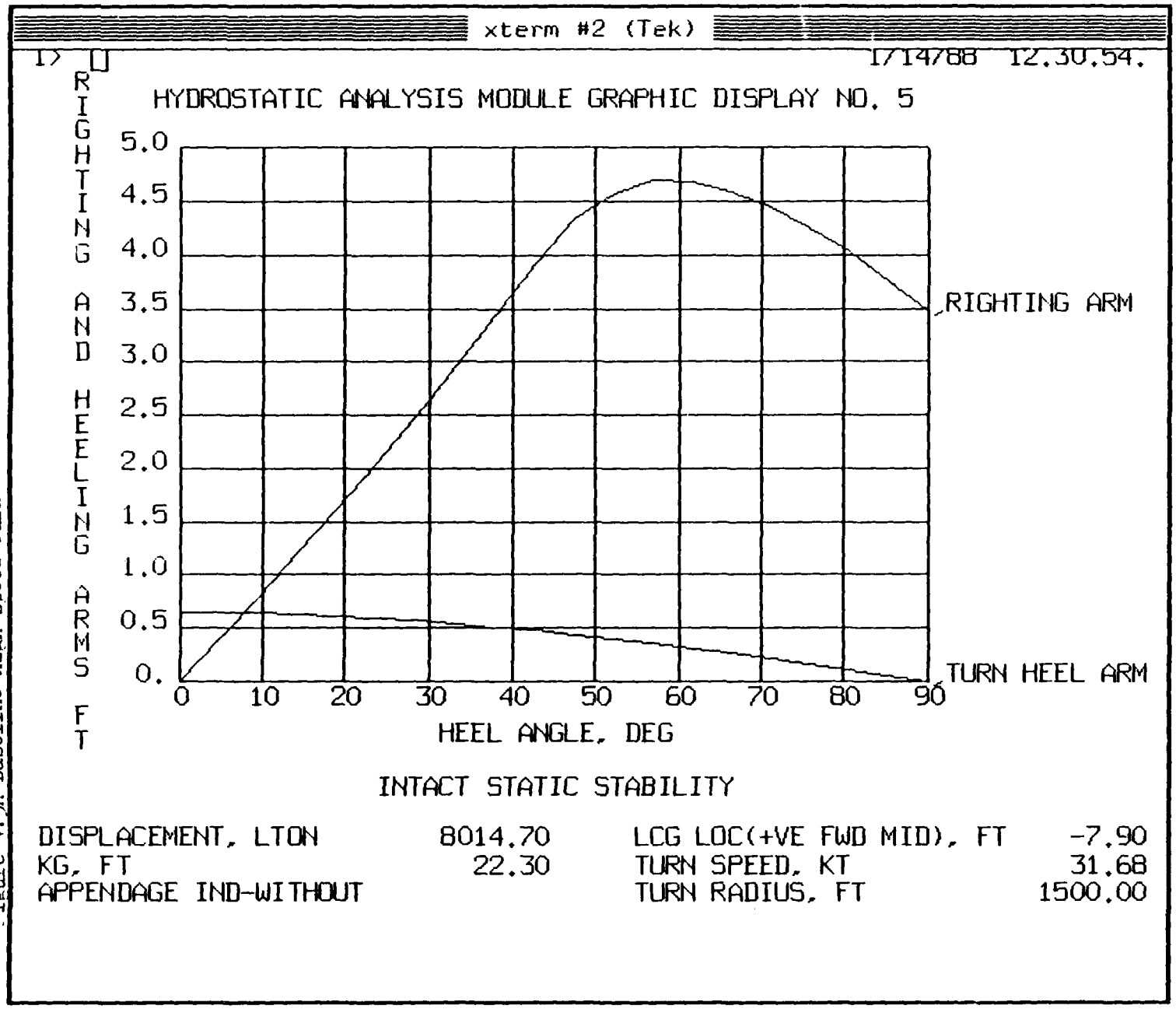

Figure 4.3A Baseline High Speed Turn

Figure 4.3B High Speed Turn For Electric Drive

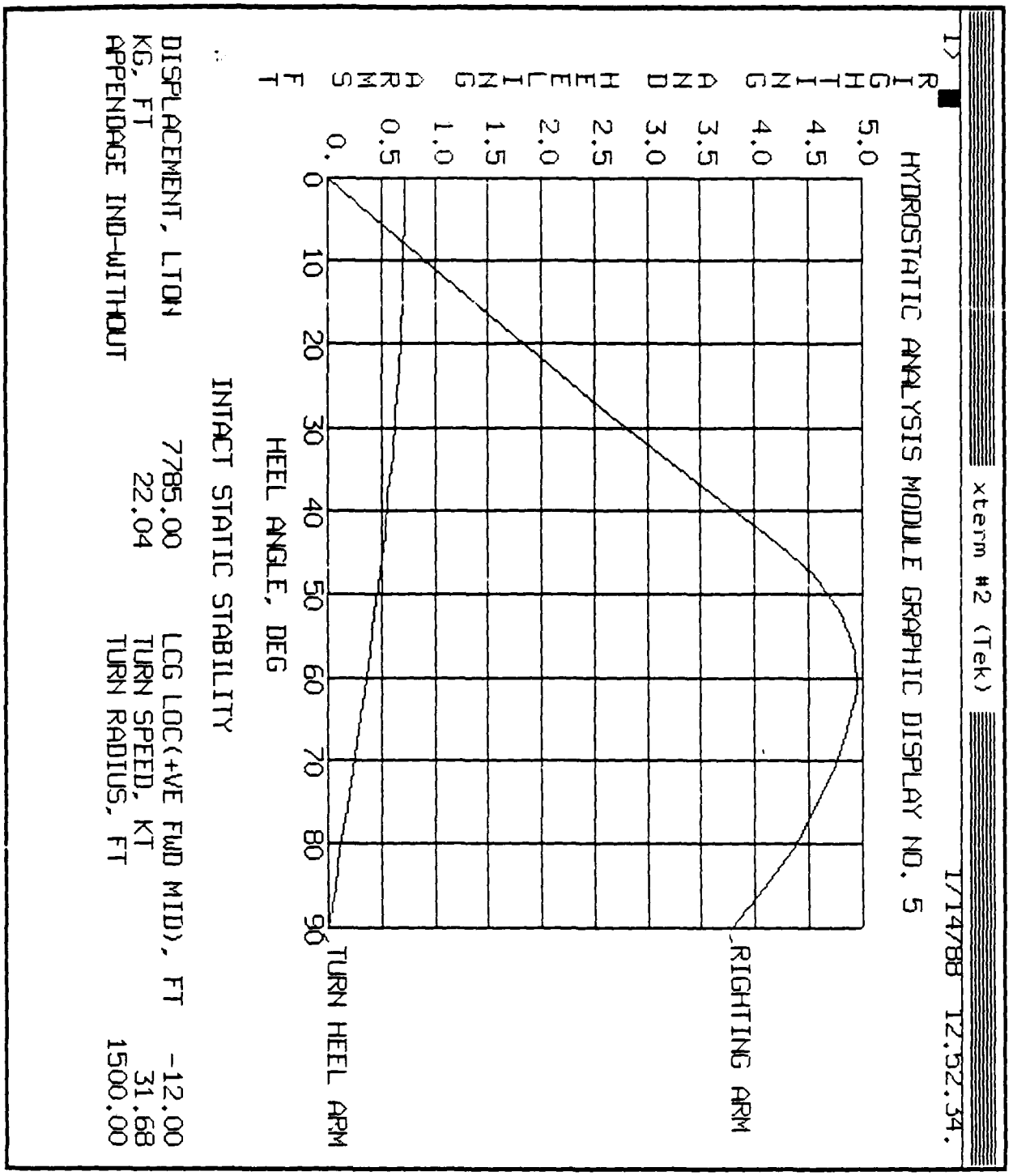

Figure 4.3C Baseline Wind Heeling Arm

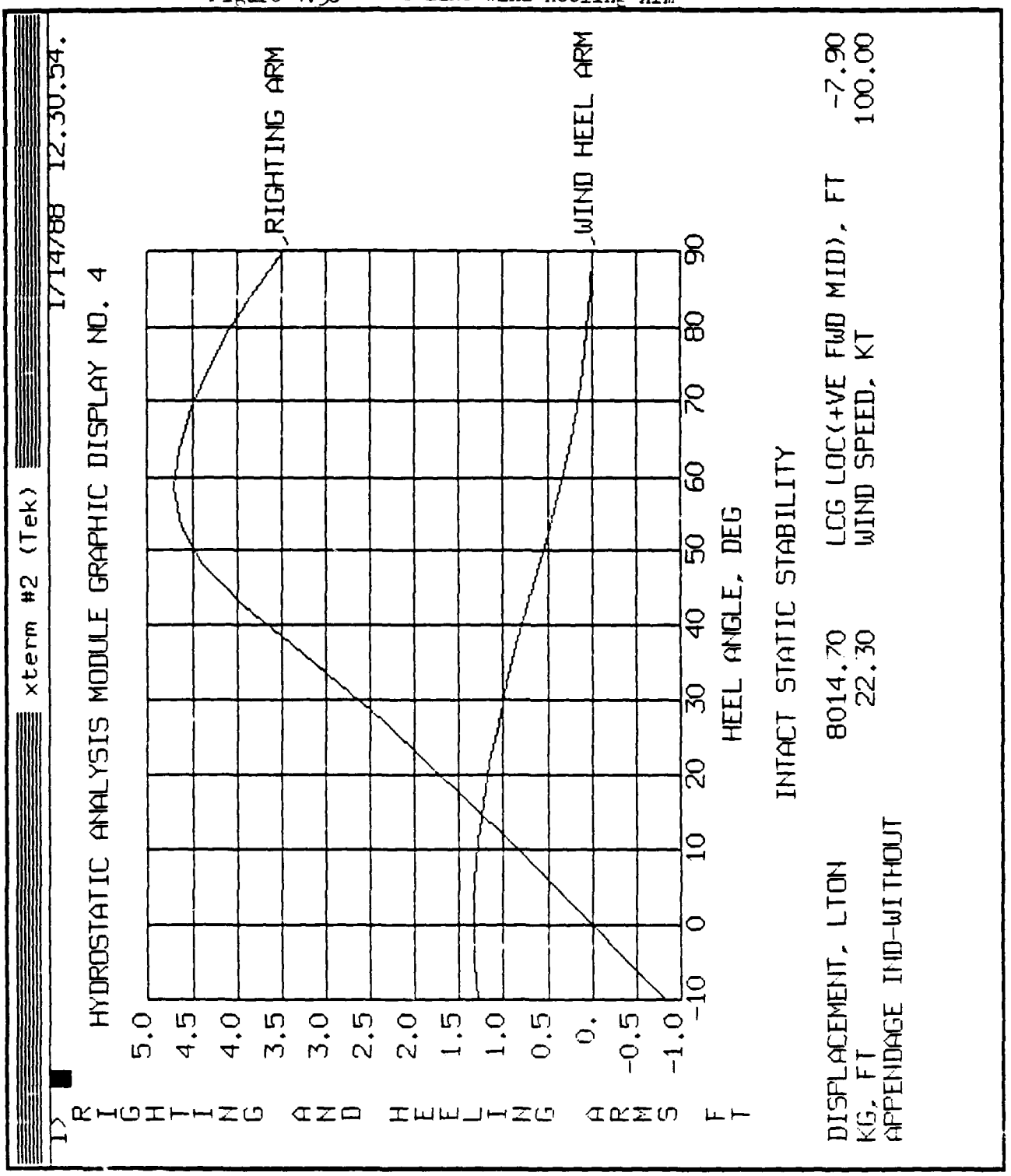

Figure 4.3D Electric Drive Wind Heeling Arm

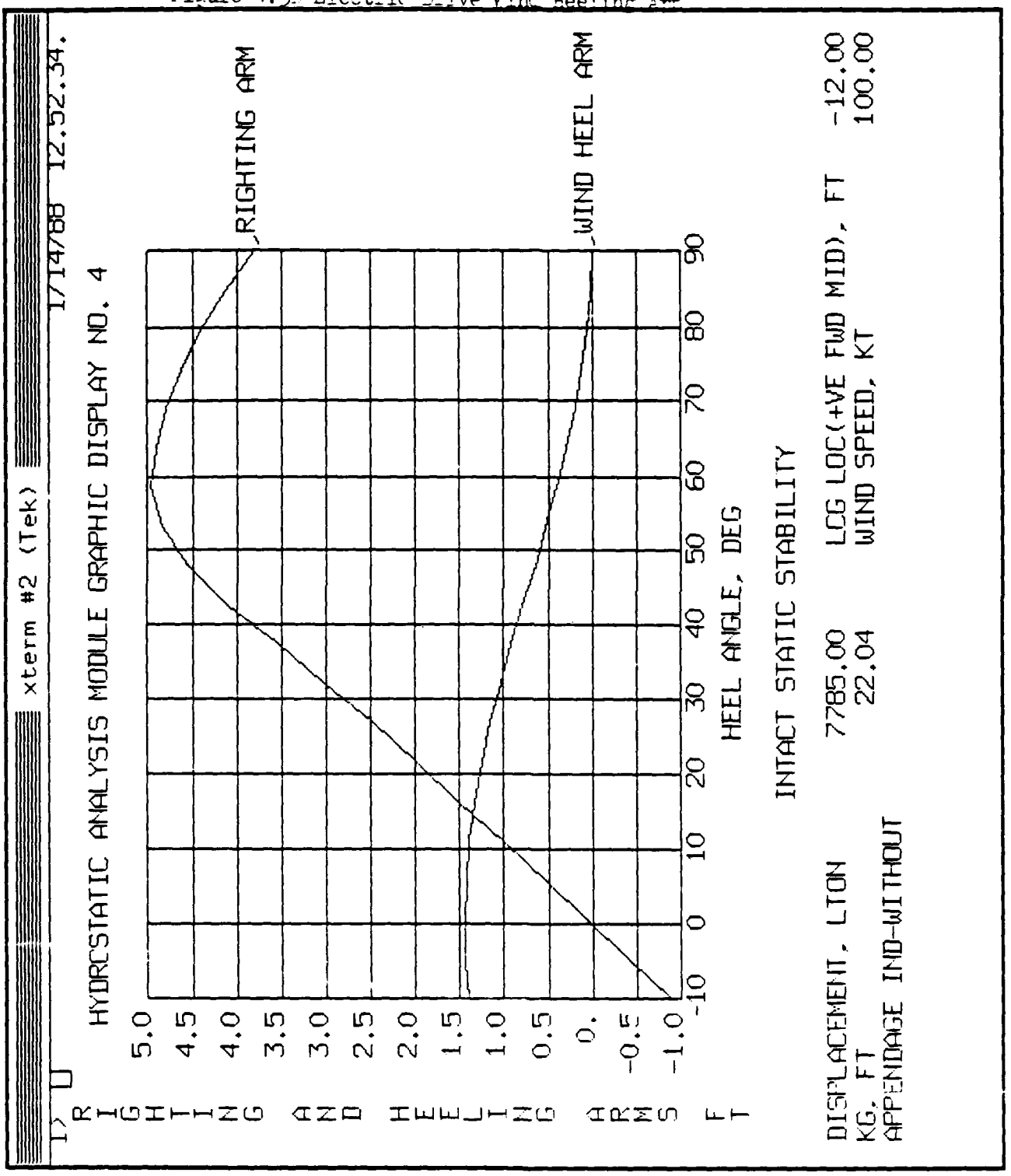

Figure 4.3E Baseline Damage Stability

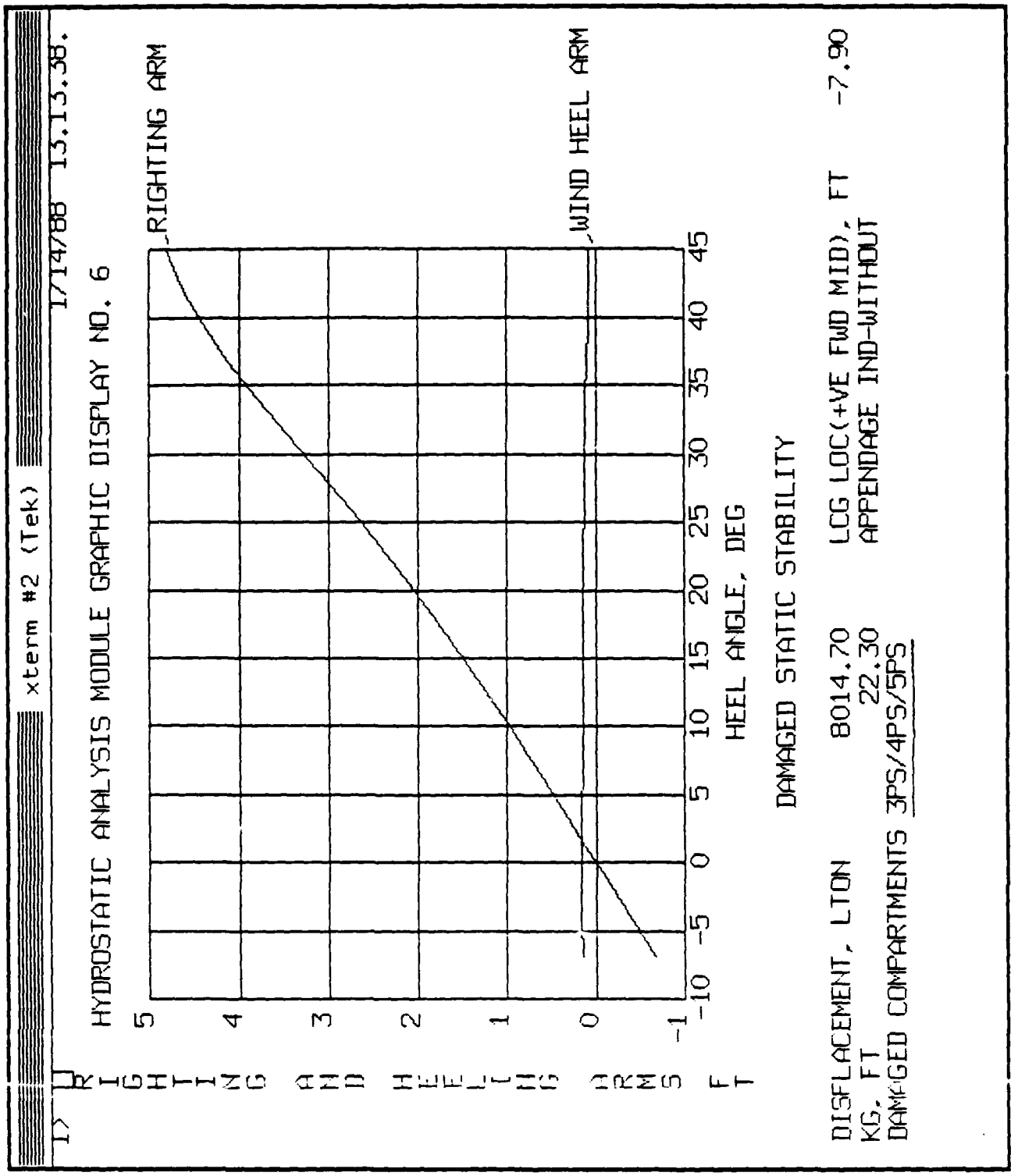

Figure 4.3F Electric Drive Damage Stability

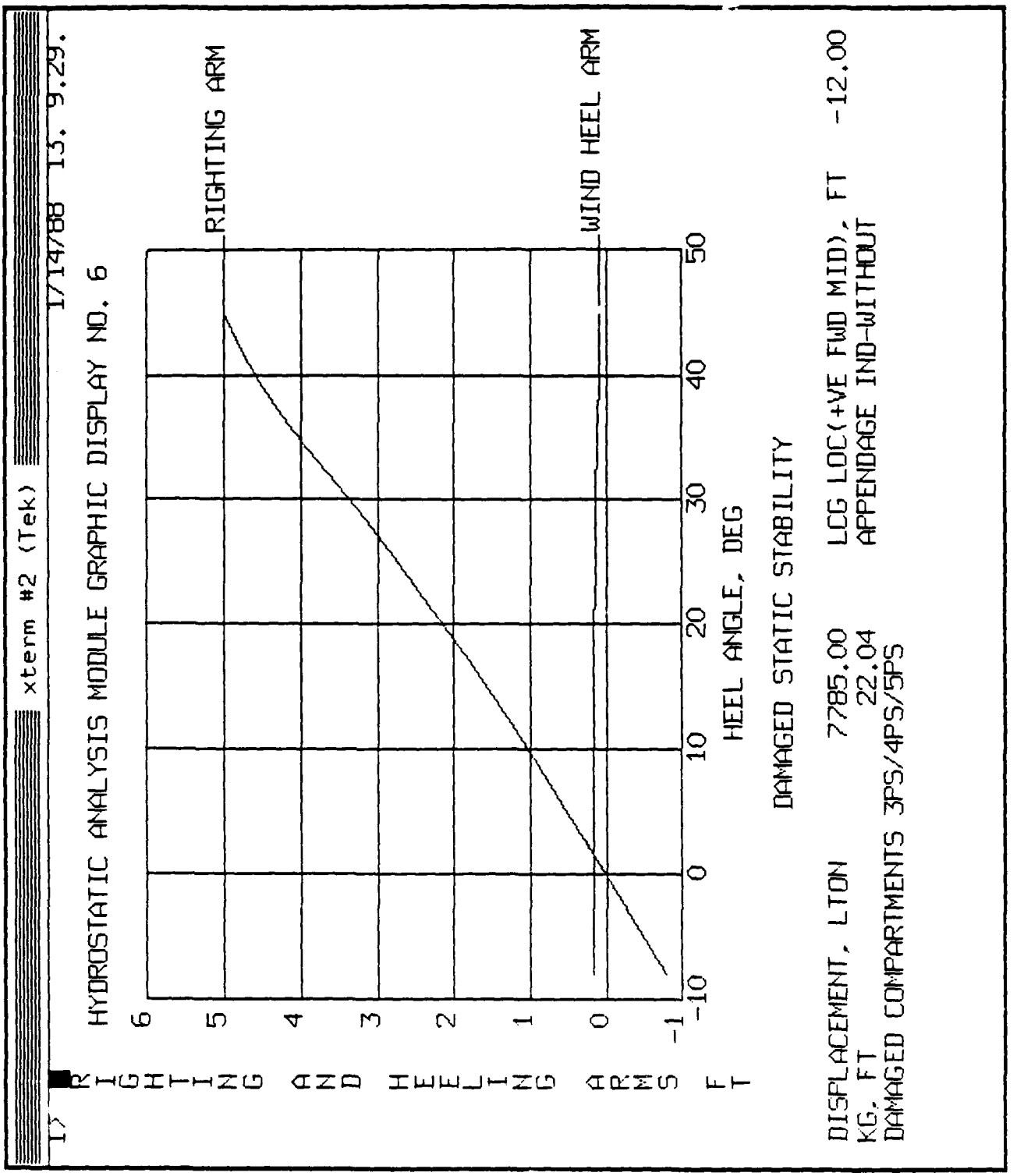

4 ENERGY

The existing mechanically driven DD963 has 80,000 HP available for propulsion provided by four HP LM-2500 gas turbines. A total of 6,000 KW is available for electrical generation from three smaller gas turbines and the majority of the auxiliary equipment is powered by the heat generated by three waste heat boilers. In contrast to this, all five gas turbines power generators of the electrically driven DD963 feed into an integrated electrical distribution system. The three 26,250 HP LM-2500's and two 2681 HP (2,000 KW) gas turbines produce a total of 84,112 HP which is used to power both propulsion requirements and ship's service electrical demand. In the worst case condition, the highest ship's service electrical load is estimated to be 4,273 KW (5,728 HP) (MIT 13A vault.) This still allows 78,834 HP available for propulsion. Conversely, when the ship is operating at endurance speed (20 knots) only 10,232 HP are required for propulsion which allows 55,114 KW (73,880 HP) available for electrical loads. Thus the integrated electrical distribution ship will be able to meet all combat system energy demands of the current DD963 with up to three gas turbines out of commission and still be able to make way through the water. The ability to provide large amounts of energy at slower speeds could be very useful for future weapons systems requiring high energy levels.

The speed of the electrically driven DD963 is expected to remain constant or increase slightly due to; no changes to the underwater hull form, the slight reduction in overall displacement (-2.83%), the installation of a more efficient propeller, and having approximately the same amount of horse power available (-1.5%) to drive the ship. Due to the small magnitude of these changes, no attempt was made to quantify an estimated change in speed.

5 PERFORMANCE

1. SURVIVABILITY:

In keeping with the initial design of the DD963, survivability was of prime concern and often was the deciding factor in all conversion design decision tradeoffs. The replacement of 146 feet of shafting with parallel path electrical cables improved the survivability of the ship considerably. The placement of the superconducting propulsion motors in the aft shaft alleys, much closer to the propeller than the existing reduction gears also improved survivability. Four separate liquid helium compressors were installed in the ship each with the ability to be cross connected to increase system reliability. Although the superconducting variant of the DD963 has two fewer gas turbines (three vs four propulsion and two vs three ship's service), the flexibility offered by the integrated electrical distribution system is more than compensated for since it allows much greater flexibility in the selection of prime movers required to be operational. Additionally, the replacement of the mechanical reduction gears with electric machinery is expected to considerably lower the self-radiated noise signature of the ship.

2. EFFICIENCY

The conversion to electric drive using superconducting machinery with an integrated electrical distribution system is expected to increase the propulsion plant overall efficiency by three percent. This is based on the fact that 20,000 to 26,250 SHP superconducting AC generators have been estimated to be 98.5% efficient (Schmucker,1988) while superconducting DC homopolar machines are 97.8% (Doyle, Green, Raphael, & Robey, 1980) as compared to the existing reduction gears which are estimated to be 98% efficient due to the inherent one percent inefficiency per reduction stage. Additionally, the change from CRP to fixed pitch propellers is expected to provide a 2.5% increase in efficiency (St. John, 1978.)

3. ENDURANCE

An increase in the overall range of the electrically driven as compared to the existing mechanically driven configuration is based on:

- fuel tankage capacity and the amount of fuel carried onboard will remain constant.

- the SFC of the electrically driven DD963 will be significantly less than the existing configuration due to the integrated electrical distribution system which will allow the most efficient loading of the operational gas turbines rather than requiring a minimum of one LM-2500 per shaft and two 2,000 KW gas turbine driven generators operational whenever underway.

-.The endurance horsepower required for the mechanically driven DD963 is 10,548 HP (St. John, 1978) which represents 5,274 HP required for each shaft. The average electrical load for ship's service needs is 1,600 KW. Based on a SFC of 0.64 lbs/Hp-hr for the LM-2500 gas turbines, 0.96 lbs/KW-hr for the 2,000 KW ship's service generators, and the total ship fuel tankage of 1606 tons, the endurance range of the mechanically driven DD963 is 6,000 NM (MIT 13A vault data.)

- As a result of the reduced displacement and more efficient propeller, it is estimated that the electrically driven DD963 will have an endurance horsepower requirement of 10,232 HP (-3.0%.) Due to the implementation of ship alt DD963-452K (all electric auxiliaries) the average electrical load for ship's services is estimated to be 2,839 KW (+77%.) Based on a SFC of 0.50 lbs/HP-hr for the LM-2500 gas turbines, 0.67 lbs/KW-hr for the 2,000 KW generators, and the total ship fuel tankage of 1,606 tons, the endurance range of the electrically driven DD963 was computed to be 10,251 NM (Table 4.8.)

TABLE 4.8 ENDURANCE CALCULATIONS

MECHANICAL DRIVE
RANGE/SPEED=TIME
6000 MILES/ 20 KNOTS=300 HOURS
TONS OF FUEL REQUIRED= (SFC) (ENDURANCE HP) (HRS) (TONS/LBS) FOR PROPULSION
=(.64) (10548) (300) (1/2240)=904 TONS
ELECTRICAL DRIVE
FIND THE TOTAL HOURS ABLE TO OPERATE AT 20 KNOTS WITH A 2839 KW
ELECTRICAL LOAD.
(SFC) (10232)(HOURS)(1/2240)+(.67)(2839)(HOURS)(1/2240)=1606
HOURS=513
ENDURANCE RANGE=(513HOURS)(20 KNOTS)=10251 MILES

c. MANNING

Presently, the DD963 has a total crew complement of 296 people, consisting of 24 officers, 21 chief petty officers, and 251 enlisted personnel. The engineering department accounts for 54 of these billets. A normal underway engineering watch section consists of ten people; five watch standers in the Central Control Station (CCS), two in each main engine room and one engineman for auxiliary equipment. The conversion of the DD963 to electric drive would have no net impact on the total ship complement nor that of the engineering department. The only difference would be a few changes to the required NEC's to provide sufficient skills and training for plant operation and maintenance for the different machinery arrangements.The addition of superconducting motors and generators and the expanded electrical distribution system associated with an integrated electrical system would require three additional electrician mates (EM's.) However, with the removal of the mechanical drive system, two gas turbines, and three waste heat boilers, the ship would require three fewer Gas Turbine Technicians (GT's.)

Additional training would be required for at least two electrician mates in the operation and maintenance of superconducting machinery. While there would no longer be the need for hydraulic training for the CRP's, at least two people would require training in the operation and maintenance of cryogenic systems.

4.6 SUPERCONDUCTING REFRIGERATION SYSTEM

a. INTRODUCTION

The methodology used for the DD-963 refrigeration system is presented in this section. For a shipboard cryogenic system there are three major issues that need to be investigated. First, helium must be transferred from the gas to the liquid state. Then it must be delivered to

the field winding. Finally, the boil off gas must be recovered in order to conserve the supply of helium.

Since minimizing conductive and convective losses are paramount, a vacuum is used to form an insulation shield. It is estimated that an appreciable portion of the liquefier output will be lost in vaporization caused by heat leakage before it ever reaches the superconducting coil. An advantage of liquid helium over other cryogenic fluids is its low viscosity. This permits ease of transfer with only a small pressure differential. The vacuum insulation jacket surrounding the liquid helium piping can be kept to a minimum.

b. METHODS OF CRYOGENIC COOLING

1. POOL BOILING VERSUS LIQUID IMMERSION

In a pool boiling cryogenic system the superconducting coil is maintained in the lower part of the cryostat. Cooling is accomplished by direct heat transfer between the coil and the liquid for the immersed part of the coil and between the coil and boil-off vapors for the unimmersed part. This is the most common method of cooling superconducting coils.

In a liquid immersion system, small superconducting coils are cooled by total immersion in liquid helium. This system is used primarily for experimental coils. Typically, the dewar is filled with sufficient liquid to last for the duration of the test. This method also provides a large heat absorption capacity so that the risk of coil damage due to heat release during a quench is greatly reduced.

In both the pool boiling and liquid immersion system a closed cycle is involved to recycle the helium. The liquid helium is boiled off at 4.2 degrees Kelvin to remove heat from the winding. The boil-off gas is used in the heat exchanger of a liquefier to produce more liquid. When an appreciable portion of the cooling capacity of the cold gas has been

the field winding. Finally, the boil off gas must be recovered in order to conserve the supply of helium.

Since minimizing conductive and convective losses are paramount, a vacuum is used to form an insulation shield. It is estimated that an appreciable portion of the liquefier output will be lost in vaporization caused by heat leakage before it ever reaches the superconducting coil. An advantage of liquid helium over other cryogenic fluids is its low viscosity. This permits ease of transfer with only a small pressure differential. The vacuum insulation jacket surrounding the liquid helium piping can be kept to a minimum.

extracted, it is returned to the compressor for recycling through the liquefier.

2. SUPERCRITICAL HELIUM

Supercritical helium is advantageous where the superconducting windings are located far away from the helium production plant. By using supercritical helium, the diameter of the transfer line can be kept to a minimum. Losses are also negligible. The use of supercritical helium reduces the storage requirements such that smaller helium inventories are required. Supercritical helium is actually a single-phase fluid that is not a liquid and is not a gas.

c. COOL-DOWN OF SUPERCONDUCTING COIL

The ultimate objective of the cool-down gas is to cool the magnet coil from room temperature (approximately 300 degrees Kelvin) to 4.2 degrees Kelvin.

This can be accomplished by two different methods. The first method is when large quantities of liquid helium are taken from a storage dewar. The second method uses a cold gas taken from a liquefier equipped with a large capacity cool-down expansion engine. For the second method,

considerably smaller quantities of liquid will be required for the final stage of cool-down. For both methods, procedures must be established for handling large quantities of gas.

It is necessary for superconducting magnets to be cooled to cryogenic temperatures and maintained at this low state the majority of the time. Exceptions are overhaul periods and field winding failures. During conditions such as a magnetic quench the system must be designed to return to cryogenic temperature (approximately 4.2 degrees Kelvin). The quench causes large amounts of magnetic heat to be generated such that the fluid can rise to considerably high temperatures. (Messinger, H., Clarke, P.B. and Bowen, W.H., 1982)

The first method in which liquid helium is used to cool the magnet is very inefficient . However, method number two uses cold helium gas from an expansion mechanism to a low temperature (approximately 30 degrees Kelvin). Liquid helium is then used during the final phase of cooling. Method number two is considerably faster than method number one. However, this method requires a separate cool-down engine.

Geofrey Green (1987) of David Taylor Naval Research Laboratories estimates that cooling with cold gas is over four times faster than cooling by liquid helium for the same power input. The application of Geofrey Green's efforts with respect to a shipboard propulsion system will be discussed below. Figure 4.4 and 4.5 illustrate a schematic that is suitable in describing the flow pattern for the cool-down to 30 degrees Kelvin. Then the gas is transferred to the compressor inlet via the counter flow heat exhanger.

The expansion engine is the brains of the operation. Dr S.C. Collins is the father of the expansion engine. The system that he designed is shown in figure 4.6. The cool-down engine consists of an expansion piston, a hydraulic piston and accumulation for extracting the energy of expansion and several pneumatically operated valves. For the hydraulic expansion

engine, the expanding helium gas forces oil through a restriction. The piston of the helium engine is connected coaxially to the piston of a hydraulic cylinder. Oil is transferred from the hydraulic cylinder into the oil accumulator during the power stroke In the accumulator is a piston in which the trapped air from the power stroke pushes oil in the hydraulic cylinder during the discharge stroke of the helium engine.

Collins designed this system such that the pressure of the expanding gas falls to approximately one atmosphere before opening the discharge valve. The air pressure in the accumulator may be as high as six atmospheres. Despite the opposing pressure in the accumulator the momentum causes the expanding piston to complete the power stroke. From figure 4.7, valve 3 is open while valve 2 is used to adjust the speed of the expansion engine. Inlet valve 3 is closed at approximately seventy percent of the expansion stroke. The function of valve 5 is to allow a large quantity of oil to flow rapidly to the accumulator. Valve 5 opens once valve 3 is closed. The helium piston accelerates but then is slowed down by the pressure developed in the accumulator. The helium piston changes direction once the accumulator develops sufficient pressure. Throttle valve 1 is used to control the speed of the helium piston during the discharge stroke. Inlet valve 3 is opened before the piston reaches the bottom of its stroke in order to prevent the piston from hitting the cylinder head.

Compressed air at 80 psig is used to operate valves 3,4, and 5. Valve 5 opens immediately during the compression stroke while the expansion of the helium gas is nearly complete when valve 4 opens. During the discharge stroke, the opening of the inlet valve and closing of the discharge valve and blowdown valve occur simultaneously. Figure 4.8 illustrates the P-V diagram for the cool-down engine.

As stated earlier, cooling with cold gas is over four times faster than cooling with liquid helium. The tradeoffs between inward verses outward cooling will be examined. When cooling gas is directed through

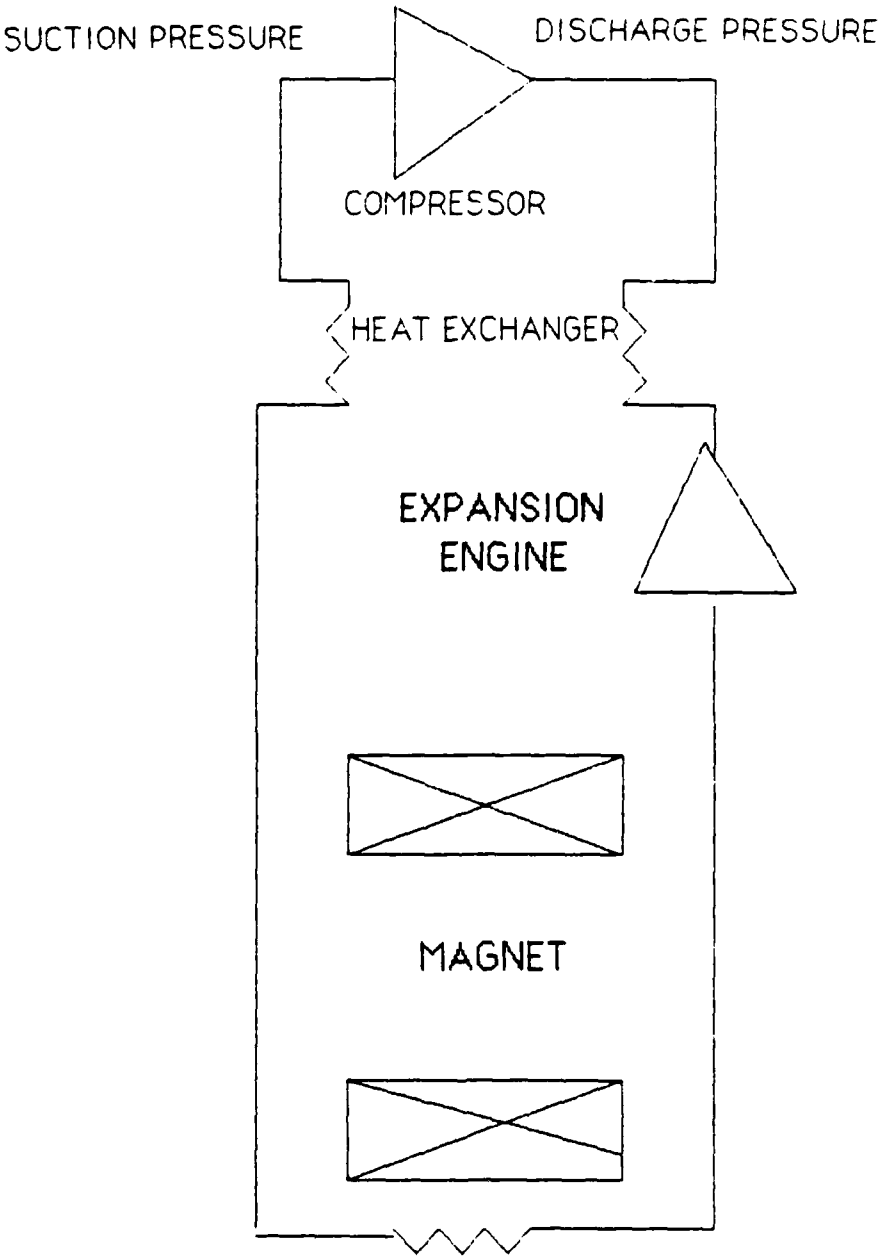

COOL DOWN SYSTEM ARRANGEMENT
FIGURE 4.4

FIGURE 4.5
COOLDOWN OF SUPERCONDUCTING COIL

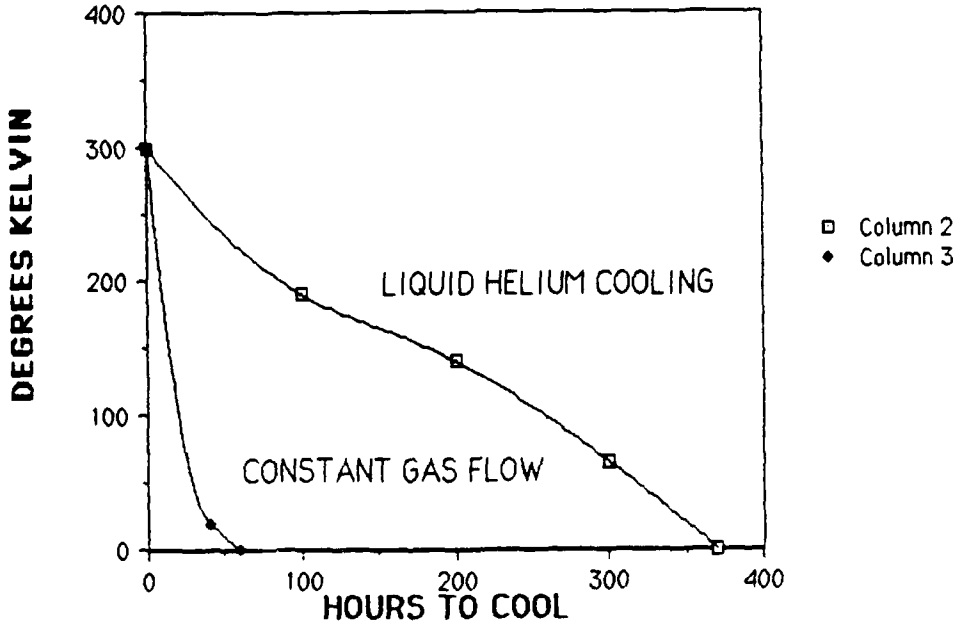

IDEAL EXPANSION ENGINE PERFORMANCE

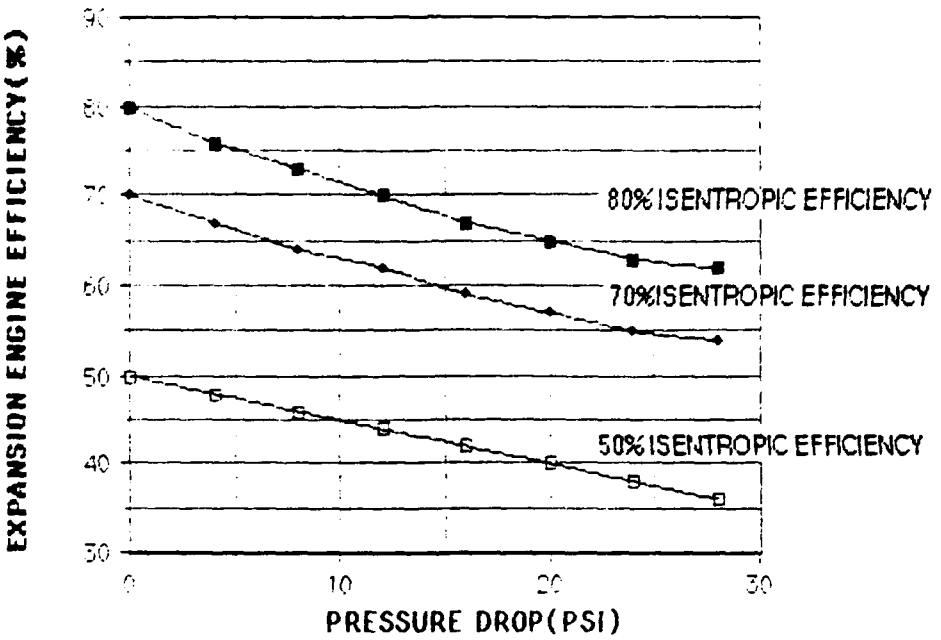

FIGURE 4.6

FIGURE 4.7
HYDRULICALLY CONTROLLED
COOL-DOWN ENGINE

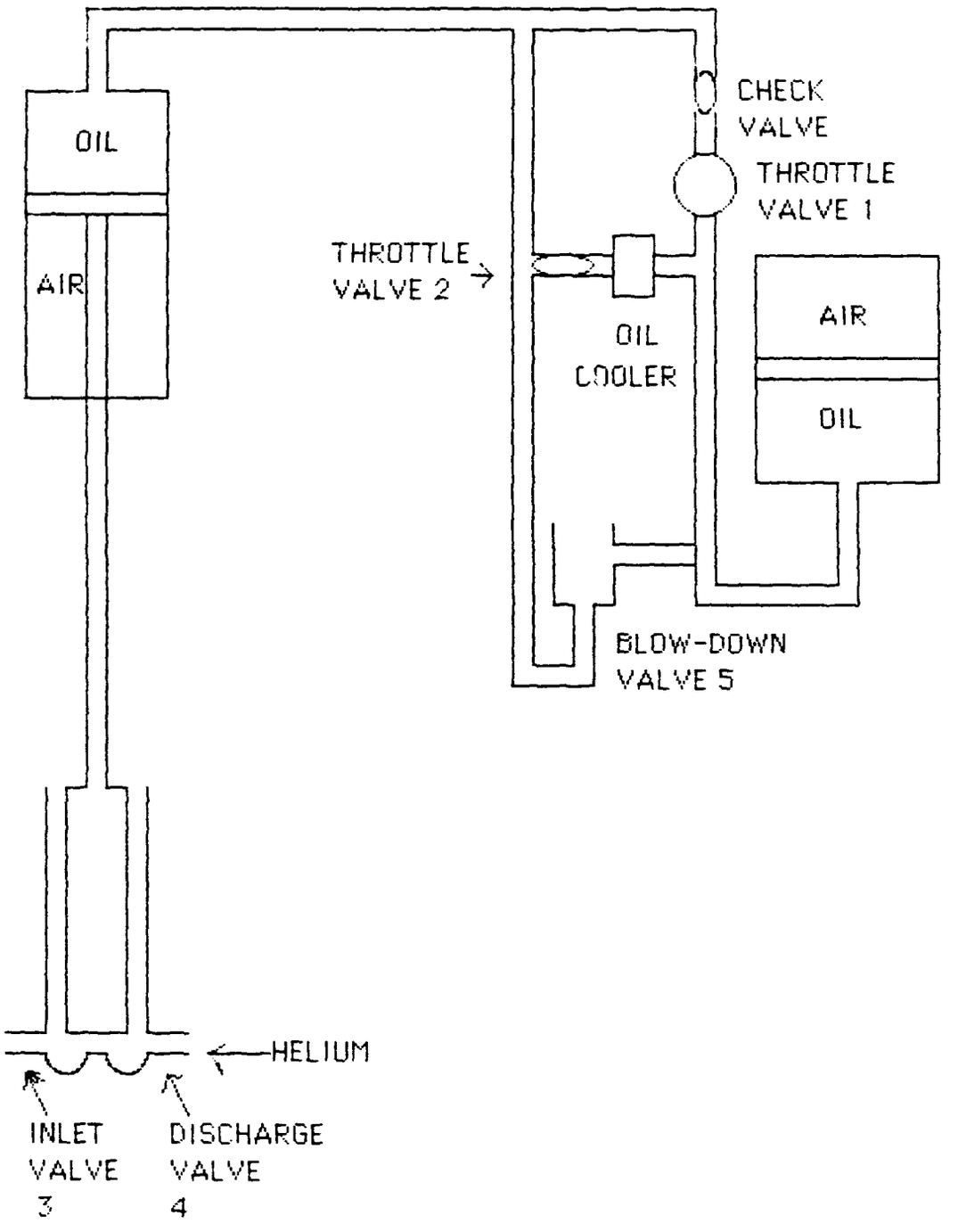

d. REFRIGERATION SYSTEM REQUIREMENTS

The objective in this section is to point out the trade-offs involved in selecting various compressor and liquefier combinations. Green provided specific component capacities and system operation information for two 40,000 HP superconducting motors. (Green, G., 1987) A twin screw system is more complex than a single screw system since liquid helium must be supplied to two propulsion motors at a constant flow rate.

As stated earlier a quench of a superconducting coil results in either a partial or complete vaporization of the liquid helium in the dewar due to the large amount of heat generated. It is estimated that 50 liters of liquid helium will be lost in the event of a quench in a 40,000 HP motor coil. Since loss of 50 liters of liquid helium will be very costly a system to recover the helium appears necessary. An emergency balloon apparatus or a fixed containment system are two alternatives.

Next, various helium systems were examined. The systems that will be discussed are 1) the separate helium system, 2) shared compressor system and 3) combination system.

Figure 4.11 illustrates a system with separate liquifiers and compressors. Both systems are completely independent. The inability to cross connect makes this system inefficient. However, contamination transfer from one system to another will not occur.

The shared compressor system is shown in figure 4.12. In this system, the compressors are connected in parallel such that a wide variation in helium gas flow rate can be achieved. System reliability is improved since failure of one compressor can be compensated for by the use of the other compressors. The cool-down can be accelerated by the use of two compressors. Once cool-down is achieved, one compressor can be shut down while the other compressor can stay available for steady-state

FIGURE4.8
P-V DIAGRAM FOR THE COOLDOWN ENGINE

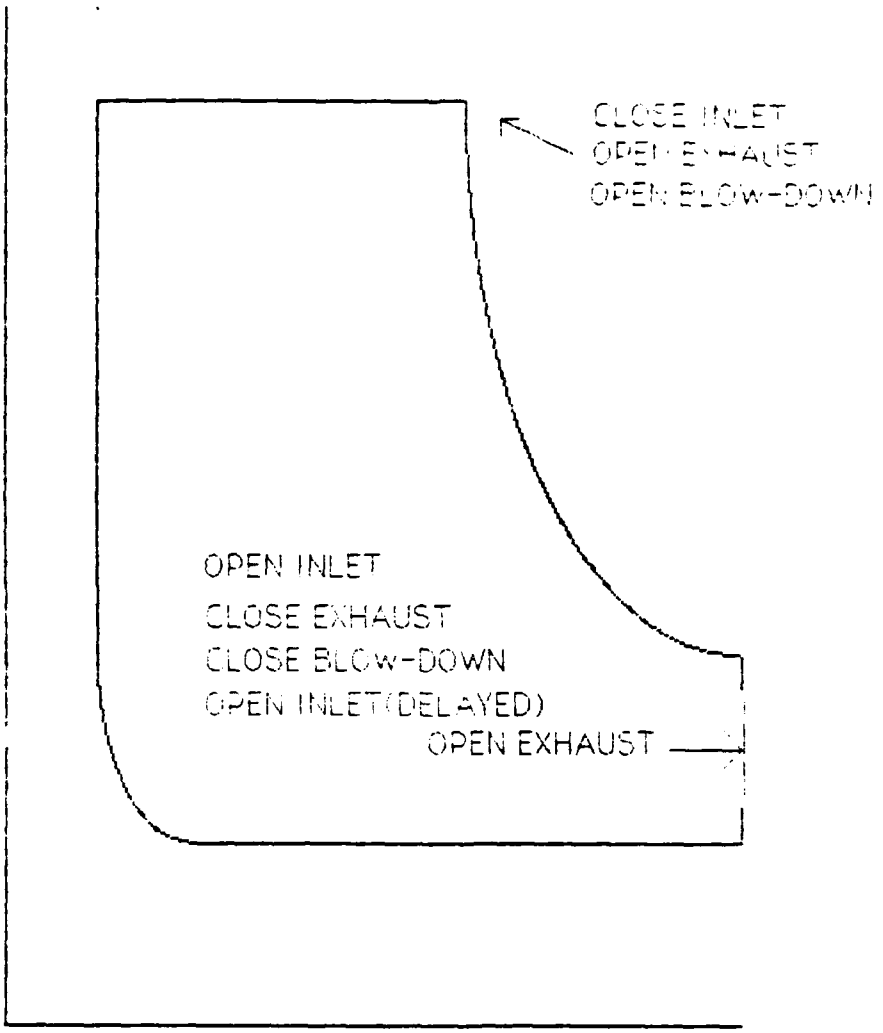

FIGURE 4.9

SUPERCONDUCTING MACHINE DESIGN

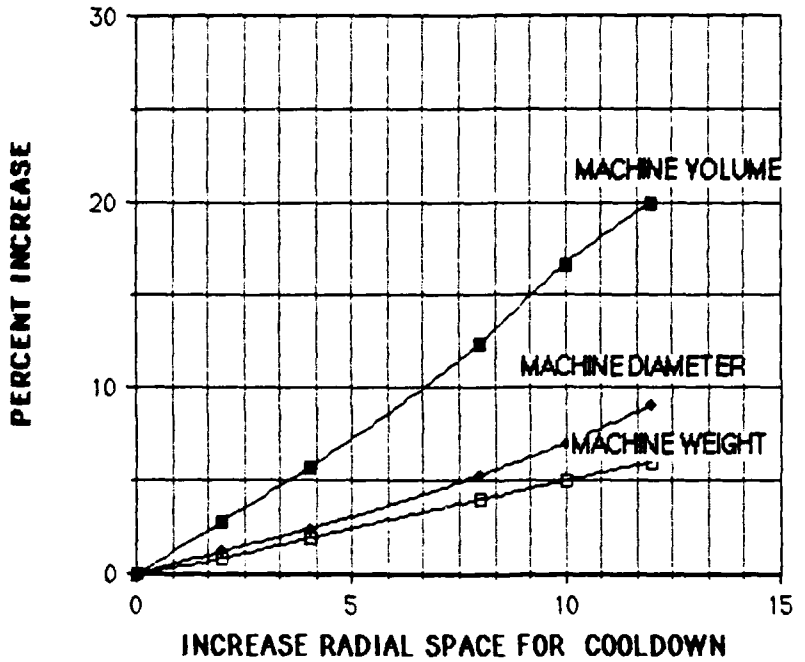

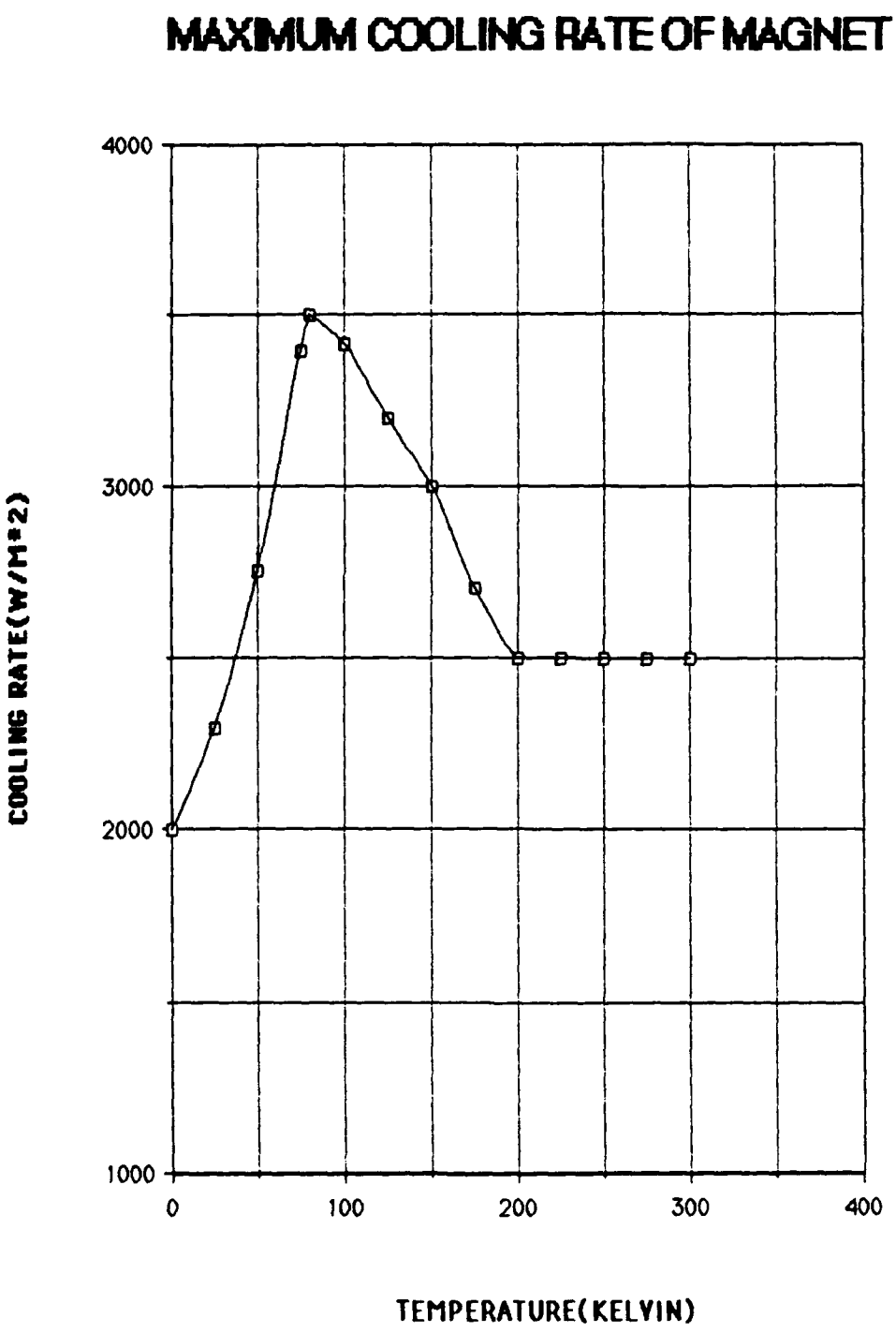
MAXIMUM COOLING RATE OF MAGNET
4000
3000
2000
1000
COOLING RATE(W/M**2)
0
100
200
300
400
TEMPERATURE(KELVIN)

FIGURE 4.10

liquid production. The disadvantage of this system is that contamination can be easily transferred from one system to another.

The combination system shown in figure 4.13 is used to provide an additional compressor and liquefier. The storage dewar is filled with liquid helium and is physically transferred to the location of the motor during a liquefier failure.

e. SELECTION OF SHIPBOARD SYSTEM

Green exmained various main shipboard helium systems with separate liquefiers. (Green, G., 1987) Various combinations to the shared compressor system appear the most suitable for a shipboard cryogenic system. The major advantages are that it provides:

1) sufficient compressor capacity to allow simultaneous cool-down of both superconducting magnet dewars,

2) safeguard against cross-contamination of liquefiers,

3) redundancy of compressors for increased system reliability.

Figure 4.14 shows a shipboard helium liquefier system to be used in conjunction with the helium system of figure 4.15. This system contains a large tank for boil-off storage along with two smaller tanks to minimize pressure surges resulting from a mismatch between helium evaporation and recondensation rates. The valves are automatically controlled by pressure, temperature and liquid level.

f. OPERATION OF SHIPBOARD HELIUM SYSTEM

The objective during this section is to discuss the specific operation of a shipboard helium system. Normal and abnormal operations will be discussed by referring to the helium system of figure 4.15. Normal operation refers to liquefier and load, liquid level buildup in the phase

separater and magnet dewar and steady-state closed cycle operation of the entire system. Abnormal operation is normally a quench of the magnet dewar. Normally, a quench does not require disconnecting from the load. However, in certain circumstances the liquefier may require disconnection from the load. A description of the valves of the shipboard helium system is shown in Table 4.9.

1 INITIAL COOL-DOWN (NORMAL OPERATION)

Helium gas at ambient temperature (300 degrees Kelvin) is cooled to liquid helium temperature. Approximately 75 cubic meters of high pressure helium gas is consumed by being converted to 100l of liquid. (Green, G., 1987)

Valves V-8 and V-9 are operated to permit flexibility of compressor use. Compressors 1 and 2 will supply helium to the starboard liquefier. Similarly, compressors 3 and 4 will supply the port liquefier. A general procedure to cool the system to cryogenic temperature is as follows:

a) Valves V-8 and V-9 are initially closed. Helium compressors 1 and 4 are started. Compressors 2 and 3 initially are not in operation.

b) Valves V-17 and V-18 are opened and valve V-19 is closed such that maximum flow is supplied to the drier.

c) Discharge gases from Engines E-1, E-2, and E-3 of figure 4.14 will return to the compressors via

d) the low pressure region of the liquefier's heat exchangers.

e) When compressor discharge pressure rises all liquefier expansion engines will start. Compressor makeup gas will flow from high-pressure storage to the compressor suction lines via valves V-16 and V-10 to maintain adequate suction pressure.

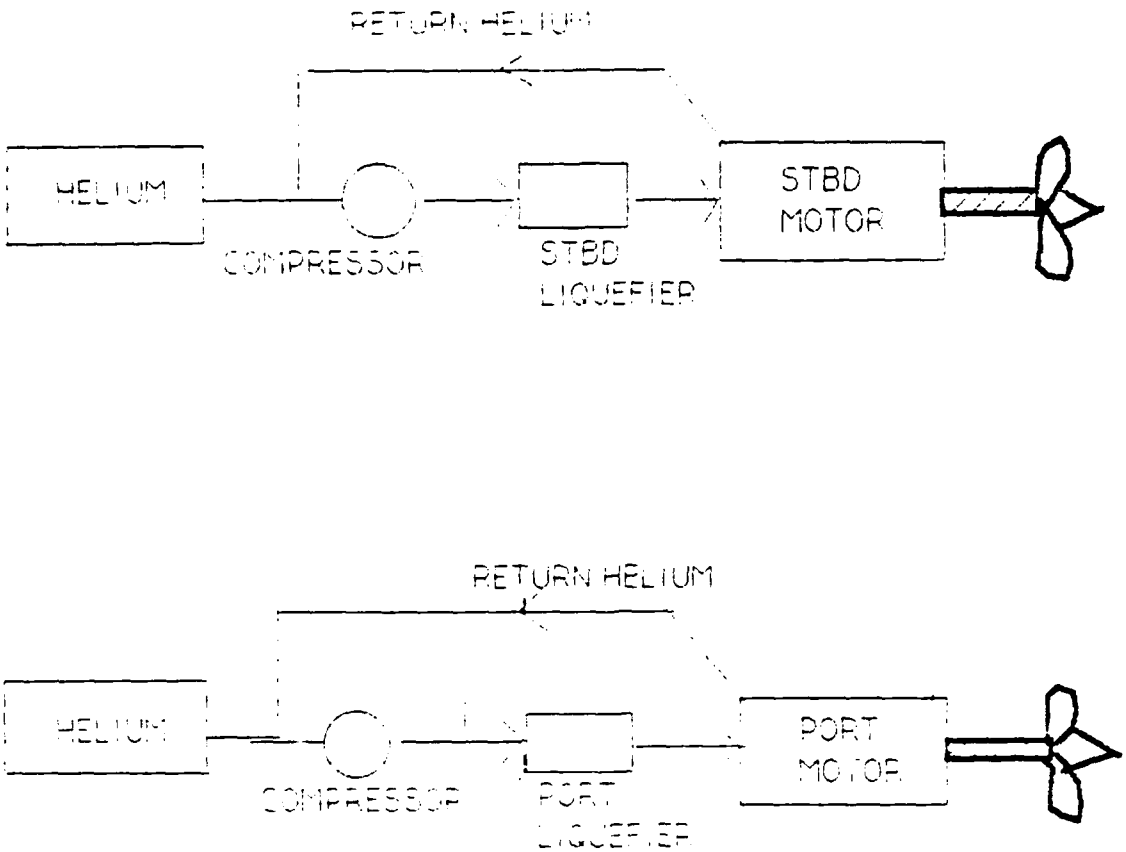

SEPERATE COMPRESSOR SYSTEM

FIGURE 4.11

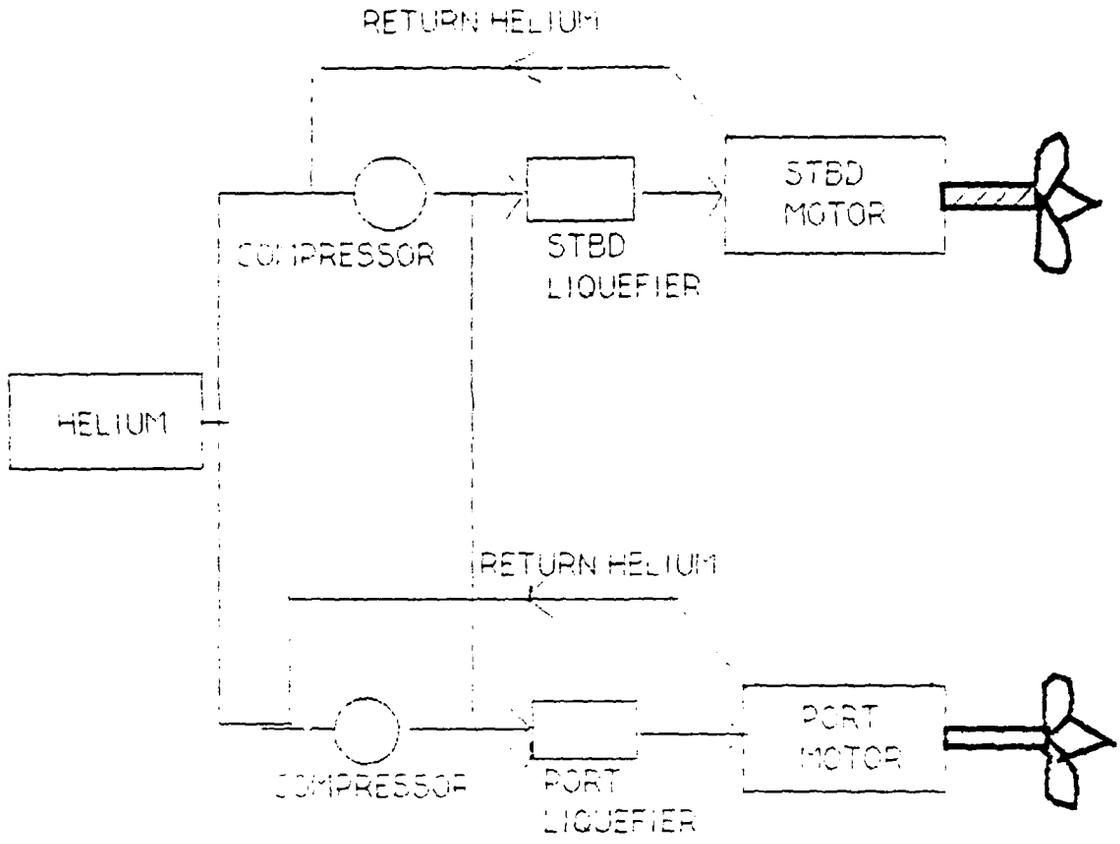

SHARED COMPRESSOR SYSTEM

FIGURE 4.12

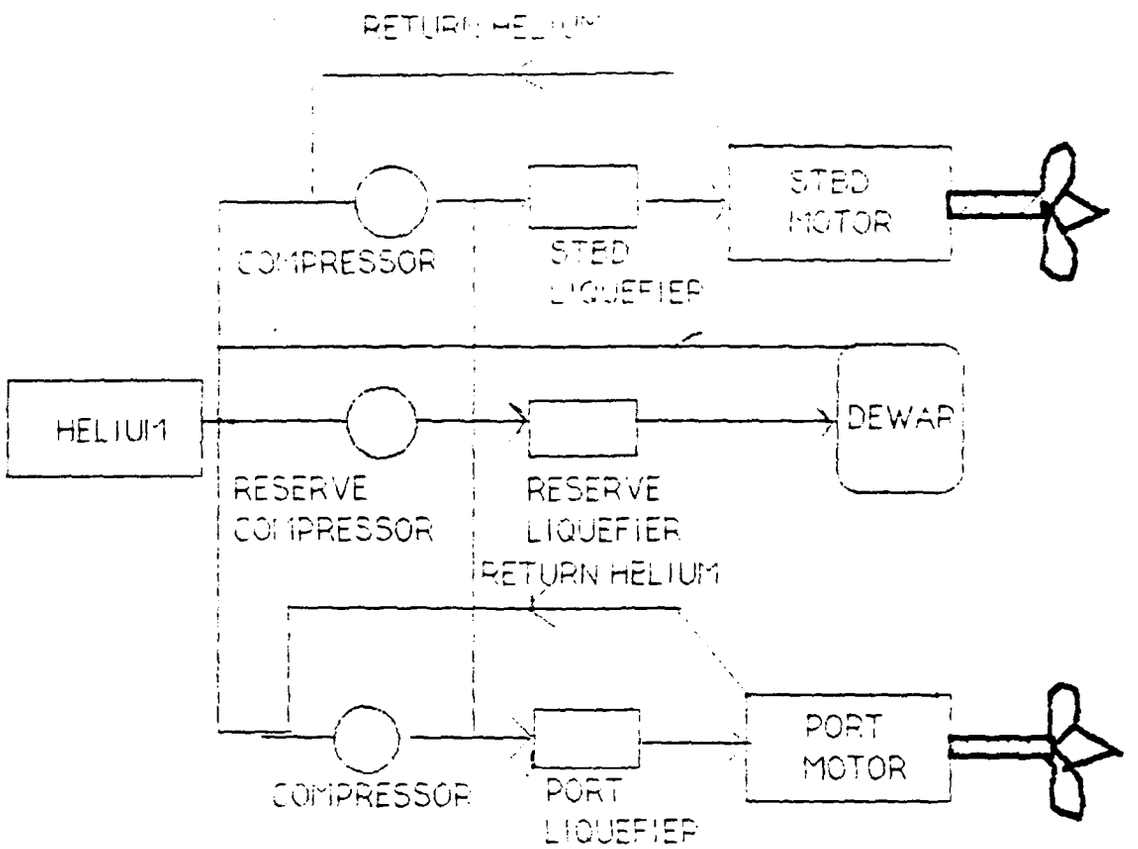

COMBINATION SYSTEM

FIGURE 4.13

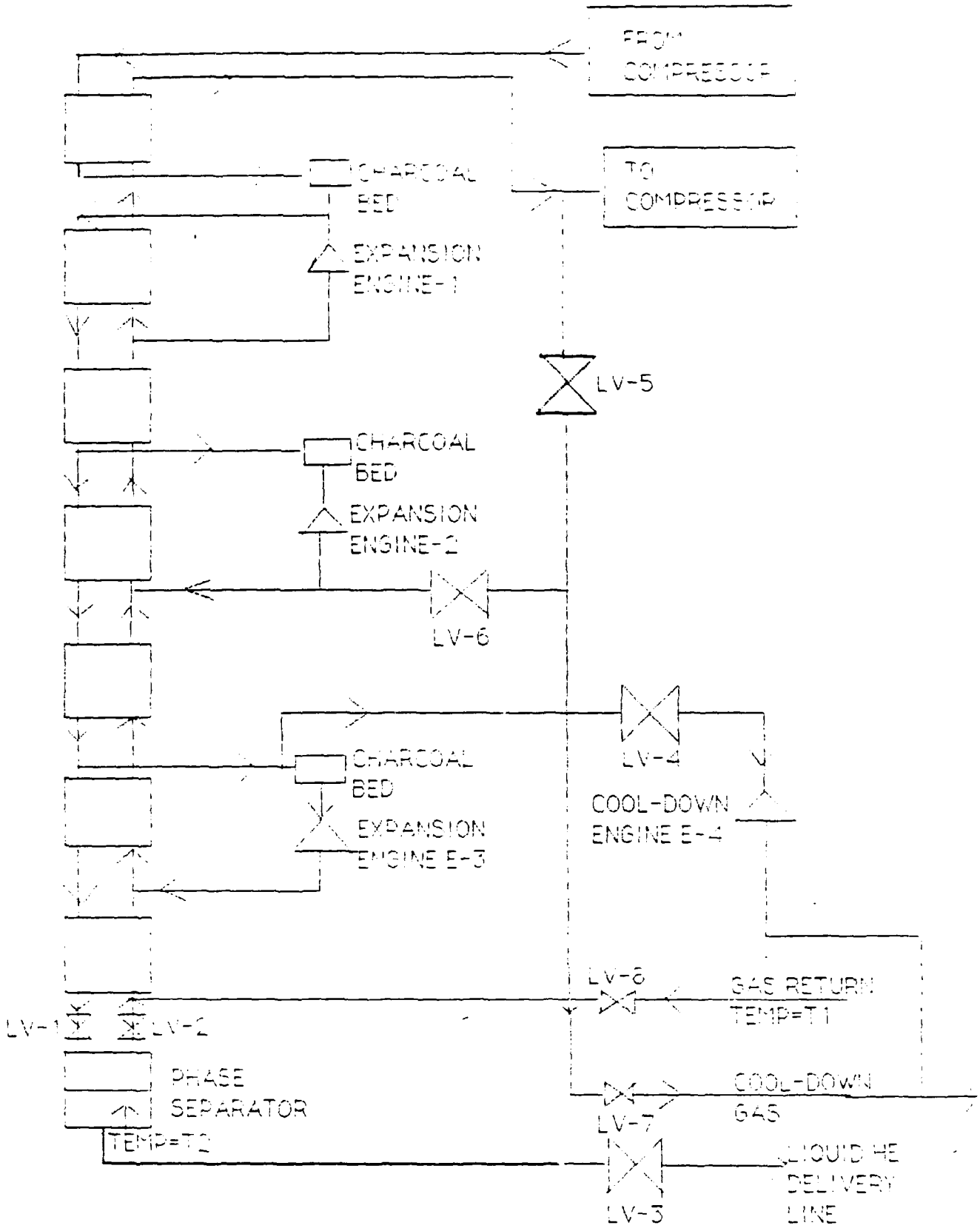

FIGURE 4.14 SHIPBOARD LIQUEFIER SYSTEM

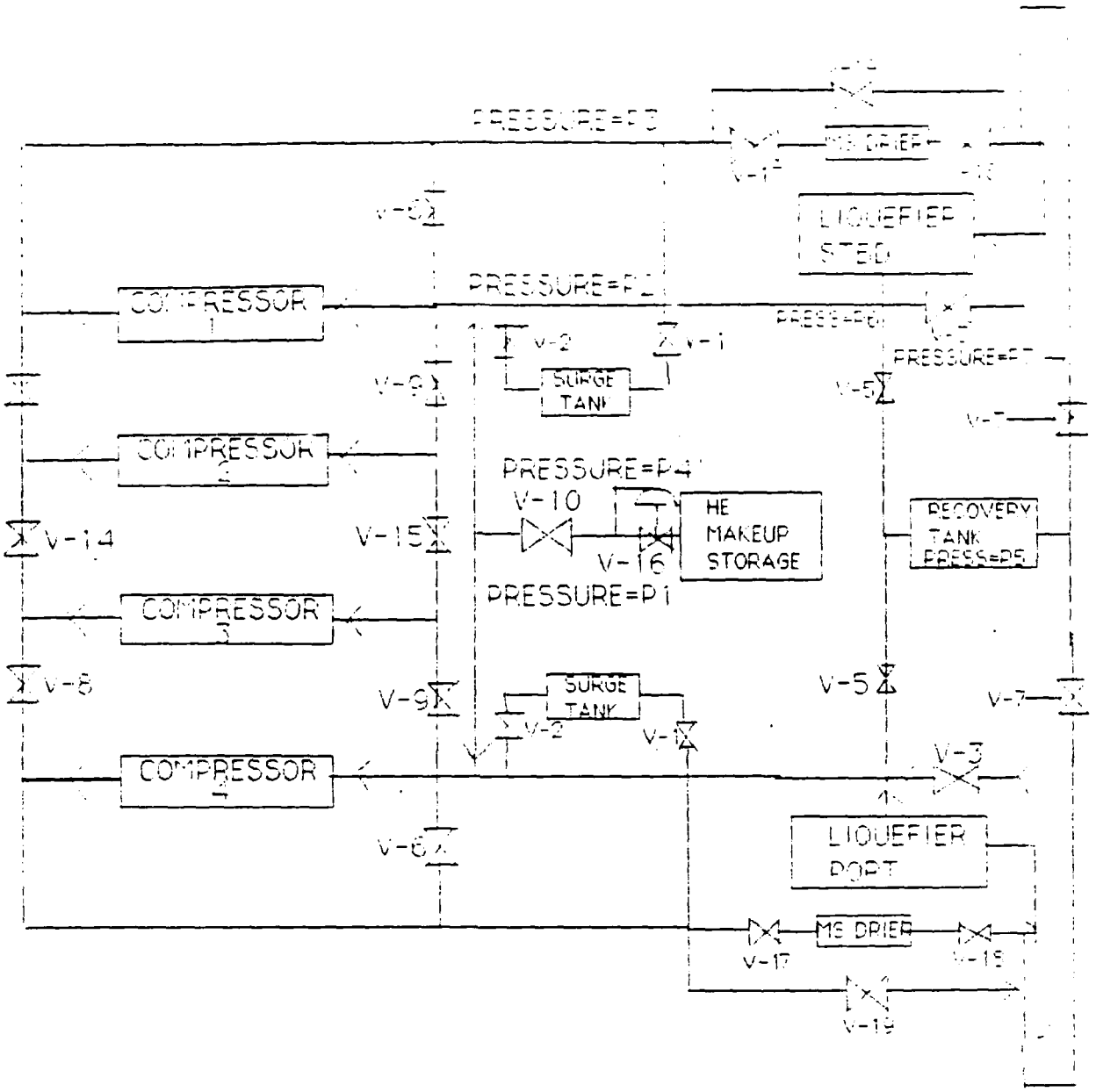

FIGURE 4.15
HELIUM SYSTEM
PART 1

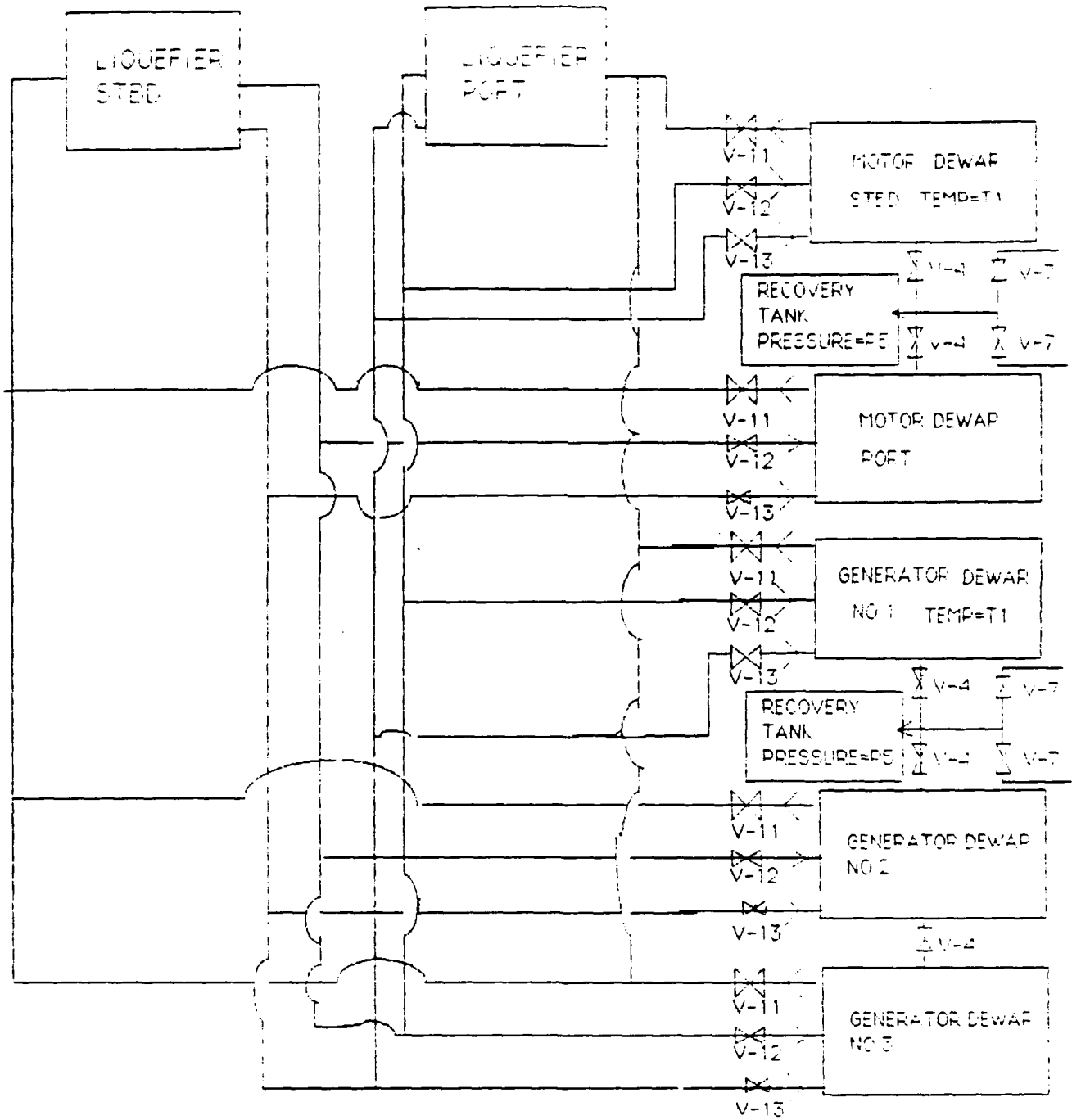

FIGURE 4.16
HELIUM SYSTEM PART 2

TABLE 4.9 SHIPBOARD HELIUM

SYSTEM VALVE DESCRIPTION

VALVE	MANUAL/AUTOMATIC	DESCRIPTION
V-1	AUTO	SURGE TANK INLET
V-2	AUTO	SURGE TANK OUTLET
V-3	AUTO	WARM GAS RETURN FROM DEWAR
V-4	AUTO	QUENCH RELIEF VALVE
V-5	AUTO	RECOVERY TANK OUTLET
V-6	AUTO	COMPRESSOR BYPASS
V-7	AUTO	RECOVERY TANK INLET
V-8,V-9	MANUAL	COMPRESSOR BLOCK VALVE
V-10	AUTO	HELIUM MAKEUP VALVE
V-11	AUTO	COOL-DOWN RETURN VALVE FROM DEWAR
V-12	AUTO	COOL-DOWN GAS INLET TO DEWAR
V-13	AUTO	LIQUID HELIUM INLET TO DEWAR
V-14,V-15	MANUAL	COMPRESSOR CROSS CONNECT VALVES
V-16	AUTO	HELIUM SUPPLY
V-17	MANUAL	MS DRIER INLET VALVE
V-18	MANUAL	MS DRIER OUTLET VLV
V-19	MANUAL	MS DRIER BYBASS VLV
LV-1	AUTO	JOULE-THOMPSON EXPANSION VALVE
LV-2	AUTO	PHASE SEPARATOR VENT VALVES

f) Engine discharge valve E-4 of Figure 4.14 is opened to begin the cool-down via valve V-12, returning to the compressor through valves V-11 and liquefier valves LV-8 and LV-6. All engines operate at maximum speed.

g) The temperature of the engine eventually falls such that a larger fraction of the compressor discharge gas passes through the engines and a smaller fraction will bypass the engine via valve V-6. As discharge pressure continues to fall, V-6 closes fully. Compressor valves V-8 and V-9 are opened and compressors 2 and 3 are started. If discharge pressure becomes excessive valve V-6 opens to reduce pressure.

h) The engine temperatures will continue to drop until each liquefier is taking full flow from two operating compressors. When the temperature of the dewar falls below 100 degrees Kelvin, the cold gas will be directed to the lowest heat exchanger by closing of valve LV-6 to ensure proper use of its refrigeration effect.

i) Valve LV-4 will close when T1 reaches 50 degrees Kelvin. Valves V-11, V-12 and LV-8 will close and the Joule-Thompson valve LV-1 will open, thereby beginning cool-down of the phase separator. Valve LV-5 will be opened manually.

j) When the phase separator temperature, T2 falls return gas from the separator is diverted through all the heat exchanges by closing valve LV-5.

k) The cool-down of the phase separator continues until T2 reaches 4.5 degrees Kelvin, at which point LV-5 will be completely closed and the gas flow directed through all heat exchangers in series. Liquid helium will begin building up in the phase separator.

l) The liquid delivery valves LV-3 and V-13 and return valve V-3 will open when the liquid level in the separator exceeds a minimum level.

This results in the final cool-down of the motor magnet dewar from 50 to 4.4 degrees Kelvin. Boil-off gas from the dewar after cooling the dewar's radiation shields and the magnet's current leads, will bypass the liquefier and return to the compressor via valve V-3.

m) Valve LV-2 is used to maintain the liquid level between the lower and upper levels. This valve opens when low level is reached and closes when high level is reached.

n) Once the magnet dewar has reached its final operating temperature of 4.4 degrees Kelvin, liquid helium will begin accumulating. When the minimum level is reached, compressors 2 and 3 are shut down and valves V-8 and V-9 manually closed.

2 STEADY-STATE OPERATION (NORMAL)

The steady-state liquefication and transfer of helium is an automatic process. Liquefier valve LV-3 is used to transfer liquid helium from the phase separator to the magnet dewar through liquefier valve LV-3. The flow rate is controlled by separator vent valve LV-2 which varies the separator pressure such that it maintains a nearly constant separator liquid level. Automatic control of the liquefier engine speed assures a constant liquid level in the magnet dewar. The rate of helium vaporization in the magnet dewar will vary such that surges in compressor suction will occur. Bypass valve V-6 will be used to maintain nearly constant discharge pressure. Valve V-1 opens automatically when P2 exceeds a specified pressure such that excess gas is dumped into the surge tanks. If the pressure P2 is reduced too low then valve V-2 is opened to return helium gas into the system. When compressor suction pressure continues to fall valve V-10 admits gas to the system from high pressure makeup storage. Valve V-16 is a pressure reducing valve.

If pressure, P4, exceeds a certain pressure, valve V-1 will close automatically and valve V-7 will open such that gas boil-off is admitted to the recovery tank. The gas will be returned to the system via valve V-5

when line pressure falls below a set pressure. The tank also stores boil-off helium gas resulting from magnet quench or normal evaporation during liquefier replacement.

The temperature of engine E-3 exhaust gas (T3) is used to control the liquefiers automatic Joule-Thompson expansion valve (LV-1). The molecular sieve drier bed is normally used when large quantities of makeup gas are added to the cryogenic system such as during a magnetic quench or a liquefier replacement. The dew point downstream of the molecular sieve will determine when a replacement is necessary. A reading of more than 1ppm indicates a replacement is required.

3 RECOVERY FROM QUENCH (ABNORMAL)

The procedure below is used to outline the steps needed to recover from the quench of a magnet. Assume that compressor 1 was in operation at the time the starboard motor magnet quenched.

a. After the quench dewar pressure P7 will rise such that valves LV-1 and LV-3 will close. System valve V-3 will also close and valve V-4 will open allowing the evaporating gas to rush into the recovery tank.

b. The quenched magnet is cooled down in much the same manner as the initial cool-down. The magnet temperature T1 will probably be below 100 degrees Kelvin. Valve LV-6 remains closed and cool-down gas from the dewar will pass into the liquefier and return to the compressor through the heat exchanger stages.

c. When valve LV-8 is opened, the residual gas in the magnetic dewar is vented into the liquefier. The gas is then pumped into the surge tank through valve V-1. Valve V-2 is then opened such that a suction can be taken on the compressor.

d. The gas generated as a result of the magnet quench which was stored in the recovery tank will also be returned to the system through V-5 during the cool-down process.

4 LIQUEFIER REPLACEMENT (ABNORMAL)

The objective during a liquefier malfunction is to remove and replace the liquefier without quenching the magnet. The liquid evaporating from the dewar will be recovered in the surge tank and in the recovery tank. Helium liquid and gas in the malfunctioning liquefier will be lost to the atmosphere. This small quantity of helium that is lost is replaced by stored high pressure makeup gas. The following procedure outlines the steps to replace the starboard malfunctioning liquefier:

a. Valves V-17, V-18 and V-19 are closed to stop the gas flow into the liquefier.

b. Drain the contents of the phase separator into the magnet dewar by manually closing LV-1 and LV-2 and opening LV-3.

c. When the separator is drained, manually open LV-2 and close LV-3. The liquid helium evaporating in the magnet dewar will pass through valve V-3 to the compressor suction piping. When the suction pressure P2 rises the valve V-1 will open to dump the excess gas into the surge tank. The pressure in the tank reaches a set pressure such that V-1 will close and valve V-7 will open and admit gas into the recovery tank.

d. Remove all piping and electrical wiring form the liquefier. The cold gas in the liquefier will be vented to the atmosphere through pressure-relief valve as it warms up.

e. Next, install the replacement liquefier, wiring and piping. Purge the liquefier and magnet dewar.

f. During the cool-down, as pressure builds up, the expansion engines E-1, E-2 and E-3 will start. The engine speed is adjusted to the maximum

to accelerate liquefier cool-down. In addition, to boost discharge pressure valves V-8 and V-9 are opened and compressor 2 is started.

g. Cool-down is continued as in initial cool-down section until cryogenic temperatures are reached.

CHAPTER 5
CONCLUSIONS AND RECOMMENDATIONS

From the results of this thesis, the following can be concluded:

1. High temperature superconductors are not yet technically feasible for a shipboard superconducting propulsion system. Technical barriers still exist such as low critical current densities and manufacturing difficulties. The most current density that high temperature wires have been made to carry is1000 amperes per square centimeter at 1 Tesla. Superconductors used in motors must be able to carry up to 100 times this amount. The ceramic's low current density problem appears to be attributed to their anisotropic character. The ceramic samples consist of individual superconducting crystals with nonsuperconducting areas in between. This results in noncontinuos current. Also, the superconducting ceramics like other ceramics are brittle, break easily, and are difficult to manufacture into coil shapes. In addition, the ceramics are highly susceptible to environmental degradation because of their extreme sensitivity to oxygen, water, and carbon dioxide. It is recommended that research in high temperature ceramics be continued since successful implementation in a marine propulsion would lead to replacement of expensive liquid helium coolant with cheaper liquid nitrogen coolant.

2. Type 2 superconducting materials are the best candidates for a superconducting shipboard propulsion system, although these materials require expensive liquid helium cooling. The most promising type 2 material is NbTi. NbTi can generate a magnetic field of up to 9 tesla (nearly five times that of an iron magnet). It is ductile and can easily be wound into the spiral shape necessary for a magnet. It is recomended that research be continued with other type materials such as Nb3Sn, V3Ga, Nb3(AlGe), and Nb3Ge. Nb3Sn can generate a magnetic field of over 15 tesla. A process has been developed for manufacturing this brittle

material into a coil shape. However, the material is very likely to fracture under the strains and forces of the strong magnetic field. V3Ga, Nb3(AlGe), and Nb3Ge have high critical field intensities but still lack a practicle fabrication technique.

3. An overview of superconducting properties and operational limits for NbTi has been established.

4. Copper - stabilized NbTi magnets were tested at the David Taylor Naval Research Laboratory and some interesting results were produced. First, the strength of the impregnated coil appears to be more significant than the hot spot developed during a quench. Next the magnet developed several self quenches.which appear to be due to insulation breakdown and instrumentation problems during magnet constuction. However, quenching of the magnet could be a major obstacle during full - scale testing in an adverse environment such as a superconducting shipboard propulsion system Therefore it is .recommended that experiments be conducted with NbTi wire with aluminum stabiiizing elements since an improvement in magnet stability is expected compared to copper - stabilized NbTi wire.

4. Experiments performed at the David Taylor Naval Research Laboratory showed that aluminum - stabilized NbTi superconductors have improved stability over copper - stabilized NbTi superconductors. The aluminum stabilizer showed improved thermal conductivity, heat capacity, and electrical conductivity at 4.2 degrees Kelvin compared with the copper stabilizer. Also, the stability of NbTi/Al was compared with the stability of NbTi/Cu.. The energy required to quench the NbTi/Al coil was found to be approximately 30 times greater than the energy required to quench the NbTi/Cu coil. However, the experimental data for the NbTi/Al coil was not as expected at an operating current/critical current of greator than 0.9. The data points for the NbTi/Al coil were expected to show a sharp decrease in magnitude as the operating current approached the critical current. The nonuniformity of the NbTi/Al coil is a possible cause of the unpredicted behavior. Another disadvantage of aluminum is that compared

to copper it is much more difficult to combine with NbTi. It is recommended that further experiments be conducted with NbTi/Al coils.

5. NbTi superconducting technology can be applied to a U.S. Navy Spruance Class Destroyer (DD963) propulsion system conversion. A feasibility study in converting a U.S. Navy Spruance Class Destroyer from mechanical to superconducting electric drive shows the following:

6. The use of an integrated electrical distribution system would allow for optimal machinery configuration with the generators running at their most economical loadings. At lower speeds, the ship's service needs could easily be supplied by the propulsion generators which would allow for a reduction in the total number of installed generators. This conversion reduced the number of LM-2500's from four to three and the number of 2,000 KW gas turbine generator sets from three to two.

7. An advantage to an integrated distribution system would be that a very large amount of power (55,114 KW) would be made available at cruising speeds for other ship mission areas. This will benefit combat systems designers who previously have been limited by the amount of power available solely from the ship's distribution system (6,000 KW.)

8. The reduction in space required by the engineering propulsion plant provides 4954 ft2 of deck space now available for other ship's functions. The shipboard system design to optimize the electric drive conversion could best be retrofitted after the installation and evaluation of this conversion. The most promising use for this "extra" space would be to expand the combat weapons systems to make use of the significantly higher electrical power made available by the integrated electrical distribution system. Possible choices for weapons upgrade could include high energy lasers, powerful electric counter measure systems or expanded active sonar capabilities. The design philosophy was too conservative to allow the installation of a new and untried "high tech" combat weapons systems simultaneously with a new and untried superconducting integrated

electrically driven ship. In the immediate future, this "gained" space could be used for additional storage and support facilities to extend the existing operational capabilities and to upgrade the command and control and survival capabilities.

9. The total cost of removal of the existing mechanical drive equipment and the cost of acquisition and installation of new electric drive equipment is estimated to cost $118.8 million.

10. Based on a remaining useful service life of twenty years, the conversion to electric drive will save an estimated $11.9 million in fuel costs.

11. The increased flexibility of the parallel power systems in separated spaces throughout the ship have provided a more redundant and survivable engineering system using less machinery. The conversion from mechanical to electric drive is expected to yield a quieter and more capable anti-submarine platform.

12. The integrated electrical distribution system will allow the most efficient loading of the gas turbines which will result in a 71% increase in endurance range.

13. Due to the increased cruising efficiency of the electric drive system, additional space or weight on the ship could be obtained by converting fuel tanks to other uses. It would be too difficult and costly to use this space effectively for this conversion but could be considered for other design conversion. Another option, not investigated in this conversion design due to the design philosophy, would be to reduce the existing tankage volume by 40% to maintain the current endurance range. This could present additional stability problems.

14. Current manning levels on the DD963 will be unaffected by the conversion. However, additional training and maintenance required by the new superconducting and cryogenic equipment is expected to be offset by

the elimination of the CRPP equipment, main reduction gears, two gas turbines and waste heat boilers.

15. Another alternative that could be investigated in this conversion design would be the placement of the electrical propulsion motors in pods directly in front of the rudders. This concept was initially investigated, but dismissed due to the extensive hull modifications that would be required. The superconducting machinery should be more accessible to maintenance personnel in this "first" attempt.

16. Due to the high cost of this conversion compared to the relatively minor gains in operational performance, this conversion is justified as a test paper to obtain experience in electric drive that can be applied in future designs. A comprehensive combat systems conversion based on integrated electric drive that would make DD963 a multi-mission, high powered fleet escort is required to justify an entire ship class conversion program. By designing a superconducting electric drive ship from the keel up, the most benefits from this could be achieved. The space savings achieved by superconducting electric drive could be best utilized in a new ship design where advancing technologies such as external podded propulsion and high energy lasers and sonar could be readily employed in smaller high powered ships.

REFERENCES

Acker, F.E., Greene, D.L., & Jolliff, J.V. (1983). Modeling of weight and volume for advanced alternating current electric drive machinery, Naval Engineers Journal, May, 192-201.

Bishop, J., Gregory, E. and Wong, J. (Presented at ICEC 11, April 22-25, 1986). Aluminum Stabilized Multifilamentary NbTi Superconductors,

Carmichael, A.D. (1987). M.I.T. Department of Ocean Engineering course 13.21, Ship power and propulsion handout and lecture notes.

Doyle, T.J. (1977). Superconductive Propulsion Motor, Mechanical Engineering, January, 48-53.

Doyle, T.J., Green, G.F., Raphael, S., & Robey, H.W. (1980). Twin-screw swath superconductive drive system, David Taylor Naval Ship Research and Developement Center. (DTNSRDC/PAS- 79/38)

Ekin,J.(1988). National Bureau of Standards, Boulder, Colorado (Personal correspondence).

Foner, S. & Schwartz, B.E. (1981). Superconducting material science. New York: Plenum.

Green, G.F. (1987). Cool down of a large scale superconducting magnet system for naval applications. Unpublished manuscript.

Gregory, E. (March 12, 1987), Recent developments in multifilamentary Nb-Ti superconductors, Cryogenics, 1987, Vol 27, June

Waltman, D. J., McDonald, F. E. and Superczynski, M. J. Stability Measurements of Aluminum-Stabilized Nb-Ti and Bronze Matrix Nb3Sn Potted Superconducting Magnets, David Taylor Naval Ship Research and Development Center, Annapolis, Maryland. Unpublished manuscript

Jolliff, J.V. & Greene, D.L. (1982). Advanced integrated electrical propulsion - a reality of the eighties, Naval Engineers Journal, April, 232-252.

Kreilic, T. S. (June, 1987). Reduction of Coupling in Fine Filamentary Cu-NbTi Composites by the Addition of Manganese to the Matrix, Presented ICMC/CEC, St. Charles, IL.

Kreilick, T. S., Gregory, E., and Wong, J. (August 1985). Fine Filamentary NbTi Superconducting Wires, Presented at the International Cryogenic Materials Conference, Paper CZ-6, Cambridge Ma.

Messinger, H., Clarke, P.B., & Bowen, W.H., Jr. (1982). Helium man- agement aboard navy ships equipped with superconducting elec- tric propulsion systems, David Taylor Naval Ship Research and Development Center. (DTNSRDC/PAS-81/17)

Mazek, J.E. (1988). Superconductivity: super-opportunity, Proceeding U.S. Naval Institue, January, 112-115.

Newton, R.I. (1973). Computer Aided Marine Power Plant Selection, MIT O.E. Thesis.

Orlando, Terry (1988). M.I.T. Department of Electrical Engineering course 6.7633, Applied Superconductivity handout and lecture notes.

Rains, D.A. (1975). Prospects in Naval Gas Turbine Power Plant Machinery, Naval Engineers Journal, April, 126-138.

Rains, D.A. (1975). DD963 Power Plant, Marine Technology, 12(1), 1-24.

Rains, D.A., Beyer, K.M., Keene, W.P., Lindgreen, J.R., Mogil, E., Page, T.E., Untershine, J., & Youngworth, J.F. (1976). Design appraisal - DD963, Naval Engineers Journal, October, 43-61.

Schmucker, D. (1988). Naval See Systems Command (Code 56-31). Personal correspondence.

Stewart, A.J., Springer, J.H., & Doyle, T.J. (1979). Effectiveness of Superconductive Electric Drives, Naval Engineers Journal, April, 109-119.

St. John, L.G. (1978). Analysis of Superconducting Electric Machines for Naval Ship Propulsion, MIT O.E. Thesis.

Waltman, D.J.(1988). David Taylor Naval Research Laboratory, Personal correspondence.

Ware, R. (Ed.) (1975). USS Spruance (DD963), Marine Engineering/ Log, May, 37-51.

The following DD963 reference material, found in the MIT 13A vault, was used:

DD963 Basic Ship Full Load Condition DD963 Class Booklet of General Drawings - FINAL DD963 Class War Fighting Improvement Program Engineering (WIPE) September 1986 DD963 Class Weight Report - FINAL DD963 Compartment List DD963 Compartment Volumes and Deck Areas DD963 Electrical Load Analysis DD963 Speed and Power Report DD963 Volume Statement